Vol. 3, No. 4, p. 253-328, July/August 1960

An International Journal on Fundamentals of Friction, Lubrication, Wear, and their Control in Industry

WEAR

USURE VERSCHLEISS

ELSEVIER

WEAR

Usure *Verschleiss*

AN INTERNATIONAL JOURNAL
ON FUNDAMENTALS OF FRICTION, LUBRICATION, WEAR,
AND THEIR CONTROL IN INDUSTRY

HONORARY EDITORIAL BOARD

F. T. BARWELL, *London*
W. BOAS, *Melbourne*
F. P. BOWDEN, *Cambridge*
B. V. DERYAGUIN, *Moscow*
I. SAKURADA, *Kyoto*
M. C. SHAW, *Cambridge, Mass.*
E. M. SIMONS, *Columbus, Ohio*
H. WAHL, *Stuttgart*
K. WELLINGER, *Stuttgart*

Editor:

G. SALOMON

Delft

HONORARY ADVISORY BOARD

E. E. BISSON, *Cleveland, Ohio*
H. BLOK, *Delft*
E. BRANDENBERGER, *Zurich*
J. T. BURWELL, JR., *New York*
A. A. CAPOCACCIA, *Genoa*
M. M. KHRUSCHOV, *Moscow*
B. LUNN, *Copenhagen*
M. E. MERCHANT, *Cincinnati, Ohio*
P. NICOLAU, *Paris*
T. SATA, *Tokyo*
R. S. VARMA, *New Delhi*

THE ROLE OF SURFACE SHEAR STRAINS IN THE ADHESION OF METALS. PART I

O. L. ANDERSON

Bell Telephone Laboratories, Murray Hill, New Jersey (U.S.A.)

SUMMARY

The effect of surface shear strains on the adhesion of copper, aluminum, and gold surfaces is examined. In particular, the effect of shear strains on the structure of metal surfaces and substrata subsequent to adhesion is elucidated. It is shown that shear strains are necessary for adhesion to occur under most circumstances when unlubricated metals are in contact. Shear strains are very effective in removing surface oxides, and these oxides are buried at below the common interface. Shear strains roughen the surface, increase the amount of atomic contact, and produce a work-hardened zone near the common interface, all of which tend to make the adhesion more effective. In general, the concept of friction and adhesion advocated by the Cambridge school is confirmed.

ZUSAMMENFASSUNG

DER EINFLUSS VON SCHUBDEFORMATION IN DER OBERFLÄCHE AUF DIE ADHÄSION VON METALLEN

Der Einfluss von Schubdeformationen auf die Adhäsion von Kupfer-, Aluminium- und Goldoberflächen wird untersucht. Im Besonderen wird dieser Effekt auf die Struktur der Metalloberfläche und der Unterschicht, *nachdem* Adhäsion eingetreten ist, aufgeklärt. Es zeigt sich, dass Schubdeformation für Adhäsion nötig ist und zwar unter den meisten Bedingungen unter denen ungeschmierte Metalle miteinander in Kontakt kommen. Die Oberflächenoxyde werden durch Schubdeformation abgetrennt und unter der Oberfläche der gemeinsamen Grenzfläche begraben. Die Oberfläche wird durch Schubdeformationen aufgerauht, es entstehen mehr Kontakte zwischen Atomen und es wird eine ausgehärtete Zone nahe bei der Grenzfläche gebildet, dies alles trägt dazu bei die Adhäsion wirksamer zu machen. In allgemeinen wurde die Auffassung über Reibung und Adhäsion, die durch die Cambridge'r Schule vertreten wird, bestätigt.

INTRODUCTION

The adhesion of sliding metal surfaces is the fundamental cause of friction and wear[1]. The elimination of friction and wear has always been a critical problem in engineering design, but the central problem of the nature of adhesion has usually played a secondary role to the search for better lubricants and the understanding of boundary hydrodynamics. Recent work has reopened the whole question of the mechanism of adhesion itself, quite apart from its consequences on friction and wear. For instance, it has become evident that adhesion of solid surfaces can be maximized sufficiently to replace, in certain cases, older methods of joining solids such as soldering and welding[2].

The general nature of adhesion is understood. According to the "adhesion theory of friction" sponsored by the Cambridge school, adhesion occurs when surface barriers (such as oxides and adsorbed gases) are removed so that the underlying structures are brought into atomically close contact. This permits primary chemical bonds to seize and the two solids then become as one. The adhesion, measured as a breaking force, is large or small as the area of close contact is large or small. The critical stage is the removal of surface barriers, which can be stripped off by tangential surface strains. It has been shown that when surfaces slide, or even tend to slide, adhesion increases[3] and the real area of contact as measured by electrical resistance increases[4]. It has been shown that tangential surface strains, when exerted in a rigorous manner, will cause metallic rods to seize at room temperature[5] with high adhesive loads. As a result of this work it is evident that tangential surface strains are the dominant, and probably the crucial, factor in adhesion.

Admitting that shear stresses are effective in permitting denuded metallic surfaces to come into close contact, there is still the deeper problem of why the adhesion of the newly bonded surfaces is greater than the cohesion of the materials just interior to the bonded region. This problem has received the attention of DE BRUYNE[6], who concluded that solids have very powerful molecular forces emanating from their surfaces which seize other solids unless there are obstructions. In support of his position, DE BRUYNE used thermochemical data to prove that the energy required to break a water film away from an aluminum surface is comparable to the lattice energy of aluminum. Furthermore, EISNER[7] has pointed out that it is not necessary for the adhesive forces to be stronger than the lattice forces to obtain adhesion; it is only necessary for the adhesive force to be larger than the effective lattice force at a surface which is considerably reduced from its theoretical value by the presence of cracks, dislocations, grain boundaries, and other imperfections.

The purpose of this paper is to present experimental results which show in a specific way what happens to the surfaces of metals when seizure occurs, and the role of shear strains in causing the seizure. We present results of the adhesion of idealized plastic spheres, the adhesion of metallic rods, the effect of shear stresses on the stripping of oxide films, and the effect of shear stresses on the structure of metals just below the adhered surfaces.

GENERAL EQUATIONS AND BACKGROUND

The physical property which is important to the understanding of adhesion is submicroscopic roughness. The consequence of roughness is the following. If two apparently smooth surfaces are pressed together, their surfaces appear to be in perfect contact, whereas they actually adjoin in only a few isolated spots. Ordinarily, the real area of contact A_r, such as might be found from resistivity measurements, is very much smaller than the apparent area of contact A_a, such as might be measured with a micrometer.

The stress at each point of contact is large, even for light loads, because the actual area of contact is small. Consequently, even when the nominal stress, which is

determined by A_a, is small, plastic conditions prevail in the immediate vicinity of contact. The magnitude of A_r is just sufficient to keep the pressure at the contact points equal to the flow pressure. However, two situations are to be distinguished; either the metal in the plastic zone is being work-hardened, or it is fully work-hardened.

For work-hardening metals, where a spherical indenter is pushed in the surface, the force W is related to the area of contact by

$$W = \text{const} \cdot A_a^n \tag{1}$$

which is known as Meyer's law[8]. (For instance, n is about 5/4 for annealed gold and copper, and the apparent pressure is thus proportional to $W^{\frac{1}{4}}$.) When the metal is fully work-hardened (or does not work-harden), $n = 1$ and the pressure is independent of load. This law also holds for cylinders in compression and soft spheres against hard planes[9]. We shall see examples of the application of Meyer's law to the adhesion of gold spheres in the next section. The real area of contact of a contact region is given by w/p, where w is the load on that contact point and p is the maximum flow pressure. The real area of contact, composed of the total of all contact regions, is given in terms of the applied load by

$$A_r = W/p \tag{2}$$

where W is the observed total load. The ratio of the real and the apparent area is

$$\beta = A_r/A_a = W/pA_a \tag{3}$$

When the metal surface is fully work-hardened, p will take on the value of σ_{max} found on the stress–strain curve at large compressive strains, and if not p will be less. Thus β is greater than or equal to the value of eqn. 3 when σ_{max} is substituted for p. Consequently, the lower limit of β is determinable from experimentally measured quantities,

$$\beta_{min} = W/(\sigma_{max} \cdot A_a) \tag{4}$$

Knowledge of σ_{max} permits the value of β_{min} to be determined if A_a and W are measured simultaneously. In general, β will be greater than the value found from eqn. 4, but, of course, less than unity.

The electrical resistivity of the two surfaces in contact is composed of a size effect due to the constriction of the current through the asperities, and a film effect due to surface films which usually have high specific resistivity. The constrictive resistance of a (circular) contact point is inversely proportional to the diameter of the individual contact. To a fair approximation, the total constrictive resistance of a surface made up of a number of contact points is inversely proportional to the one-half power of the real contact area*,

$$R_c = \text{const} \cdot A_r^{-\frac{1}{2}} \tag{5}$$

* This equation is plausible for small balls with large value of β, the case for which it is applied in the following section. It is less true for the case of a large number of contact points.

Neglecting changes in the contact flow pressure, using eqns. 1 and 2, the above can be written as

$$R_c = \text{const} \cdot A_r^{-\frac{1}{2}} \tag{6}$$

or if the apparent area is a circle of diameter d

$$R_c = \text{const} \cdot d^{-n} \tag{7}$$

The film resistance of a contact spot is inversely proportional to the area of contact. Under the same conditions as above, the total film resistance is related to the apparent contact diameter by

$$R_f = \text{const} \cdot d^{-2n} \tag{8}$$

During work-hardening, the value of n is slightly above unity and becomes unity when the metal in the immediate vicinity of the contact surface is fully work-hardened.

Equations 7 and 8 will be used to exhibit the effective removal of a surface barrier. In plots of log R (resistance) *vs.* log d (diameter of contact), the sudden reduction of the slope to about one-half its former value is indicative of film removal. An abrupt drop of resistance is sometimes used as evidence of film penetration, but this interpretation can be misleading since the magnitude of the resistance is sometimes very sensitive to the film thickness. In particular, wear of a thin film often causes large resistance drops because of the quantum mechanical tunneling effect[10].

THE DEFORMATION AND SEIZURE OF SOFT SPHERES

The root of the problem in adhesion experiments is: how do the asperities seize? In this section some new experimental results will be described which illustrate the behavior of a single asperity at the instant of seizure.

The mechanical behavior of metals in contact is the consequence of a number of adjoining asperities which are deformed plastically. The experiments described in this section are intended to show the reaction of a single soft sphere to various loading conditions. This sphere, which is large enough to be observed in the optical microscope, constitutes a model of the asperity. By observing the sphere's reactions, deductions are made on the physics of the ordinary adhesion process which results from the reaction of many individual — but invisible — asperities.

A very soft, very smooth, spherical ball is made as follows. The end of a piece of gold wire is heated until it becomes molten, whereupon it is quenched in air. As the molten gold cools, surface-tension forces shape a large sphere on the end of the wire. (For wire 0.005 in. in diameter, a ball 5 times as thick as the wire easily forms.) The sphere is easily manipulated by inserting the end of the wire into a capillary tube; for example, a 0.025-in. sphere held in a ceramic capillary in contact with a similar sphere held in a collet is shown in Fig. 1. Spheres made in this manner are very smooth. The smoothness of one sphere was examined, by electron micrographs using replica techniques, in which no roughness was discerned at 11,000 diameters. Electron reflection photographs with a resolution of about 1 μ also showed large

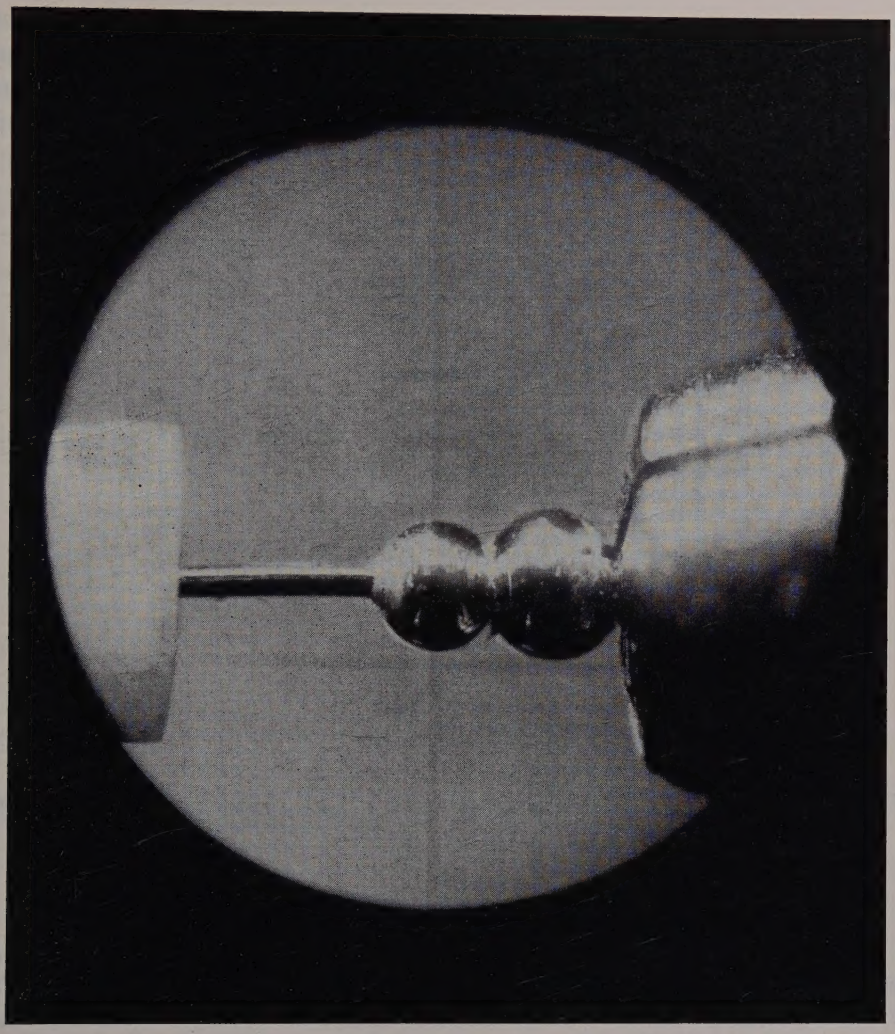

Fig. 1. A photomicrograph showing two gold spheres in contact. The spheres are formed by surface tension on the ends of 0.005-in. gold wires. One sphere is held firmly in a collet, while the other is manipulated in a ceramic capillary tube.

regions with no roughness*. Of course, it is not certain that the surface is molecularly smooth, but the sphere is very much smoother than other metallic surfaces. Surface tension appears to give the gold ball the smoothness that is found on glass microscope slides, where the surface is also formed by surface tension. The sphere is, of course, very soft. The softness and smoothness of the sphere make it a good model for one asperity.

The deformation of the ball follows eqn. 1 as shown in Fig. 2, where force is plotted against apparent area of contact. The exponent $n = 1.35$, found from Fig. 2, agrees

* The electron reflection photographs were kindly made by Dr. M. SEAL of Cambridge University.

with the original work of O'NEILL[8]. The ball was pressed against surfaces of various roughness including glass microscope slides, etched germanium, tarnished copper, and lapped steel; but the value of n did not change. Nor did the value of n change for ball diameters ranging from 0.005 to 0.05 inch. The area of contact was measured

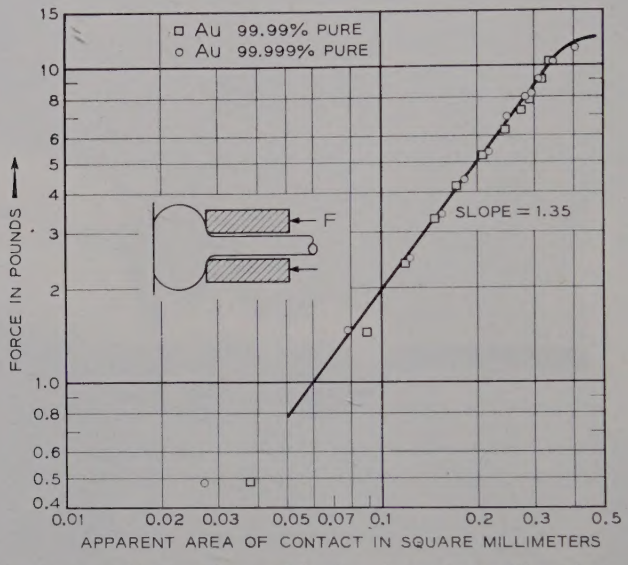

Fig. 2. A plot of log force *vs.* log area for a gold sphere in contact with a plane. The slope of this line determines the value of n for Meyer's law, eqn. 1.

by magnified shadowgraph techniques so that the diameter of contact could be measured at different positions. There was a small ellipticity of area of contact; but the maximum diameters, a and b, were measured, and the apparent area was defined as $A_a = (\pi/4)ab$, and the diameter of contact as $(a + b)/2$.

The next experiment was to determine the value of the ratio of the real and apparent area of contact, β_{min}, defined by eqn. 4. To use eqn. 4 the maximum yield pressure of bulk gold is needed, but a survey of the literature showed conflicting values. Consequently, the stress–strain curves of pure (99.999%) gold cylinders were measured both in compression and tension. The cylinders were annealed for two hours at 300°C. The data from the compression curves were corrected for friction and size effects, after the method of COOKE AND LARKE[11], yielding five points of the true stress–strain curve in compression. These five points superimposed upon the stress–strain curve in tension, as theory requires, show it is permissible to use the tension stress–strain curve in place of the true compressive stress–strain curve. The stress–strain curve is plotted in Fig. 3, where the solid line is the tension curve, and the circles are corrected points of the compression curve. The inset shows that gold

is an ideal work-hardening metal with a low yield point (2,000 p.s.i. or 141 kg/cm²) and shows no hysteresis loss as the load is cycled. The asymptotic value of stress, reached at a strain of about 0.5, is about 30,000 p.s.i. or 2,000 kg/cm². (It is interesting to note that the stress–strain curve for the plastic sphere which is obtained from

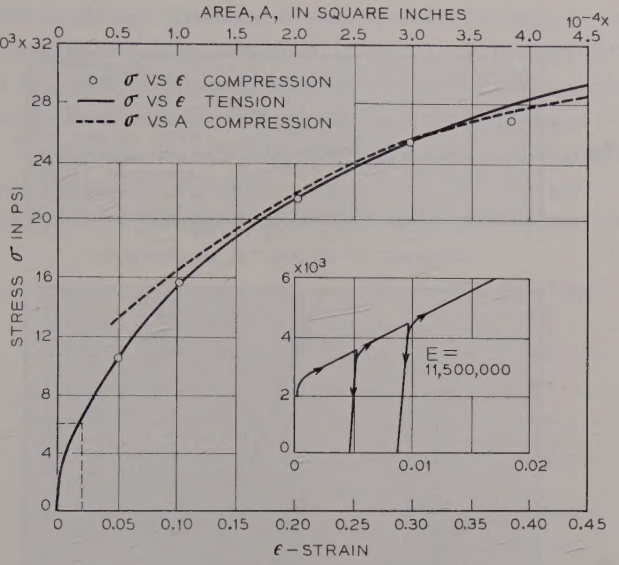

Fig. 3. The stress–strain curve of pure (99.999%) gold. The solid line is for tension; the circles are for compression of cylinders after friction and size effects have been extrapolated out; the dashed line is stress *vs.* area of contact for the data shown in Fig. 2.

Fig. 2 can be superimposed on the tensile stress–strain curve of the cylinders. The stress–strain curve of the sphere is shown by the dashed line in Fig. 3. This means that A_a is proportional to the strain and, in fact, $A_a = 10^{-3}\ \varepsilon$ sq.cm.)

Using Fig. 3, the ratio of the real to the apparent area of contact of the ball and the plane is found to vary from $\beta_{min} = 0.6$ at the smaller loads to $\beta_{min} = 0.95$ at the larger loads in these experiments. Knowing the lower limit of β, we are in a position to place limits on the extent that a sudden change in resistivity of the sphere is due to sudden increase in the area of contact. Since the value of β_{min} does not depart significantly from unity, the reaction of one sphere against a plane or another sphere is a good model of the reaction of one asperity against another.

The next set of experiments was made to show the behavior of the electrical resistance between a sphere and plane, or between two spheres, at the moment of seizure.

The resistance across the common interface of the gold ball and a plane metallic surface was measured as a function of load and diameter of contact. The resistance was measured by measuring the voltage drop at constant current with a Leeds and

Northrop microvoltmeter and a #7752 potentiometer. The resistance arising from the electrical leads in this device is self-compensating, so that the measured resistance is very accurate on a relative basis and reasonably accurate on an absolute basis*. The maximum and minimum apparent diameters of contact were measured by shadowgraph techniques, and the effective diameter of contact $d = (a + b)/2$ was plotted against resistance.

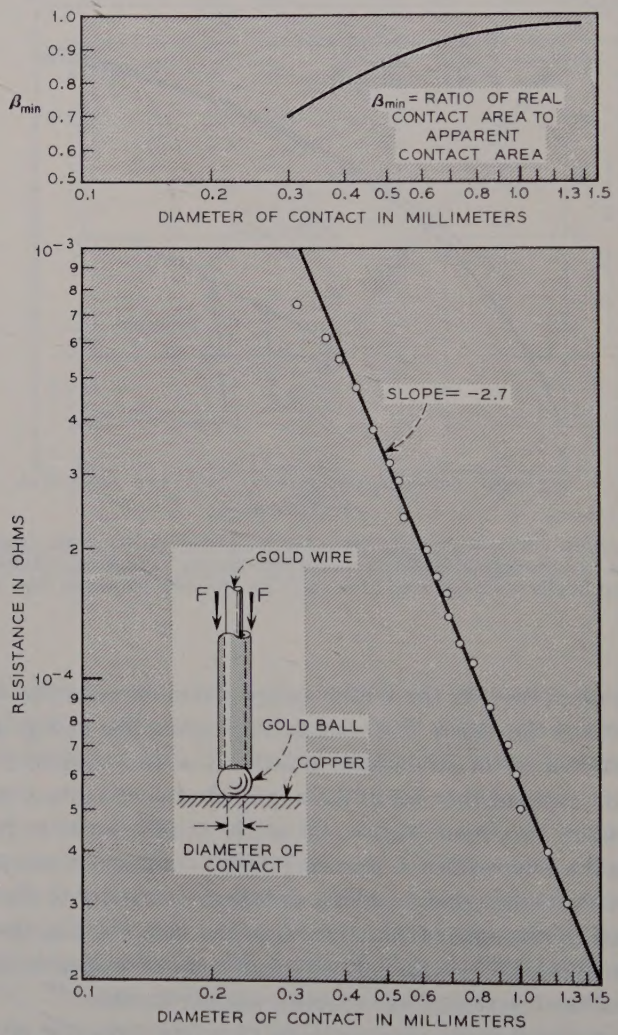

Fig. 4. The variation of contact resistance R and β_{min} *vs.* diameter of contact for a gold sphere against a copper plane. The salient features are that the slope of the line in the lower curve is exactly double the slope found in Fig. 2, and that the real area of contact is nearly equal to the apparent area of contact.

* Uncertainty about the absolute value of the resistance arises from the estimated voltage drop due to the metal between the potential leads. This must be subtracted from measured voltage drop.

Fig. 4 shows the result of the measurements of area, resistance, and load when a gold sphere is pushed against a polished copper plane. The bottom graph shows resistance *vs.* diameter of contact, while the top graph shows β_{min} *vs.* diameter of contact. The solid line passing through the experimental points has a slope of —2.7. Since the absolute magnitude of this slope is about 2, it is concluded that the resistance is primarily due to a film barrier. Because the slope is greater than 2, the gold is being steadily work-hardened. Knowing W and d, and using $\sigma_{max} = 30{,}000$ p.s.i. as found in Fig. 3, the value of β_{min} is determined by eqn. 4 and plotted against diameter of contact. From this plot, it is apparent that the gold surface is always in very intimate contact with the metallic surface, especially in the later stages of deformation. Actually, since p is less than σ_{max} in the beginning stages of deformation, β will be closer to unity than indicated by β_{min}.

The plot of resistance *vs.* diameter of contact for a gold sphere and a polished

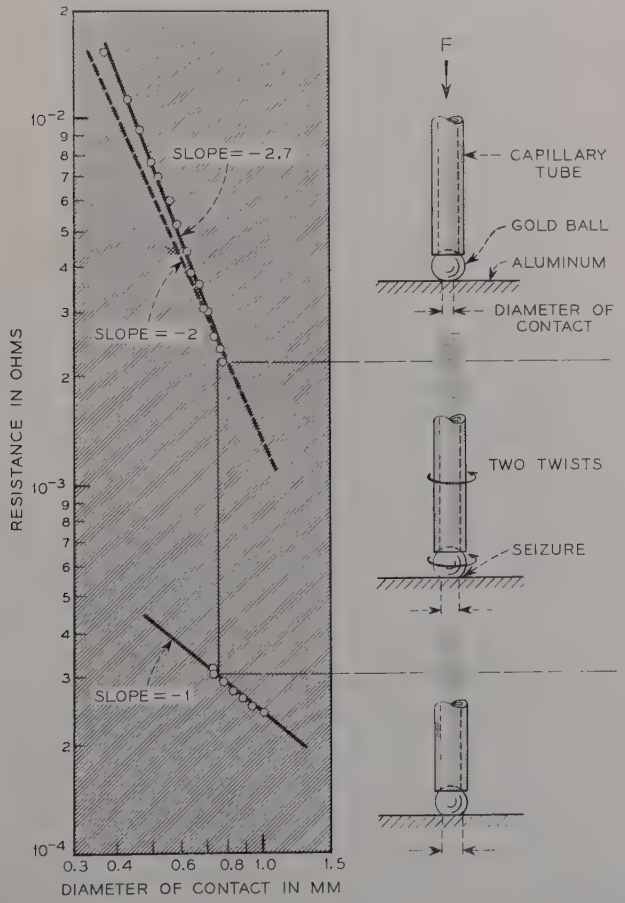

Fig. 5. A plot showing the behavior of the resistance as shear strains are imposed on a sphere, causing seizure. The salient features are that the slope changes from —2.7 to —1 upon seizure, and the resistance drop is too large to be ascribed to an increase in real area of contact.

aluminum plane is shown in Fig. 5. The dashed line showing the slope of —2 corresponds to a film on fully work-hardened metal, but this line is a much poorer fit to the data. It is apparent that a line with the slope —2.70 fits the data points very well; and, consequently, the value of n determined from resistance measurements is in very good agreement with the value of n determined from the mechanical measurements, as shown in Fig. 2. The resistivity follows eqn. 8 until the point where the ball is twisted with respect to the aluminum, causing seizure between the ball and plane*. At that point the resistance drops by about a decade, and further load shows that

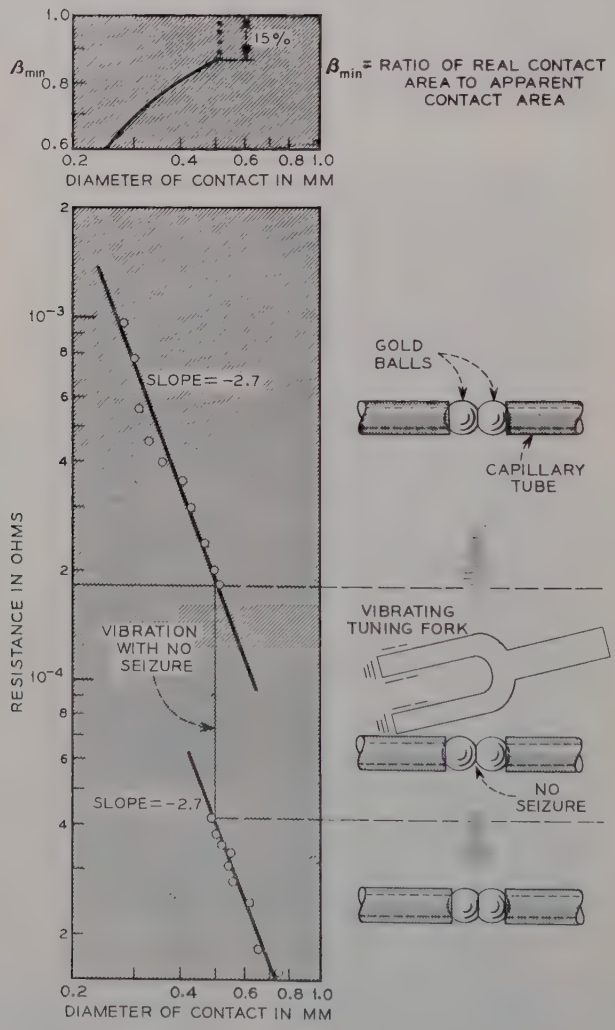

Fig. 6. A plot showing the behavior of resistance when the shearing strains are not strong enough to cause seizure. In this case the slope does not change, although there is a large resistance drop.

* Twisting consists of rotation of the ball 180° in one direction. Cyclic rotation produces stronger adhesion, in general, but was not used in order to obtain more reproducible results.

the resistivity subsequently follows eqn. 7 rather than eqn. 8. The final slope being —1.0 rather than —1.35 indicates that the surface is fully work-hardened according to eqn. 1. The drop in resistance could conceivably be caused by an increase of real area of contact or film penetration. However, a calculation of β_{min} shows that at the moment of seizure the real area of contact can increase at most by only about 8 per cent, whereas the resistance drops by nearly one order of magnitude. Consequently, the drop in resistance must be caused primarily by the degradation of the surface barrier.

When the ball is twisted relative to the plane, seizure occurs and the power law changes. Usually seizure is so complete that the coefficient of adhesion is meaningless when measured*. If a large traction is exerted, either the gold wire is broken or the ball pulls out a chunk of the other metal surface. Seizure was always found when the power law changed. Seizure did not always occur with a resistance drop, however, as the following experiment shows.

Two gold balls were squeezed together, and the resistance plotted against diameter. Their behavior was the same as one gold ball against an aluminum or copper plane. No seizure occurred unless the balls were twisted with respect to each other while under load. In other words, direct pressure without shear did not produce adhesion. The log R *vs.* log d curves were similar to Fig. 4. It was found that a large drop in resistance could be obtained without seizure by slight shear strains. A tuning fork was vibrated and then dampened on one of the capillary tubes holding the gold balls, thus creating small shear strains between the surfaces. The results of the log R *vs.* log d curve for gold on gold is shown in Fig. 6.

Here we see that the slope is about —2.7 before and after the shearing strains, which shows that a high resistive film remains even though the resistivity has dropped by nearly a decade. In general, our results were as follows. When the shearing strains were sufficiently large to produce adhesion, the slope of log R *vs.* log d curve changed from $-2\ n$ to —1; and conversely, when the shearing strains were so small that no adhesion occurred, the slope remained unchanged. However, shearing strains always produced a resistance drop of about one decade, which was too large to be attributed to an increase in the real area of contact. In no case did seizure occur unless shear strains were imposed (in this case by rotating one of the balls).

We interpret these results as follows. Some high resistive film—perhaps an oxide—blocks the adhesive forces (such as conjectured by DE BRUYNE) emanating from the surface of metals. These films are easily degraded by shear strains but not by direct compression. Sometimes these films are worn down by shear strains, but not to the point where they lose their effectiveness in blocking adhesive forces. In the latter case, it is possible to reduce the resistance by a large amount without adhesion, very likely by a small change in a very thin film because of the tunneling effect.

If film degradation can occur without adhesion, the question of the converse arises: Can adhesion occur without complete film degradation? An experiment revealed that

* The coefficient of adhesion is the force required to separate the surfaces divided by the force used to push them together.

this possibility also exists. A gold ball was pushed against a copper plane and twisted, producing seizure; the load was increased and the ball then twisted, and this operation was repeated several times. The results are plotted in Fig. 7.

During the first twisting operation, the resistance drops by nearly one decade. Each successive twisting operation reduces the resistance by an abrupt amount,

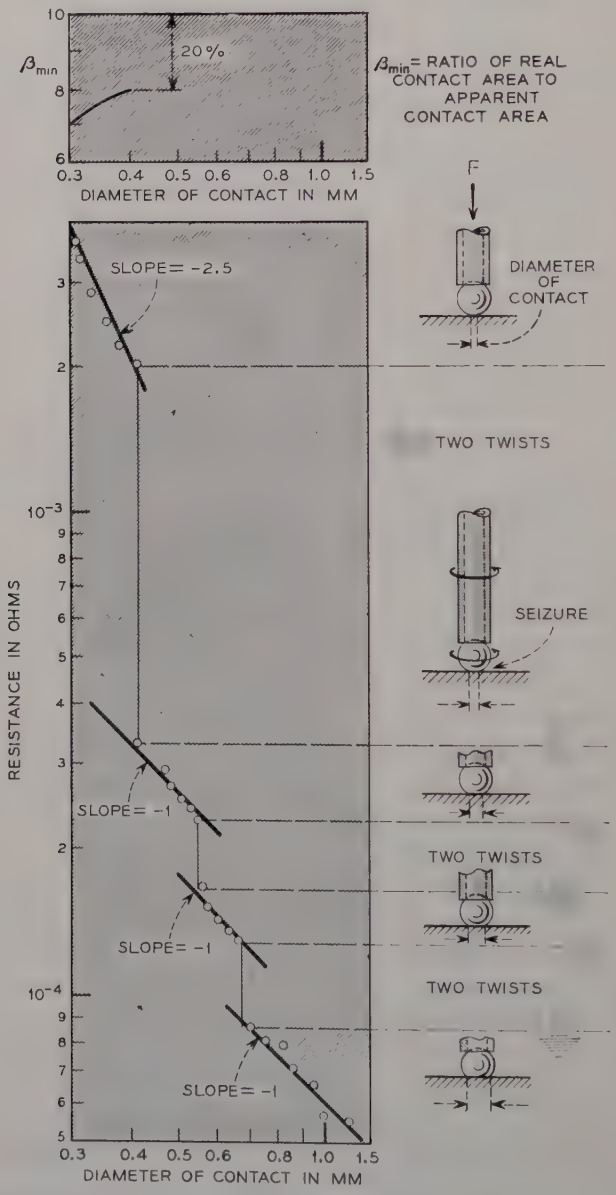

Fig. 7. A plot showing the behavior of resistance when further shearing strains are imposed subsequent to seizure.

although not as much as in the first operation. Very little of the resistance drop can be attributed to an increase in A_r. This resistance drop must arise from further degradation of surface barriers, which occurs in the presence of adhesion, and one concludes that very strong adhesion can take place without the complete degradation of surface films* on the two gold balls.

The observations made on the deformation and seizure of soft gold balls verify the mechanism that has been conjectured for the deformation and seizure of asperities in the "adhesion theory of friction". However, our results go further. Our gold ball is a good model of the asperity; and we have shown that the seizure of a single sphere occurs after film degradation has occurred, but that this degradation does not occur simply because of plastic flow. Thus asperities will not seize unless there is motion which introduces a surface shearing strain. Since this shearing strain is required to produce seizure of very pure gold, which is sometimes regarded as an oxide-free metal, we conclude that shearing strains are even more necessary for the seizure of less noble metals.

THE ADHESION OF METALLIC RODS

The adhesion of gold spheres, such as described in the previous section, is a go or no-go phenomenon. Adhesion does not occur if shear strains are not imposed, whereas adhesion is complete if shear strains are imposed. The force measured in separating the gold spheres is not meaningful since the spheres do not break along their initial plane of contact. What is in fact measured is the strength of the gold. This is no doubt due to the fact that adhesion occurs over virtually the total area of contact, and the cross section of contact is greater than the cross section of the wire.

If two metallic rods with ends cut in planes normal to their axes are pressed together so that their axes are co-linear, and if one rod is twisted with respect to the other, adhesion will often occur[5]. In this case the value of β is low since the contact area is limited to a number of isolated spots. When the rods are pulled apart, they break roughly along their plane of contact so the force measured to pull them apart represents adhesion. This force divided by the initial normal force is the coefficient of adhesion γ. It turns out that the value of γ is not reproducible from test to test. However, the values of γ are contained within a reproducible distribution; and for a large number of tests, the median $\tilde{\gamma}$ (or $\tilde{F}$) is well defined[12]. The distribution for 1,190 tests of $\frac{1}{4}$-inch rods (copper on copper) pressed together with five pounds is shown in Fig. 8. The distribution is log-normal, which means that the factors affecting adhesion are related to each in a multiplicative way, whereas in ordinary normal distributions the unknown factors enter in an additive way. In these experiments

* The presence of surface films was verified by electron diffraction. Gold balls (99.999% pure) were pressed against clean microscope slides, and the flat surfaces examined. In all cases there was evidence of extraneous material on the surface. All types of patterns appeared. In one case crystallites 1 μ in size were seen. In some cases there appeared to be two phases or a single phase with a complex structure. In one case an amorphous structure appeared.

the value of $\tilde{\gamma}$ was found to be independent of load and nominal area of contact[12]. Consequently, the laws of adhesion read exactly like Amontons' laws of friction, provided the words "median coefficient of adhesion" are substituted for "coefficient of friction".

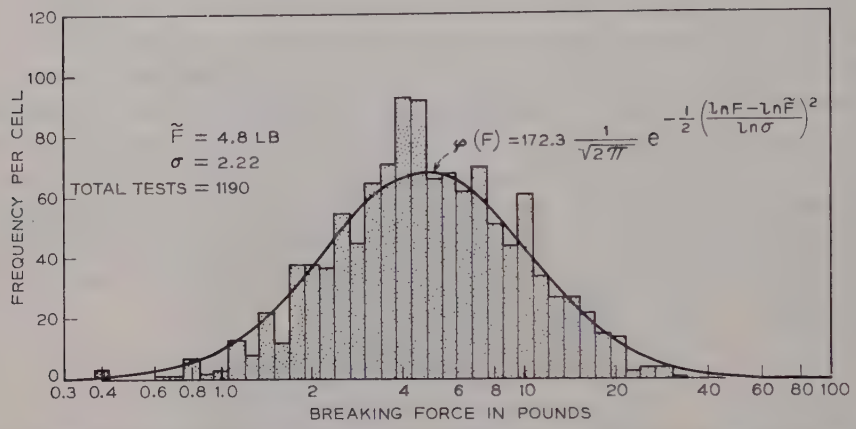

Fig. 8. A histogram showing the distribution of adhesive forces which were required to separate copper rods when the imposed load was 5 lb.

Since the median coefficient of adhesion is independent of applied load, the median adhesive load is proportional to the applied load (the proportionality constant is about unity)*. This implies that the real surface of contact is proportional to the adhesive load. To prove this, a large number of copper rods were adhered and their surfaces examined after they had been pulled apart. The real contact area was quite evident in the microscope, and this area divided into the adhesive load was reasonably constant (about 30,000 p.s.i.). This shows that the observed variability in γ is due to the variability of the area of contact, and that the adhesion had a uniformly high value over the region of contact. Since A_r is so variable, the fundamental relation $A_r = W/p$ is destroyed by shear strains imposed by this geometry.

No correlation between $\tilde{\gamma}$ and the angle of twist could be found. No correlation between $\tilde{\gamma}$ and the roughness of copper rods could be found (the roughness varied over a factor of 50). No correlation between $\tilde{\gamma}$ and the thickness of the oxide film on aluminum could be found. No correlation between the hardness of copper rods and $\tilde{\gamma}$ was found, although for the case of aluminum, very soft aluminum yielded a higher value of $\tilde{\gamma}$ than the corresponding harder varieties. In order to explain these results, a number of photomicrographs were made to examine the structure of the metals in the region next to the area of contact. This will be discussed in the next two sections.

* The dependence of γ upon structure and atomic weight will be treated in the second paper of this series.

THE DISRUPTION AND ABRASION OF OXIDE SURFACES BY SHEAR STRAINS

In this section photographic evidence is presented which shows the visible surface damage that results from the shearing strains induced in creating the degree of adhesion which is reported in the previous section. These photographs are in some ways similar to those obtained by others in the investigation of friction and wear. This similarity serves to emphasize that friction, wear, and adhesion are interrelated phenomena. The difference between the surface damage associated with adhesion and that of friction is largely that of scale: for a large value of γ, the damage covers a large fraction of the area of contact.

The photomicrographs show details revealed at a magnification of 100 $\times$. Color contrast was provided in the following manner. Aluminum rods were anodized in a black dye, providing a thick (0.001 in.) oxide which gave a surface layer with a color contrast to that of aluminum substrate. Thus, a white color indicated aluminum in which the original oxide had been completely stripped off, gray indicated oxide which was partially worn, and black indicated undamaged oxide.

Such an anodized aluminum rod was placed in the experimental apparatus described in the previous section, and a hardened steel rod was pushed against the end of the aluminum rod and then rotated. Very little adhesion occurred between the aluminum and steel, but the conditions of load and twist were the same as those producing adhesion described in the previous section.

Fig. 9 shows two typical photomicrographs which reveal very extensive and non-uniform wear. In some regions the black oxide has been completely ripped off, whereas in other regions the oxide has been worn down. Very little of the surface is undamaged. The oxide has been worn down by abrasive action as shown by the swirls and skid marks in the gray regions. Careful examination revealed no evidence of wear from the steel rod. Consequently, the oxide abrades itself. The mechanism which suggests itself is that the bits of oxide which are sheared off during initial stages of the shearing become abrasive particles which tear out more oxide in an accumulative way. This observation is in agreement with that of MOORE AND TEGART for copper[13].

The normal force used during the twisting action was not large—the force divided by the apparent area of contact was found to be about 3,000 p.s.i. (200 kg/cm^2). Microscopic examination showed no evidence of surface damage when a normal force was imposed without simultaneous shearing strains. Examination of several photomicrographs indicated that the surface damage was, on the average, just as great in the center of rotation as on the edge. In the next section some photographic evidence will be presented which indicates that the stripped oxide is buried beneath the surface. This method of the disposal of the debris reveals information on two different problems in adhesion. First, it is evident that burial of the stripped oxide below the surface allows the denuded metals to come into atomically close contact. The photographic evidence indicates that bonding probably occurs between the metals themselves, and not between the metals and an intermediate phase (such as the Beilby layer). Second, there is no evidence of melting phenomena or hot spots. It is difficult to

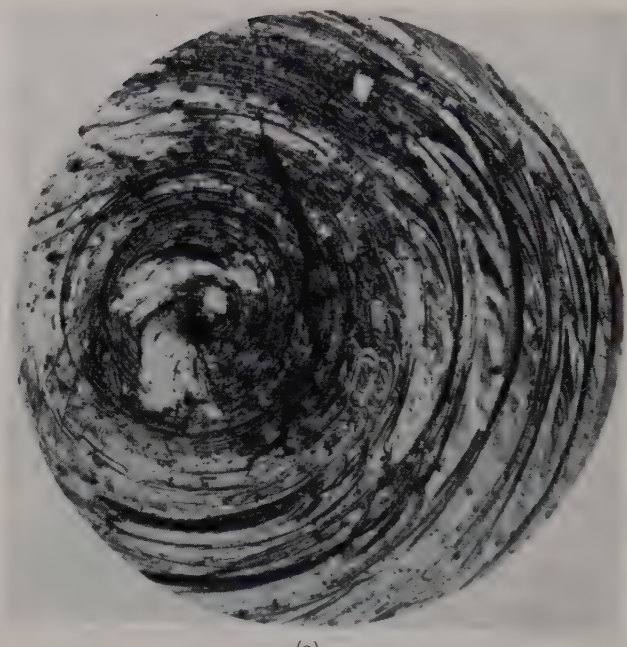

(a)

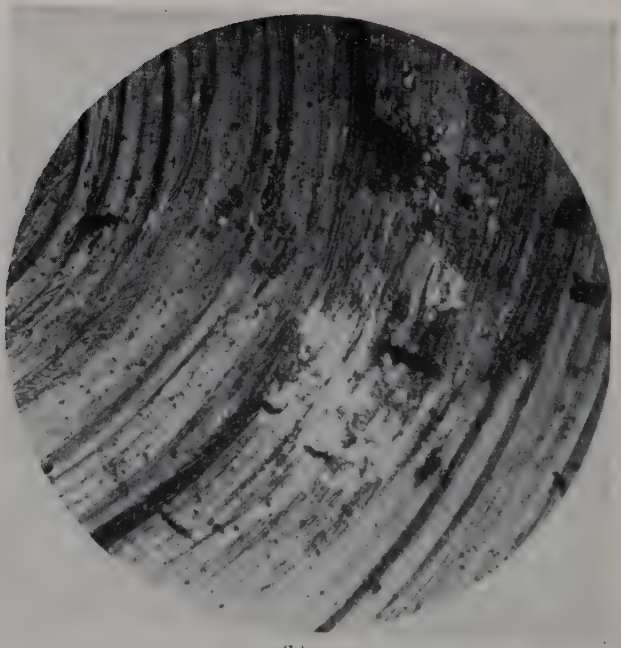

(b)

Fig. 9. The abrasion of dyed aluminum oxide film by shearing strains similar to those which produced the adhesive load shown in Fig. 8. The black regions show undamaged oxide, the white regions show oxide completely removed, and the gray regions are abraded oxide. Magnification 100 ×.

support the hypothesis that a significant temperature increase occurs at the surface owing to the scrubbing action. Using the heat conduction equation which was used successfully by BOWDEN AND TABOR[14] to account for the hot spots measured at high speeds, and using the measured normal force and the measured velocity of rotation, it turns out that the coefficient of friction would have to be unreasonably high (about 30) for the transient surface temperature to be equal to 100°C. It is, of course, impossible to know the temperature in the first few atomic layers during the shear strains. However, our experiments reveal no evidence which supports the idea that melting is essential to the oxide removal; and further, we found no experimental evidence to show the existence of a Beilby layer.

The evidence presented in Fig. 9 shows why $\tilde{\gamma}$ is independent of the thickness of the oxide for aluminum. The oxide removal occurs in an accumulative way; the total oxide layer, thick or thin, is removed shortly after the first few particles which are dislodged by the shearing strains.

THE INTERPENETRATION OF COPPER AND ALUMINUM BY SHEAR STRAINS

In this section, photomicrographs will be presented which show the cross section of the aluminum–copper interface after adhesion has occurred. Aluminum and copper were chosen because of the color contrast. Adhesion between $\frac{1}{4}$-in. rods was produced by the method already described. The rods were forcibly separated and a transverse section in a plane 45° to the axis of the rod was ground and polished using standard microscopic preparation techniques.

Aluminum was plucked off by the copper in large (0.001 in. thick) patches. The two photographs shown in Fig. 10 are typical of areas found at the common interface. The light color areas represent aluminum, while the mottled areas represent copper.

The size of the grains shown in the copper is related to the hardness. It is seen that the amount of work-hardening next to the interface and in a zone to a depth of about 0.001 in. is much greater than in the bulk of the copper. Since a harder material is stronger in tension, the copper is stronger near the interface than some distance below. The thickness of the plucked metal is always about the same as the depth of the work-hardened region. The amount of work-hardening produced at the surface by the shear strains was very large. This explains why the value of $\tilde{\gamma}$ was independent of the hardness of copper: the work-hardened surface obliterated any previous history of anneal in the copper.

In Fig. 10b, the roughness of the copper surface (hill to valley dimension) is over ten times the roughness of the original surface before adhesion. Consequently, the tangential strains which are necessary for adhesion produce very roughened surfaces. This shows why the value of $\tilde{\gamma}$ is independent of the roughness: the roughened surface obliterated any previous history of roughness in the copper.

The boundary between the aluminum and copper is sharp and clearly marked in Fig. 10b. However, photomicrographs show that interpenetration of two surfaces sometimes occurs; Fig. 11 shows one example of the interpenetration of copper and

aluminum. In this case the $\frac{1}{4}$-in. diameter was sheared under a normal force of 10 lb. at room temperature, and the adhesive load required to break them was 22 lb.

It is seen that large chunks of aluminum are found below the copper surface. For example, in Fig. 11a, the amount of aluminum driven below the surface is large

Fig. 10a

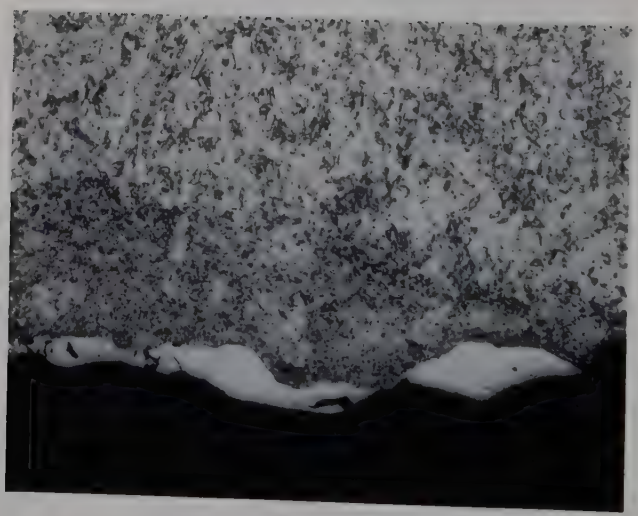

Fig. 10b

Fig. 10. A cross section through the common interface of copper and aluminum rods after adhesion has occurred and the rods have been separated. The white regions show the aluminum which was plucked by the copper as the adhesive load was measured. In Fig. 10a, the fudge-like regions near the aluminum may be aluminum oxide. In Fig. 10b, the fine grain structure of the copper near the surface indicates the work-hardening produced by shear strains. Magnification 150 ×.

considering the fact that this intermixing occurred at room temperature in less than 2 sec at an apparent pressure of less than 100 p.s.i. This intermixing is not diffusion, nor alloying.

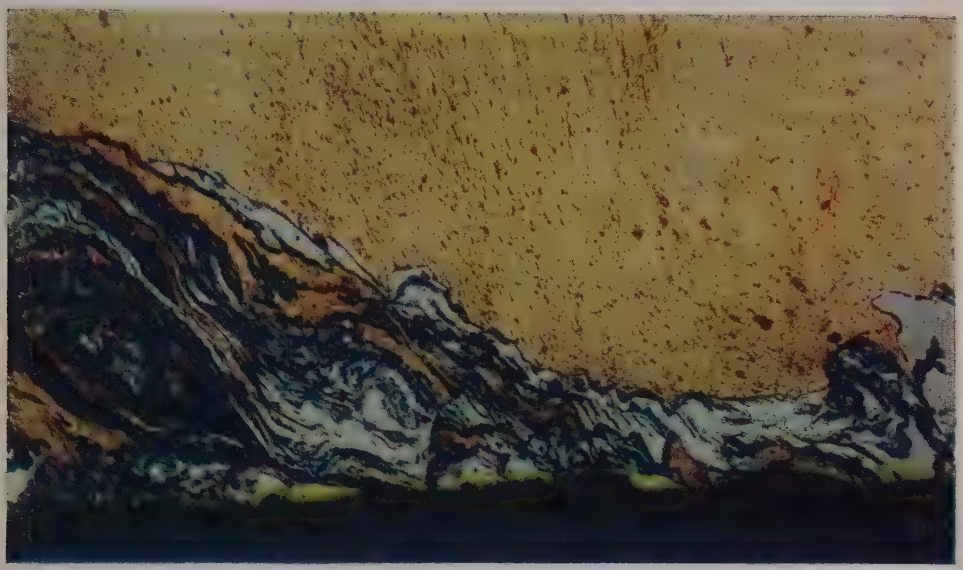

Fig. 11a

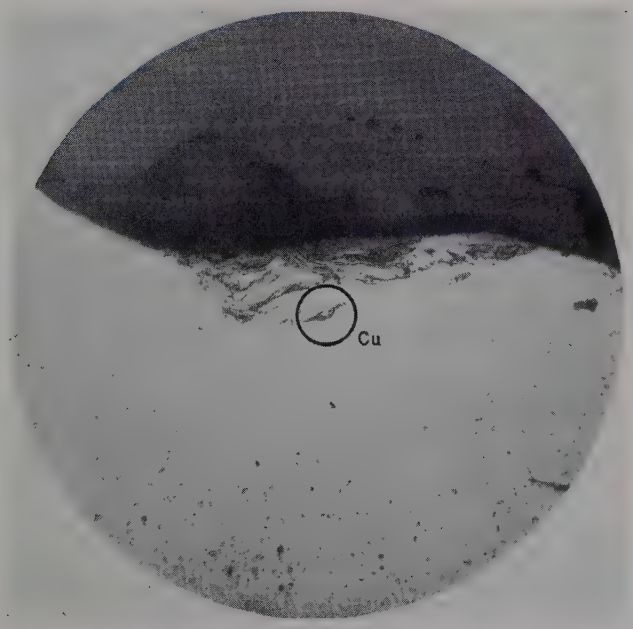

Fig. 11b

Fig. 11. Photomicrographs showing the interpenetration of copper and aluminum. Fig. 11a shows aluminum completely surrounded by copper at depths of about $\frac{1}{2}$ mm. Fig. 11b shows copper buried below the surface of aluminum. *Photography by F. G. Foster*

In view of this evidence of interpenetration of the two metals, the phenomenon of adhesion itself is not surprising. What is surprising is that the shearing strains resulting from simple twisting under load produce mechanical intermixing to such an extent.

In some regions the transverse section of the common interface looks like Fig. 10b, in others like Fig. 11a. The regions similar to Fig. 10b outnumber those in Fig. 11a, but our sampling indicates that regions like Fig. 11a are not rare.

In Fig. 10a, there are some blackish regions with a fudge-like appearance. The most careful attempts to resolve these regions so as to distinguish between the copper color and the aluminum color have failed. This region appears to be composed of tiny black-colored particles. These fudge-like regions are probably the aluminum oxide which has been stripped off the surface and buried by the action of the shear stresses.

Attempts to find copper within the aluminum rod showed that this type of penetration is much rarer than the penetration of aluminum in copper. Fig. 11b shows a region where copper has penetrated aluminum. In this case, the fudge-like blackish regions were clearly identified as copper oxide, because copper oxide turns a glassy ruby red color under polarized light. What is significant in this photograph is that the copper oxide debris has been buried in the aluminum rod in regions that are completely surrounded by the aluminum. The clear-cut identification of the fudge-like material in Fig. 11b as copper oxide lends credence to the conclusion that the fudge-like material in Fig. 10a is aluminum oxide.

It is concluded from Figs. 10 and 11 that metallic oxides and films, after being stripped off, are then buried at great depths—depths of the order of microns—by the action of the shearing strains. It is concluded that the penetration of the oxides is sometimes accompanied by an intermingling of the basic metals. The fraction of the surface area through which the oxides interpenetrate is small compared to the amount of remaining surface area, which is merely denuded. It is concluded that the common interface, such as seen in Fig. 10a, is largely devoid of surface barriers. The oxides formerly present in this region have been stripped off, swept away, and buried in another region, such as shown in Figs. 10a and 11a and b.

CONCLUSION

The experimental results of this paper tend to confirm the concept of adhesion and friction advocated by the Cambridge school. It is shown that surface shear strains are necessary for adhesion to occur. It is shown for the metals examined that surface shear strains do the following:

(1) Strip off the surface barriers.
(2) Roughen the surfaces.
(3) Produce a work-hardened zone just below the surface.
(4) Cause the denuded metals to come into atomically close contact.
(5) Bury the surface barrier debris below the surface at great depths.
(6) Sometimes cause interpenetration of the two metals.

It is shown that vigorous surface shear strains often cause very high adhesion — comparable to that produced between denuded metals in very high vacuum. It is shown that the laws of adhesion are similar to Amontons' laws of friction. The results of this section confirm the concept that dry friction and wear result from adhesion.

Part II of this series will deal with the correlation of the coefficient of adhesion with other mechanical properties for a number of different metals.

ACKNOWLEDGEMENT

The author wishes to acknowledge the measurements of Mr. PETER ANDREATCH and the helpful discussions of Dr. W. P. MASON, Dr. J. S. COURTNEY-PRATT, and Mr. HOWARD CHRISTENSEN.

REFERENCES

1 E. F. BOWDEN AND D. TABOR, *The Friction and Lubrication of Solids*, Oxford University Press, London, 1954.
2 O. L. ANDERSON, H. CHRISTENSEN, AND P. ANDREATCH, *J. Appl. Phys., 28* (1957) 923.
3 F. R. BOWDEN AND G. W. ROWE, *Proc. Roy. Soc. (London), A 223* (1956) 429.
4 J. S. COURTNEY-PRATT AND E. EISNER, *Proc. Roy. Soc. (London), A 238* (1957) 529.
5 P. ANDREATCH AND O. L. ANDERSON, *Rev. Sci. Instr., 30* (1959) 498.
6 N. A. DE BRUYNE, *Nature, 180* (1957) 262.
7 E. EISNER, *Ph. D. Thesis*, Cambridge University, 1954.
8 H. O'NEILL, *The Hardness of Metals and Its Measurement*, Chapman and Hall, Ltd., London, 1934, p. 49.
9 D. TABOR, *The Hardness of Metals*, Oxford University Press, London, 1951.
10 R. HOLM, *Electric Contacts Handbook*, 3rd edn., Springer-Verlag, Berlin, 1958, p. 121.
11 M. COOKE AND E. C. LARKE, *J. Inst. Metals, 71* (1945) 377.
12 O. L. ANDERSON, *J. Appl. Phys., 30* (1959) 593.
13 A. J. W. MOORE AND W. J. MCG. TEGART, *Australian J. Sci. Research, 4* (1951) 181.
14 F. P. BOWDEN AND D. TABOR, *Friction and Lubrication*, Methuen & Co. Ltd., London and John Wiley and Sons, Inc., New York, 1956.

Received for review November 2, 1959
Accepted January 10, 1960

Wear, 3 (1960) 253–273

SOME OBSERVATIONS ON THE FRICTIONAL BEHAVIOUR OF BORON NITRIDE AND OF GRAPHITE

G. W. ROWE

Tube Investments Research Laboratories, Hinxton Hall, Cambridge (Great Britain)

SUMMARY

This paper describes experiments with layer-lattice crystals in pure chemical form. The specimens are cleaned by outgassing at high temperatures (1,000–1,200°C) *in vacuo* ($5 \cdot 10^{-4}$ microns) and purified gases and vapours are admitted. It is found that the friction of outgassed graphite is reduced from about $\mu = 0.45$ to about $\mu = 0.15$ by many different gases. The friction of outgassed boron nitride is similarly reduced from about $\mu = 0.5$ to about $\mu = 0.18$ by organic vapours but not by oxygen or nitrogen. Compounds such as MoS_2 and $CrCl_2$ show low friction in the absence of vapours.

The friction of outgassed graphite and boron nitride falls markedly as the specimen temperature is increased, but that of MoS_2 and $CrCl_3$ is almost unchanged at temperatures below those at which the films are decomposed.

It is suggested that the low friction exhibited by these materials is attributable to their common layer-lattice structure, with weak interlayer bonding. The interlayer bonding in graphite and boron nitride is initially stronger than in the other compounds, but can be reduced by increasing the temperature or admitting vapours.

ZUSAMMENFASSUNG

EINIGE BEOBACHTUNGEN ÜBER DAS REIBUNGSVERHALTEN VON BORNITRID UND GRAPHIT

Versuche mit Schichtgitterkristallen in chemisch reinem Zustand werden beschrieben. Die Proben wurden durch entgasen bei hoher Temperatur in Vakuum gereinigt und dann an gereinigte Gase und Dämpfe ausgesetzt. Es zeigt sich dass der Reibungskoeffizient von entgastem Graphit durch viele, verschiedenartige Gase von $\mu = 0.45$ auf etwa $\mu = 0.15$ erniedrigt wird. Auch die Reibung von entgastem Bornitrid nimmt ähnlich von $\mu = 0.5$ auf etwa $\mu = 0.18$ ab und zwar unter dem Einfluss organischer Dämpfe jedoch nicht durch Sauerstoff oder Stickstoff. Verbindungen wie etwa MoS_2 und $CrCl_2$ zeigen auch bei Abwesenheit von Dämpfen niedrige Reibung.

Die Reibung des entgasten Graphits und des Bornitrides nimmt wesentlich ab mit zunehmender Temperatur der Probe, dagegen wird die von MoS_2 und $CrCl_2$ unterhalb der Zersetzungstemperatur des Films kaum durch die Temperatur beeinflusst.

Es wird vorgeschlagen, dass die niedrige Reibung dieser Stoffe durch die ihnen gemeinsame Schichtgitterstruktur, mit schwacher Bindung zwischen den Schichten, verursacht wird. Diese Zwischenschichtbindung ist in Graphit und Bornitrid anfänglich stärker als in den übrigen Stoffen, kann jedoch durch Temperaturerhöhung oder durch die Wirkung von Dämpfen erniedrigt werden.

INTRODUCTION

The lattice structure of boron nitride closely resembles that of graphite. This has led to the supposition that, like graphite, boron nitride should show low friction. There have, however, been varying reports of the efficiency of boron nitride as a lubricant. Most of the work reported has been complicated by some special feature; in particular the method of bonding the boron nitride to a substrate is important, and oxidation has been thought to play a significant part.

The present note describes simple experiments with graphite and boron nitride under controlled conditions using a high-vacuum apparatus, and also for comparison some experiments with a commercial form of boron nitride in a bonding agent.

EXPERIMENTAL

The working parts of the high-vacuum apparatus are shown in Fig. 1. This was developed from an earlier design[1] and is made entirely of fused silica. A small slider A is held on a cantilever extending from a carriage C running on sapphire balls. The lower slider B, which has a flat surface, is mounted by parallel-motion silica springs on the static framework. An iron bar D, encased in silica, is carried backwards and forwards by an electromagnet surrounding the vacuum envelope. The slider A thus reciprocates slowly, on B. The deflection of the silica springs is optically magnified and recorded to measure the friction. In this apparatus loads up to 15 g can be applied by a bifilar silica spring in the upper cantilever. A silicone oil vapour pump with two liquid nitrogen traps provides a working vacuum at about $5 \cdot 10^{-4}$ microns ($5 \cdot 10^{7}$ mm Hg).

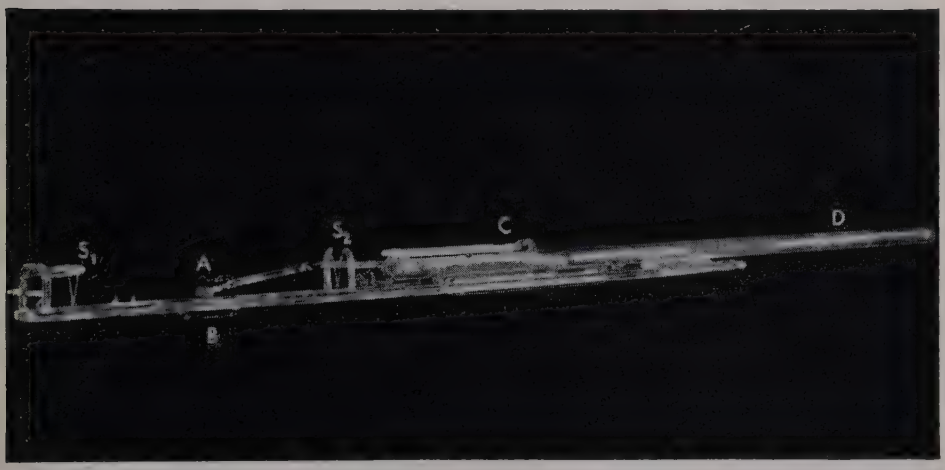

Fig. 1. A photograph of the silica friction mechanism, which is contained in a silica tube evacuated to about 10^{-7} mm Hg. A reciprocating magnetic force applied to the iron bar D moves the specimen A slowly over the lower specimen B, which is restrained by two silica springs S. The force of friction is recorded by the deflection of these springs, shown by a thin pointer whose image is projected onto a moving-paper camera.

Specimens such as graphite which are electrically conducting can be heated directly by an induction furnace, while non-conducting specimens such as boron nitride can be heated by surrounding them with a tantalum susceptor. The vapour pressure of this metal is sufficiently low at the temperatures used that, in the outgassed state, it introduces no contamination.

The temperatures recorded are those measured with a disappearing-filament pyrometer. No correction has been applied for emissivity since this is not known

for either boron or boron nitride. If we suppose the emissivity of BN to be the same as that of thoria (0.6) the actual temperatures would be about 40°C higher than the quoted value at 1,000°C. The correction for boron is likely to be about 12° at 1,000°C.

The apparatus used in air is generally similar to that designed by ELDREDGE AND TABOR[2], incorporating some of the modifications made by DEACON AND GOODMAN[3]. The upper slider, in the form of a hemisphere 4 mm in radius, is mounted by parallel-motion springs on a hinged arm. Loads up to 4 kg are applied by weights. The lower specimen is a flat block traversed beneath the slider by a lathe saddle. The friction force deflects the springs, whose movement is mechanically linked to a pen recording on moving paper. A furnace with silicon carbide elements heats the sliders to 1,000°C. A small subsidiary heater with Kanthal windings surrounding the upper slider equalises the temperatures.

RESULTS

Boron nitride

The effect of thorough cleaning on the friction of boron

The susceptor was first outgassed and the apparatus was then assembled with pure crystalline boron specimens. In high vacuum the friction was $\mu = 0.4$. They were heated to various temperatures and then cooled to room temperature in vacuum. The friction rose to $\mu = 0.9$ after heating to 660°C and was unchanged by further outgassing at temperatures up to 1,000°C. The friction rose slightly as the temperature of the specimens was increased, reaching $\mu = 1.1$ at 1,000°C.

The effect of nitrogen and ammonia on the friction of boron

Pure dry nitrogen was admitted to the vacuum tank. The nitrogen had been freed as far as possible from oxygen by conventional methods. It is of course not possible to remove all traces, but under the particular circumstances of the experiment some further purification may occur in the vacuum chamber, since the hot metal susceptor is a good getter for oxygen.

The friction measured at room temperature after the specimens had been heated in nitrogen is shown in Fig. 2. Similar results obtained with dry ammonia vapour are also given in the figure. It will be seen that both nitrogen and ammonia show some effect immediately on the cold specimens, ammonia having slightly greater influence. To form a thicker film some other specimens were heated in a separate apparatus for five hours at 1,200°C in a stream of pure nitrogen flowing at 4 l/min. These formed white crystals at the edges, and the flat surface was covered by a thin film showing interference colours. Examination by electron diffraction[4] (GLOSSOP AND PASHLEY) showed well-defined patterns from both. The evidence supported the identification of the surface film as boron nitride with the usual hexagonal structure. It was not, however, possible to distinguish unambiguously between boron nitride and graphite although the intensity of the (101) reflection relative to the (100) accorded better with boron nitride than with graphite. Furthermore, the crystals were obviously white and there is no reason to suppose that carbon was present. A further important

result from the electron diffraction study was that no boron oxide could be detected, though again it cannot be stated with certainty that no oxide in any form was present. It may reasonably be concluded that the only crystalline material present was boron nitride, and there is no real reason to suspect the presence of other materials.

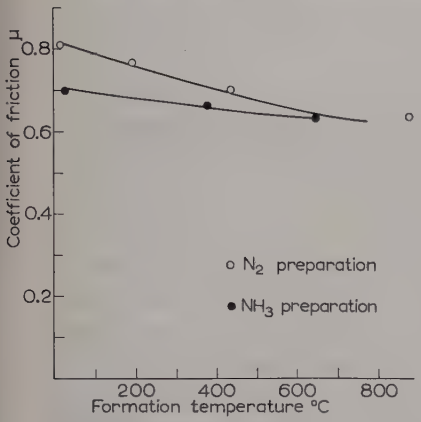

Fig. 2. Friction at 20°C between boron sliders previously heated in N_2 or NH_3 to form boron nitride.

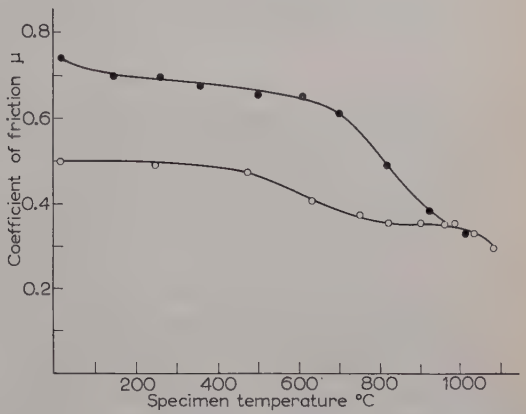

Fig. 3. The influence of temperature on the friction of outgassed boron nitride. ● Boron nitride coating on boron sliders; ○ Sintered boron nitride sliders.

The friction of boron sliders coated with boron nitride

Specimens were prepared by heating boron crystals in nitrogen at 1,200°C, as above, and then rapidly transferring them to the vacuum apparatus. The friction measured *in vacuo* was found to be $\mu = 0.7$, comparable with that of the clean specimens on which the film had been formed in the vacuum apparatus itself. They were outgassed by heating to 1,000°C but this did not materially influence the room-temperature friction, suggesting that little contamination had occurred while the specimens were being transferred.

The friction was then measured as a function of specimen temperature. The results shown in Fig. 3 were found to be reproducible and reversible, and the film was found to be very durable.

Neither oxygen nor nitrogen had an appreciable influence on the friction of the coated sliders at room temperature.

The friction of boron sliders coated with boron oxide

A visible oxide coating was formed on some other boron specimens by heating them in a stream of oxygen for 17 h at 350–400°C. The friction at room temperature was then found to be $\mu = 0.7$, comparable with that of the nitride film. However, when the specimen temperature was increased the friction rose fairly steadily to $\mu = 1.2$ at 900°C. After this treatment the friction remained at its high value and was sensibly unaltered by changes in specimen temperature between 20° and 900°C.

The friction of blocks of sintered boron nitride in vacuo

Two blocks of sintered boron nitride were obtained by courtesy of the Carborundum Company. These were carefully abraded to provide fresh surfaces and were then washed. (This should remove any oxide. Specimens installed with no pretreatment showed appreciably higher friction.) The washed sliders were then installed in the silica vacuum apparatus. Their friction was increased from 0.1 to 0.52 by outgassing at 1,060°C.

The specimens were then reheated *in vacuo* and the friction was measured as a function of specimen temperature (Fig. 3). Again the fall in friction with increasing temperature was found to be reversible, but the highest friction was less than that found with the thin coating.

The influence of vapours on the friction of sintered boron nitride

A small dosing vessel attached to the vacuum line allowed small quantities of gas to be admitted to the outgassed specimens. Measurements of the friction were made at intervals after each admission of gas. In general the effect was, however, found to be sensibly complete in less than one minute. Fig. 4 shows the results for dry atmospheric gases, water vapour, and three widely differing organic vapours. Each point in Fig. 4 represents ten minutes exposure to the gas pressure. After each complete run in a given vapour the system was evacuated and the specimens were outgassed. The reproducibility of the friction in the outgassed state shows that no permanent changes occurred, so the order of admission of the vapours was unimportant.

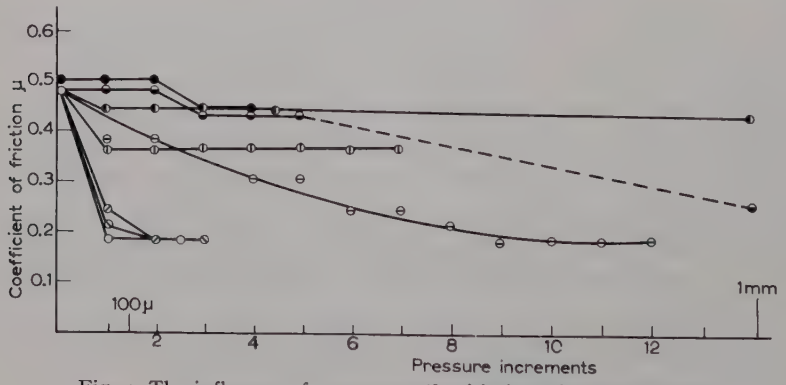

Fig. 4. The influence of vapour on the friction of boron nitride.

⊖ water vapour ◐ nitrogen ○ heptane
● oxygen ◒ dry air ⊘ ethyl alcohol
◑ hydrogen ⊘ caproic acid

The water vapour was taken from a distilled water doser, which was repeatedly frozen in liquid nitrogen and thawed in vacuum to remove gases. When the water vapour was finally pumped away from the specimens the friction rose to $\mu = 0.3$.

The caproic acid vapour was similarly freed from gases. The friction was unaffected

by pumping away the vapour. Ethyl alcohol was also chemisorbed and indeed the adsorbed product withstood heating at 800°C *in vacuo*.

The friction in heptane also remained low when the vapour was pumped away ($\mu = 0.18$ at 200 μ pressure and $\mu = 0.21$ at 10^{-2} μ).

When exposed to the laboratory atmosphere the friction was $\mu = 0.18$.

Graphite

The effect of thorough cleaning on the friction of graphite

The graphite specimens were in the form of 3 mm rods, spectrographically standardised. The room-temperature friction was increased to $\mu = 0.45$ after the specimens had been outgassed at 1,100°C *in vacuo*. Fig. 5 shows the friction of the outgassed specimens at various temperatures. To extend the range of temperature, Fig. 5 includes some results from another apparatus[5].

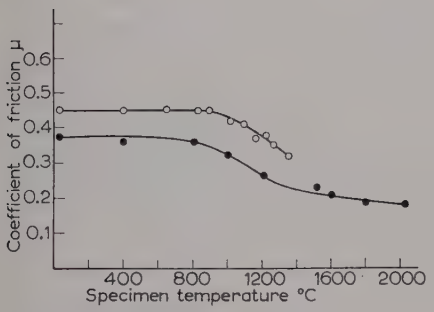

Fig. 5. The infuence of temperature on the friction of outgassed graphite. ○ spectrographically standardised graphite; ● Acheson AGR graphite

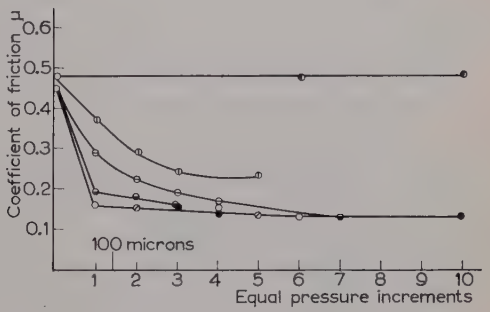

Fig. 6. The influence of vapours on the friction of spectrographically standardized graphite.
◐ nitrogen ● oxygen ○ heptane
◑ hydrogen ⊖ water vapour
⊘ ethyl alcohol ◒ dry air

The influence of vapours on the friction of graphite

Vapours were admitted in small quantities in exactly the same way as for the boron nitride specimens. It was found that all the gases except nitrogen reduced the friction considerably (Fig. 6). However, the results depend upon the type of graphite used. It was found that the friction of spectrographically standardised graphite is much more sensitive to vapours than that of common grades. Moreover, if the outgassing procedure is repeated many times the denuded graphite becomes increasingly difficult to retain in its initial state, although the initial friction itself remains remarkably reproducible. This implies that the residual impurities, whatever they may be, do not in themselves greatly influence the friction but do prevent or hinder adsorption of friction-reducing vapours. With the high purity graphite the reduction in friction was almost entirely irreversible after long exposure to the organic vapours.

Friction of boron nitride in air

Since in most practical applications the boron nitride or graphite must be used in air, it is interesting to consider the behaviour under atmospheric conditions.

Fig 7 shows the friction of a boron nitride slider made from sintered material, on stainless steel. The friction remains low, at least up to 700°C. Fig. 7 also shows the friction of stainless steel sliders coated with a commercial graphite suspension (in water), a commercial graphite suspension in silicone oil, and the latter suspension with addition of 5% boron nitride. All show low friction up to high temperatures, but the boron nitride addition extends the temperature range.

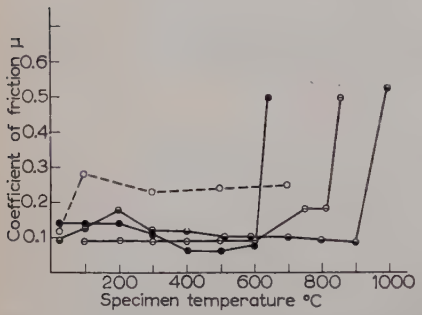

Fig. 7. The friction between stainless steel sliders in air at high temperatures, with different coatings.
● graphite suspension in water (a)
⊖ graphite suspension in silicone fluid (b)
◒ suspension (b) with 5% BN powder (c)
○ sintered BN sliding on steel.

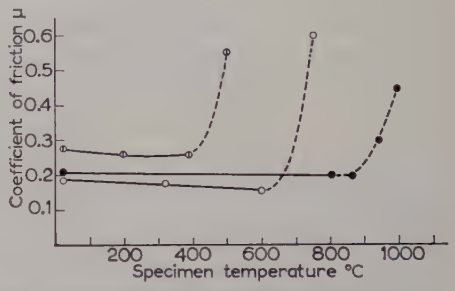

Fig. 8. The friction of metallic sliders coated with layer-lattice compound formed *in situ*. ⓘ TiI_2 coating on Ti; ○ $CrCl_3$ coating on Cr; ● MoS_2 coating on Mo.

Friction of other lamellar compounds

In these experiments, more fully discussed earlier[7], sliders of spectrographically standardised metal were outgassed in the high-vacuum apparatus. Purified dry gas was then admitted and the specimens were heated to form coatings. Fig. 8 shows the friction between pairs of identical coated sliders as a function of temperature. These coatings show a low friction at room temperature, which is not dependent upon the presence of vapours. On the contrary, TiI_2 for example, is rapidly hydrolysed by water vapour and then shows a high friction.

DISCUSSION

The friction of outgassed graphite and boron nitride

Both graphite and boron nitride show a high friction in the outgassed state. Boron nitride formed on a boron surface shows $\mu = 0.7$, and the sintered material $\mu = 0.5$. Spectrographically standardised graphite shows $\mu = 0.45$, and the commercially pure AGR material $\mu = 0.4$. These values are higher than those found under similar conditions for other layer-lattice compounds such as TiI_2 ($\mu = 0.25$) $CrCl_3$ ($\mu = 0.19$)

and MoS_2 ($\mu = 0.19$). They are in fact closer to the value found for the more isotropic carbon bonding in diamond ($\mu = 0.4$–0.5 at this load).

The low friction of graphite normally recorded in air was originally attributed to ease of shear of the lamellar crystal lattice. However, it is found that graphite does not shear readily; mechanical tests show tensile failure unless a high compression is superimposed. The bonding in the carbon lattice is such that each C atom operates three valence electrons. The C atom possesses two *s* and two *p* electrons. The three σ bonds thus require both the *p* and one of the *s* electrons so the latter pair become uncoupled. The odd one is available as a π electron, which is responsible for the highly directional electrical conductivity of graphite. It can take part in intercalation reactions[6], but in the outgassed material provides additional bonding between the layers. Under these conditions there is thus a considerable resistance to shear, as was pointed out by FINCH[8], and the cleavage strength will also be higher. In boron nitride both types of atom possess the co-ordination number 3 and each operates three valence electrons paired off in σ bonds. The boron atoms utilise completely their two *s* and one *p* electrons and the nitrogen atoms contribute only their three *p* electrons. The lone electron pair of the *s* subgroup remains, and, as the absence of colour shows, is relatively firmly bound. Their only action is to reinforce the Van der Waals forces between the layers. Here again there is fairly strong resistance to shear over the layer plane.

The structure of boron nitride is essentially the same as that of graphite and the same number of electrons are used, but there is this characteristic difference in the bonding, which we shall see leads to a difference in the influence of adsorbed vapours. Though the structures are clearly anisotropic, the simple picture of shearing over lamellae leading to low friction is not applicable to the outgassed conditions.

The bonding in layer-lattice materials of the PbI_2 type is not easy to envisage on this electrostatic basis. Since the substitution of the dipole OH in a PbI_2 lattice gives the same structure as the original iodide ion, it has been suggested that the bonding arises from unilateral polarisation of the anion. Each Pb ion, with co-ordination number 6, is surrounded by six I ions with co-ordination number 3, but not all are geometrically equivalent, each I being bounded on one side by only three Pb ions. The bonding within each layer is thus strong while the bonding between layers is almost entirely Van der Waals. Criticisms of this simplified explanation have been made but it will suffice for the present purpose. Thus we should expect the interlayer strength to be lower for this type of lattice than for one with the reinforced Van der Waals bonds in outgassed graphite or boron nitride. The friction is found to be lower.

Temperature dependence of the friction of outgassed materials

As the temperature of the specimens is increased, the strength of the bonds will decrease. In a homogeneous material this does not usually cause a marked change in the friction since in general the shear strength and hardness vary together. Bulk graphite is a reasonably uniform polycrystalline material and it has been shown that the tensile and shear strength are not greatly influenced by temperature[5]. Earlier

reports[9] that the strength of graphite increases with temperature are probably attributable to removal of contamination, which markedly influences the strength. At the surface, the material can no longer be regarded as homogeneous and in fact it has been shown that during lubricated sliding the surface becomes highly oriented[10].

This offers a possible explanation of the low friction of outgassed graphite at high temperatures. The bond weakening due to thermal agitation allows the surface crystals to become favourably orientated and the weakening of the π bond allows easier shear or cleavage on the layer plane. The σ bonding within the layer remains relatively strong at the temperatures we are considering, 1,000–1,800°C; at about 2,200°C the π bonding is so weakened that the graphite evaporates in high vacuum. At the surface there is a marked anisotropy of bond strengths which can be so ordered by repeated sliding that low friction results.

There is at present no information on the strength of outgassed boron nitride. The friction of a boron nitride film on a boron substrate shows the same sort of temperature dependence as the friction of the bulk solid, which supports the suggestion that it is the change in the surface layers which reduces the friction. The substrate can remain unchanged.

The actual value of the coefficient of friction of outgassed graphite, and the temperature range over which it falls, depend upon the type and purity of the material; and also presumably on the binder, when present. However, all graphites and boron nitride appear to show a reversible fall in friction as the temperature is raised. It is important to recognise that this is a property common to these two materials of the same structure, not a coincidental correlation between the bond weakening in graphite and an oxidation behaviour of boron nitride. Fig. 3 shows that the friction of the sintered BN material and of the specially-prepared films begins to fall at about 500°C, lower than that at which pure graphite begins to fall. DEACON AND GOODMAN[3] also record a reversible drop in friction in their experiments with boron nitride. Their conditions were, however, different; the boron nitride was used as a powder rubbed on to platinum bars, and sliding took place in air. Thus the coating was subject to oxidation and indeed a sharp increase was found at about 900°C, attributed to the formation of boric oxide. This led them to postulate that the decrease in friction at 500°C was due to a weakening of intercrystallite bonds which resulted from melting of boric oxide. This could occur, they supposed, if boric oxide was present as a surface film surrounding the crystallites. However, when it was present in larger quantities, as mentioned above, a large irreversible rise in friction was found. Their theory thus required the presence of a critical amount of oxide in a particular distribution.

In the high vacuum experiments careful precautions were taken to exclude oxygen. While this can never be completely certain, there is no prior reason to consider oxygen as the major factor in the frictional behaviour. As shown in Fig. 4, low-pressure oxygen has no detectable influence on the friction of cold outgassed boron nitride. The friction of sliders deliberately coated with oxide is high at room temperature and increases as the temperature is raised. Also the specimens were initially outgassed at 1,100°C–1,200°C, which should remove any oxide present (the dissociation pressure[11]

is 9.4 mm at 1,200°C). If, however, we suppose for the moment that oxide does form and subsequently melt at 450°C we should expect it to convert to the glassy amorphous form on subsequent cooling[12]. The frictional behaviour would therefore not be reversible. DEACON AND GOODMAN did in fact find an irreversible behaviour of this type when definite oxidation occurred (on heating above 900°C) and, moreover, they state that the irreversible change became more pronounced after repeated high temperature oxidation. Only when the specimens were heated at temperatures well below that at which appreciable oxidation occurred could the reversible behaviour be found. Electron diffraction then showed no change in the specimen.

This reversible fall in friction above 500°C in the absence of deliberate oxidation accords well with the present high-vacuum results. The present experiments show, however, that the reduction in friction continues to temperatures well in excess of 1,000°C, limited only by the apparatus, and the friction does not increase between 500°C and 900°C as happens in the presence of oxygen.

It seems reasonable to conclude that the results recorded in Figs. 3 and 6 really refer to graphite and boron nitride themselves, and not to fortuitous quantities of impurity. This suggests that the high initial friction and the reduction in friction at high temperatures are properties of the common crystal structure.

There is a sharp contrast in the behaviour of lamellar solids of the MoS_2 type. These all show a low friction at room temperature[7], which is sensibly constant, perhaps falling slightly, as the temperature is increased. Eventually a temperature is reached at which the compounds decompose or volatilise and then of course the friction rises very rapidly on further heating. An attempt has been made to explain the low friction of MoS_2 in terms of an oxide coating on the crystallites[3]. This again involves the special postulate of oxide impurity in the molybdenum specimens or the sulphide gas used to form the coating. Various preparations of both in an attempt to remove oxygen and water all gave essentially the same results, while deliberate admission of water vapour[13] is known to destroy the lubricating properties of MoS_2. In the presence of oxygen MoS_2 oxidises rapidly at high temperatures and the low friction is again lost. Another theory attributes the low friction at high speeds to an amorphous layer of sulphur[14]. The high volatility of sulphur makes it impossible to account for the low friction of MoS_2 at high temperature in vacuum on this theory. The same arguments apply to the postulate of amorphous sulphur as the low-friction agent in WS_2[15]. Clearly, the low friction of $CrCl_3$, for example, cannot be accounted for in this way.

It seems more likely that the close resemblance between such diverse materials as $CrCl_3$, TiI_2 and WS_2 depends on the feature all share in common: their lattice structure. The larger spacing between the layers in MoS_2($C_0 = 3.66$ a.u.) compared with that of graphite (3.35 a.u.) and BN (3.33 a.u.) reflects the weaker, Van der Waals, bonding and associated lower friction.

Influence of vapours on the friction of graphite and boron nitride

The high friction of graphite can be reduced by many vapours. BOWDEN AND

YOUNG[1] found that both oxygen and water vapour caused a reversible reduction in friction when present at pressures greater than about 100 μ. GOODMAN AND ROWE[10] confirmed this behaviour but found that there was also an irreversible component; when oxygen or water vapour was admitted to the surfaces the friction fell, but it could not be restored to its initial high value simply by pumping away the gas.

The present experiments show that all the vapours examined, except nitrogen and hydrogen, reduced the friction of graphite at room temperature to a value close to that of outgassed graphite at very high temperatures. This agrees well with the results of SAVAGE[19]. RÜDORFF[6] has shown that many elements can be chemisorbed in graphite by reaction with the π electron. This weakens the interlayer bond and is evidenced by an increase in the layer spacing from 3.4 a.u. to 6.1 a.u. with oxygen and even 10.4 with bromine. Bromine can eventually so weaken the lattice that the whole specimen will spontaneously crumble. Bromine gives the lowest friction.

Now boron nitride does not form these intercalation compounds with inorganic gases[16]. It does eventually oxidise at high temperatures but then the B atom combines with oxygen preferentially and N oxides are not formed. On the other hand N is a powerful donor atom in forming organic complexes by disruption of the *s* electron pair, which otherwise increases the interlayer bond[17]. Hydrogen also may form $B_3N_3H_6$ in this way[18]. It will be seen from Fig. 4 that the inorganic gases have little influence on the friction of boron nitride, while all the organic vapours produce a large fall in friction, which is irreversible. When the reinforcement of the Van der Waals bond is reduced by reaction with the π electron in graphite or by disruption of the *s* electron pair in boron nitride, it appears that the friction is reduced to a value comparable with that of layer-lattice compounds such as MoS_2 and $CrCl_3$ *in vacuo*.

The friction of these materials with initially weak interlayer bonding may, conversely, be increased by the presence of vapours. HALTNER AND OLIVER[13] for example find that water vapour, and even toluene and heptane, are chemisorbed on MoS_2 and all increase the friction.

CONCLUSION

The general similarity between the temperature dependence of the friction of graphite and boron nitride and their difference in this respect from MoS_2, $CrCl_3$, and TiI_2 suggests that the greater interlayer bonding in graphite and boron nitride is important. This is further borne out by the observation that compounds like MoS_2 with Van der Waals interlayer bonding all show low friction when formed under vacuum conditions and higher friction in the presence of chemical vapours, while the high friction of outgassed graphite can be reduced by almost any vapours which decrease the strength of the interlayer π bonding. Boron nitride does not form intercalation products like those of graphite, and oxygen has no influence on its friction. Organic compounds do, however, form complexes with *s* electrons of the N atom of boron nitride which otherwise increase the interlayer bonding. Vapours of these compounds reduce the friction of outgassed boron nitride.

These experimental results support a reversion to the earlier hypothesis that the friction of lamellar solids is directly a function of their lattice structure rather than dependent on special circumstances of oxidation or decomposition.

ACKNOWLEDGEMENTS

I should like to thank the Chairman of Tube Investments Ltd. for permission to publish these results, and Mr. D. J. BALDWIN for performing the experiments.

REFERENCES

1 F. P. BOWDEN AND J. E. YOUNG, *Proc. Roy. Soc. (London), A, 208* (1951) 444.
2 K. R. ELDREDGE AND D. TABOR, *Proc. Roy. Soc. (London) A, 229* (1955) 181.
3 R. F. DEACON AND J. F. GOODMAN, *Proc. Roy. Soc. (London), A, 243* (1958) 464.
4 A. B. GLOSSOP AND D. W. PASHLEY, *Tube Investments Research Lab. Tech. Memo, 33* (1957).
5 G. W. ROWE, *Tube Investments Research Lab. Rept., No. 62* (1958).
6 W. RÜDORFF, *Z. anorg. Chem., 245* (1940) 121.
7 G. W. ROWE, *Instn. Mech. Eng. Lubrication and Wear Conf., London, 1957*, (paper 5).
8 G. I. FINCH, *Proc. Phys. Soc. (London), A, 63* (1950) 785.
9 C. MALMSTRON, R. KEEN AND L. GREEN, *J. Appl. Phys., 22* (1951) 593.
10 J. F. GOODMAN AND G. W. ROWE, *Chem. Soc. Symposium "Chemisorption", 1956.*
11 R. E. SLADE AND G. I. HIGSON, *Brit. Assoc. Advance. Sci. Rept.*, (1913) 451.
12 F. C. KRACEK, G. W. MOREY AND H. E. MERWIN, *Am. J. Sci., A35* (1938) 143.
13 A. G. HALTNER AND C. S. OLIVER, *Gen. Elec. Rep. 58-RL-2018* (1958).
14 V. R. JOHNSON AND G. W. VAUGHN, *J. Appl. Phys., 27* (1956) 1173.
15 M. T. LAVIK, G. E. GROSS AND G. W. VAUGHN, *Lubrication Eng., 15* (1959) 246.
16 W. RÜDORFF, *Z. Naturforsch, 136* (1958) 459.
17 N. V. SIDGWICK, *Chemical Elements and their Compounds*, Oxford Univ. Press, 1950.
18 S. H. BARRER, *J. Am. Chem. Soc., 60* (1938) 524.
19 R. H. SAVAGE, *J. Appl. Phys., 19* (1948) 1.

Received November 2, 1959

Wear, 3 (1960) 274–285

SURFACE CHEMICAL BEHAVIOR OF POLAR COMPOUNDS IN NONAQUEOUS LIQUIDS
DISPERSING EFFECT OF THE SOAP SOLUTION

TOSHIO SAKURAI AND TETSURO BABA

Tokyo Institute of Technology, Tokyo (Japan)

SUMMARY

A study has been made of the surface chemical behavior of fatty acid–hydrocarbon solutions in which a steel plate is dipped or iron powder immersed and which is heated to 100°C. The amount of iron soap formed in the solution gradually increased with the lapse of time. Even when the concentration of fatty acid was greatly changed, the formation of soap was not greatly affected. In the experiments using iron powder, the critical temperature for adsorption was still high, even when the concentration of stearic acid in the cetane solution decreased to as little as $4.45 \cdot 10^{-4}$ *M*.

Rhodamine B was added to the liquid paraffin solution of Al stearate and Fe stearate or the solution in which the iron powder was immersed in order to measure their absorption and fluorescence spectra. It was then observed that the maximum absorption spectrum was 546 mμ, while the maximum fluorescence spectrum was 560 mμ, and further that micelles were formed in these soap solutions.

The critical micelle concentration values for the liquid paraffin solution of Al stearate and Fe stearate measured by a fluorescence spectrum method were $1.05 \cdot 10^{-5}$ *M* and $4.0 \cdot 10^{-5}$ *M* respectively. Meanwhile, it was observed that the iron soap concentration of the solution in contact with the iron powder was more than the above concentration after 3 hours. The solution whose concentration had reached the above soap concentration showed a dispersing effect upon iron powder and carbon black. It can therefore be concluded that the metal soap formed in the lubricating oils will serve to disperse worn debris and other solid matter, and that an effective adsorption film can be formed by bringing about the formation of metal soap and so increasing the critical temperature.

ZUSAMMENFASSUNG

Das kapillarchemische Verhalten von Fettsäure-Kohlenwasserstofflösungen wurde untersucht, nachdem eine Stahlplatte oder Eisenpulver eingetaucht und bis zu 100°C erwärmt wurden. Die Menge der Eisenseifen, die in der Lösung gebildet wurden, vermehrte sich allmählich mit der Zeit. Jedoch wurde die Seifenbildung nicht beeinflusst, wenn die Konzentration der Fettsäure auch beträchtlich verändert wurde.

Mit Eisenpulver war die Kritische Temperatur der Absorption auch dann hoch, wenn die Konzentration der Stearinsäure in der Cetanelösung bis auf $4.45 \cdot 10^{-4}$ mole/l erniedrigt wurde.

Rhodamin B wurde an diese Lösungen zugefügt und ihre Absorptions- und Fluoreszenzspektra gemessen. Das Maximum des Absorptionspektrum wurde bei 546 mμ gefunden, während das Maximum des Fluoreszenzspektrum bei 560 mμ gemessen wurde, es zeigte sich, dass in diesen Seifelösungen Micellen gebildet wurden.

Die für die kritische Micellen-Konzentration Werte der Paraffinöllösungen des Al-stearates und des Fe-stearates, die aus dem Fluoreszenzspektrum bestimmt wurden, betrugen $1.05 \cdot 10^{-5}$ Mol/l und $4.0 \cdot 10^{-5}$ Mol/l. Andererseits wurde beobachtet, dass die Konzentration der Eisenseifen, in Lösungen, die mit Eisenpulver in Kontakt standen nach 3 Stunden zunahmen. Lösungen, welche die obengenannte Seifenkonzentration erreicht hatten, zeigten eine dispergierende Wirkung für Eisenpulver und Russ. Es folgt aus diesen Ergebnissen, dass die Metallseifen, die sich in dem Schmieröl bilden, zur Dispersion der abgeriebenen Trümmer und anderer Feststoffe beitragen. Daher kann sich ein wirksamer Adsorptionsfilm bilden, wenn die entstandenen Metallseifen die kritische Temperatur erhöhen.

INTRODUCTION

We have recently made some interesting observations. On increasing the temperature of the hydrocarbon solution of a saturated fatty acid in which a steel plate is dipped, the critical temperature of the solution rises, while the thermal critical concentration moves gradually to the low concentration side when the solution is kept at a particular temperature for a long time.

Both the critical temperature of solution and the thermal critical concentration were obtained from the observations.

It was found that the critical temperature varied with the nature and concentration of solute and also with the nature of the solvent. This effect could be reproduced to within $\pm$ 1°C at Pt/Pt and was reversible with temperature unless decomposition, oxidation, or other chemical changes occurred in solute or solvent. When the fatty acid solution containing sufficient soap was employed for steel/steel, however, the reproducibility was within $\pm$ 2°C.

A transition from smooth sliding to stick-slip occurred at or above a critical temperature that was characteristic of the metals, the polar compound and the concentration.

It is assumed that the transition effect is due to the disorientation or desorption of the polar molecules above a critical value, which depends upon the nature of the metal surface, the chain length, and the active end group of the polar compound.

The thermal critical concentration was defined by the authors as a point on which two straight lines crossed each other in the diagram of the relation between log $C-1/T$ for the adsorption isostere, where C is the concentration of the solution, and T is the absolute temperatue. The thermal critical concentration is therefore the minimum concentration of the solute on which the maximum critical temperature can be observed. Even if the concentration of solute is increased to a critical value, the critical temperature does not rise.

In this connection, we previously reported[1] that the above results are due to the formation of iron soap in the solution, and to the increase in the soap concentration. Many studies so far published have confirmed that metal reacts with fatty acid to form a metal soap. Little investigation has been made, however, as to the behavior of the metal soap formed in the solution.

SINGLETERRY[2] discovered that the metal soap formed micelles in nonaqueous liquids. Subsequently, ZISMAN[3], PERI[4] and DENISON[5] observed that the micelle formation was effective in dispersing fine solid material in lubricating oils. In other words, the metal soap micelle present in the lubricating oils can not only disperse or solubilize the initially formed oxide of lubricating oils, but also disperse the fine solid particles in the lubricating oil. Not only that; we believe it possible that the metal soap micelle can disperse in the oil the worn debris formed by contact between the metals during the lubrication, and thereby enhance the lubrication effect. We report here on an investigation into the dispersing action of iron soap formed in a fatty acid–hydrocarbon solution that is in contact with steel plate or iron powder.

EXPERIMENTAL

Materials

Palmitic and stearic acid were used as the saturated fatty acid. They were refined by a recrystallization method. As solvents, cetane, decalin and liquid paraffin were used. They were refined by a normal method. Their characteristics are as follows:

Cetane: d_4^{20} 0.7750, n_D^{20} 1.4352, m.p. 18.1°C.

Decalin: d_4^{20} 0.8950, n_D^{20} 1.4797, b.p. 185–187°C.

Liquid paraffin: d_4^{20} 0.8660, n_D^{20} 1.471, molecular weight 310, ring analysis naphthene ring 45.5%, paraffin chain 54.5%.

Palmitic acid: m.p. 62.4–62.6°C, neutralization value 215.1 (calculated value 218.8); Stearic acid; m.p. 69.2–70.5°C, neutralization value 197.7 (calculated value 197.3).

The soaps used were Fe distearate and Al distearate (neither of which correspond analytically to the distearate hereafter termed "refined Fe stearate" and "refined Al stearate" respectively). They were made from the sodium salt by means of double decomposition, and thereafter refined by a recrystallization method. Their characteristics are shown in Table 1. As for the quantitative analysis of the iron in the soap, orthophenanthroline was used as a reagent, and the optical density was measured at approximately 500 mμ, when the photoelectric photometer was used.

TABLE I

PROPERTIES OF REFINED METAL SOAPS

Soap	*Metal content (wt%)*		*Free acid (wt%)*	*Softening point (°C)*
	*Theoretical**	*Experimental*		
Iron stearate	8.92	6.99	0.23	119.3
Alminium stearate	4.56	5.09	0.16	135.0

* Calculated as distearate.

The iron power was prepared by dispersing it in a soybean oil–acetone (1:1) mixture, and separated and cleaned by using the precipitation method. The grain size distribution of iron powder revealed by the electron microscopic test is shown in Fig. 1. The grain size of the iron powder was distributed over a relatively small range, while the average diameter of the grains was approx. 1 μ.

The carbon used in the dispersion test was a carbon (micronex) of approx. 10 mμ diameter on average. Prior to being used, the carbon was heated to 60°C and degassed.

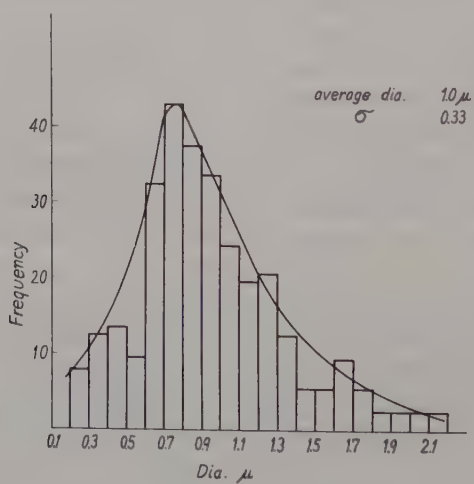

Fig. 1. Size distribution curve of the iron powder used.

Methods

Measurements of the fluorescence and absorption spectrum. Micelle formation by oil-soluble soaps in nonpolar solvents is observed from measurements of the depolarization of the fluorescence of a suitable dye molecule which has been solubilized by the micelle. The depolarization observed is a result of the Brownian rotation of the dye-bearing unit between the time of excitation and the time of the emission. The relative intensity of fluorescence depends upon the concentration of micelle formed. A dye, such as Rhodamine B, is colorless in hydrocarbon solvents, but is colored when incorporated into soap micelle. One excites the micelle-borne dye with plane-polarized light and measures the degree of polarization of the fluorescence emitted at 90° to the

incident beam. In measuring the fluorescence and absorption spectra, we employed an Hitachi spectrophotometer of EPU–2 type. The size of the cell used was 10 × 10 × 40 mm. Before and after the measurement of the fluorescence and absorption spectrum, the reading of wavelength was corrected by comparison with a standard. In measuring the fluorescence, 2 cells were used. A prepared test solution of the maximum concentration was put in one cell, while a less concentrated solution was put in another cell. Then the rhodamine B ($1.05 \cdot 10^{-4}$ *M*) was added to these two solutions. In this case, the standard was the solution of maximum concentration, which was given the value of 100%. The repeated measurements of the relative intensity for a given solution showed an average deviation of 0.5%. The glass surface of the cell was made inactive by varnishing with silicon oil; reaction of the glass surface of cell with the test solution or dyestuff would cause not only a change in the absorption and fluorescence spectrum, but also the deviation of the maximum value of the spectrum.

The fluorescence of rhodamine B was excited with the 546 mμ radiation from a SHL – 100 mV mercury vapor lamp.

Measurement of the critical temperature. As we previously reported, the rectification effect caused by the barrier of unsymmetrical oil film was utilized when the polar compounds were put between the slider consisting of three steel balls and steel plate. When the temperature of solution was increased under the minimum load, the rectified current extinguished itself owing to the disorientation of the polar compound adsorbed on the surfaces. The critical temperature, therefore, was assumed to be the temperature at the time when the rectified current extinguished itself[1].

All measurements of critical temperature were given in platinum–platinum.

RESULTS

Soap formation in the saturated fatty acid–hydrocarbon solution

The cetane solutions of palmitic acid, in which the steel plate (block gauge material), 20 × 25 × 10 mm, had been dipped, were heated at 100 ± 1°C for 2, 3, 5 and 7 h, respectively. The absorption spectra of the solutions are shown in Fig. 2. The fluorescence spectra of the solution after 7 h are shown in Fig. 3.

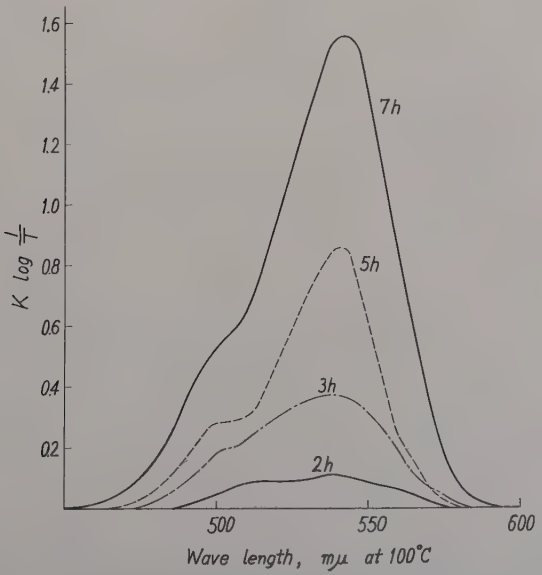

Fig. 2. Adsorption spectra for rhodamine B in $3.80 \cdot 10^{-3}$ *M* palmitic acid–cetane solution after heating with steel plate at 100°C.

As shown in Fig. 2, the absorption spectrum reached a maximum at 546 mμ. With the increase of the contact time with the steel plate, the maximum value rose. Meanwhile, the fluorescence spectrum reached a maximum at 560 mμ. With the increase of contact time, the fluorescence intensity of the solution rose.

It was also conceivable from Fig. 2 that the iron soap was easily formed only if the steel plate was dipped in a hydrocarbon solution of fatty acid, and that more iron soap was formed when the steel plate was dipped for a longer time at 100°C. In addition, the fact that the amount of iron in the solution after 7 h was $4.3 \cdot 10^{-6}$ g/g revealed that iron soap was formed in the solution. In order to advance this study of the formation of soap, various experiments were made on fatty acid solution and iron powder. In the first place, $4.45 \cdot 10^{-2}$–$4.45 \cdot 10^{-5}$ M solutions of stearic acid and cetane were prepared, and their 20 g solutions to which 5 g iron powder had been added were heated at 100 ± 1°C for 7 h. The residual iron powder was then filtered, the amount of iron that had dissolved in the solution to form a soap was analysed, and the maximum critical temperature (T_{max}) of the various resulting solutions was measured. The results are given in Table II. With the gradual decrease in the concentration of the stearic acid in the solution, the formation of iron soap decreased. The decrease of

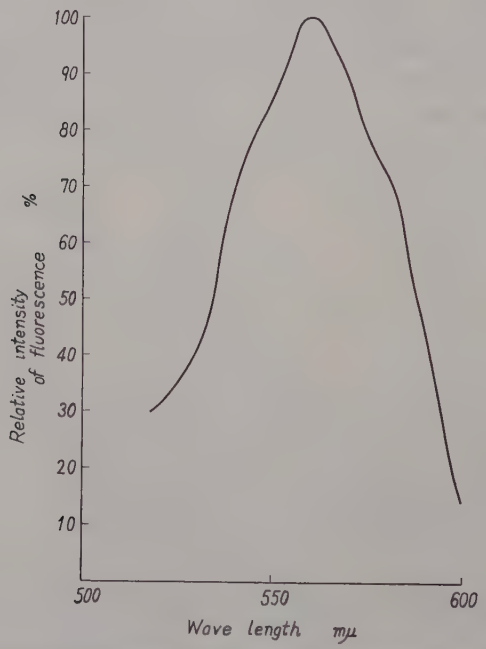

Fig. 3. Fluorescence spectra for rhodamine B in $3.80 \cdot 10^{-3}$ M stearic acid–cetane solution after 7 h heating with steel plate at 100°C.

iron soap formation, however, did not keep pace at all with the drop in the concen-concentration of stearic acid, and the formation of iron soap was observed to as low a concentration as $4.45 \cdot 10^{-4}$ M. But it was difficult, using this analytical method, to

observe iron soap formation at any concentration less than this. It was interesting that the high critical temperature also showed at a 4.45 M concentration of stearic acid. At a concentration as low as $4.45 \cdot 10^{-5}$ M, T_{max} was also less than the room temperature.

TABLE II

IRON SOAP FORMATION IN CETANE SOLUTION AT VARIOUS CONCENTRATIONS OF STEARIC ACID AND CRITICAL TEMPERATURES OF THE SOLUTION

Concn. of stearic acid, (mole/l)*	*Amount of iron dissolved in solution (g/g)*	*Critical temp., T_{max}, °C (Pt/Pt)*
$4.45 \cdot 10^{-2}$	$7.0 \cdot 10^{-6}$	116.7
$4.45 \cdot 10^{-3}$	$6.7 \cdot 10^{-6}$	116.0
$4.45 \cdot 10^{-4}$	$2.4 \cdot 10^{-6}$	103.0
$4.45 \cdot 10^{-5}$	not observed	below room temperature

* The solutions to which iron powder had been added were heated for 7 h at 100°C and filtered.

TABLE III

RELATION BETWEEN SOAP FORMATION IN STEARIC ACID–CETANE SOLUTION AND CONTACT TIME WITH IRON POWDER

Contact time (h)*	*Amount of iron dissolved in solution (g/g)*	*Concentration of iron soap (mole/l) (calc.)*	*Critical temp., T_{max}, °C (Pt/Pt)*
2	$1.4 \cdot 10^{-6}$	$2.0 \cdot 10^{-5}$	80.7
3	$2.7 \cdot 10^{-6}$	$4.1 \cdot 10^{-5}$	105.6
5	$5.3 \cdot 10^{-6}$	$8.2 \cdot 10^{-5}$	115.2
7	$6.7 \cdot 10^{-6}$	$1.0 \cdot 10^{-4}$	116.0

* $4.45 \cdot 10^{-3}$ M solution was heated with iron powder at 100°C and then filtered.

In other experiments, the 20 g solution of stearic acid ($4.45 \cdot 10^{-3}$ M)– cetane to which 5 g iron powder was added was heated at 100° ± 1°C for 2–7 h. The results obtained are shown in Table III. In the case of contact for less than 3 h, the formation of iron soap rapidly increased with the passage of time. In the case of contact for over 3 h, however, it increased slowly. This seems to be due to the fact that the reaction between the fatty acid and the metal surface is disturbed, because the soap formed adsorbs to the metal surface and forms a relatively thick adsorption film of soap regardless of the sort of solution. In other words, since the solubility of iron soap in cetane and liquid paraffin is notably low, the diffusion velocity of soap molecules into the solution, which has adsorbed to the iron surface, slows down appreciably. Consequently, the surface concentration of soap becomes larger, and the adsorption film on this surface hinders the reaction with the free fatty acid. This may be considered as a phenomenon of precipitation adsorption[7]. Table IV shows the results of an experiment in which iron and copper powder was added to the stearic acid solution of liquid paraffin. For the iron powder, the same results as the above were obtained. In the liquid paraffin without fatty acid after 7 h, an iron content of $2.3 \cdot 10^{-6}$ g/g was detected. This shows a great difference in the iron soap formation

as compared with that in the cetane: $0.3 \cdot 10^{-6}$ g/g. This difference seems to be due to the different oxidation stability of the liquid paraffin and cetane.

As shown in Table IV, almost ten times as much copper as iron was detected. In the case of liquid paraffin alone, the T_{max} showed a high value. Sodium diethyl dithiocarbamate was used for the analysis of the copper. Then the optical density of copper was measured at 420 mμ by a photoelectric photometer, and the formation

TABLE IV

RELATION BETWEEN SOAP FORMATION IN STEARIC ACID–LIQUID PARAFFIN SOLUTION AND CONTACT TIME WITH IRON POWDER OR COPPER POWDER

Contact time (h)*	*Amount of iron dissolved in solution, 10^{-6} g/g*	*Critical temp., T_{max}, °C (Pt/Pt)*	*Amount of copper dissolved in solution**, 10^{-5} g/g*	*Critical temp., T_{max}, °C (Pt/Pt)*
1	1.0	76.0	3.6	110.6
2	3.2	108.5	7.4	118.5
3	5.3	112.0	9.7	120.3
5	5.9	116.5	9.8	120.0
7	7.0	117.4	11.9	121.7
Liquid paraffin (7 h)***	2.3	72.3	3.5	102.0

* A $4.45 \cdot 10^{-3}$ *M* solution was heated with iron powder at 100°C and then filtered.
** A $4.05 \cdot 10^{-3}$ *M* solution was heated with copper powder at 100°C and then filtered.
*** Blank test.

of copper soap in the solution was evaluated. The results of these experiments are almost the same as those of the GREENHILL[8] experiment. The maximum critical temperature of various solutions was measured between platinum and platinum.

When iron powder or steel plate is in contact with the hydrocarbon oil solution of stearic acid, iron soap can easily be formed. Though the rate of soap formation is then naturally affected by the temperature, it is little affected by the concentration except in the case of stearic acid of very low concentration. It can be considered that an effective lubricating oil film may be formed even at such a low concentration, since the solution has a high critical temperature even at a concentration of $4.45 \cdot 10^{-4}$ *M*.

Micelle formation

It is conceivable in view of the above facts that the iron soap formed in the fatty acid solution forms micelles in the solution, and that, as is typical of nonaqueous colloidal solutions, a dispersing action may be observed.

The absorption and fluorescence spectra of the cetane solutions containing refined Al or Fe stearate were measured using rhodamine B. The maximum of the absorption for the two was 546 mμ, almost in agreement with that for calcium xenyl stearate obtained by SINGLETERRY. The fact that the maximum fluorescence spectrum for the two was 560 mμ shows that the soap formed micelles in the solution. The fluorescence intensity at 560 mμ is plotted against the concentration in Fig. 4. If the curves in Fig. 4 are extrapolated to the zero point of fluorescence intensity, this point

is a concentration corresponding to the so-called "C.M.C.". The concentration for the refined Al stearate was $1.05 \cdot 10^{-5}$ M, while that for the defined Fe stearate was $4.0 \cdot 10^{-5}$ M.

Table III additionally shows the concentration of iron soap formed when the iron powder was added to the solution of stearic acid and cetane. The concentration values were calculated from the analysis of free fatty acid and iron, on the assumption that

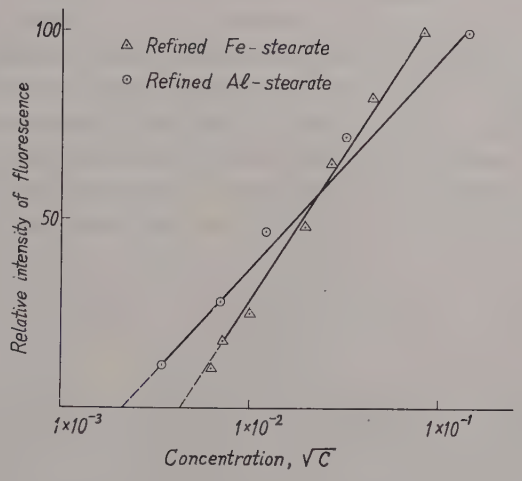

Fig. 4. Fluorescence intensity of $1.05 \cdot 10^{-4}$ M rhodamine B in cetane as a function of soap concentration.

the ratio of the stearic acid molecule to the iron atom in the average structure of iron soap in the solution is 1.5 : 1. Table III shows the following: the concentration of iron soap in the solution after 3 h is $4.1 \cdot 10^{-5}$ M, corresponding to the zero point of fluorescence for the refined Fe stearate. Therefore, if the solution is in contact with the iron powder for more than 3 h, the concentration of the soap formed in the solution becomes sufficiently high to form micelles. The micelles formed may contain a complex of soap and free fatty acid.

Dispersing effect

Dispersion of iron powder. It is evident that the iron or copper soap formed in the fatty acid solution of hydrocarbon increases the critical temperature of the solution and plays an important role in the lubrication. It is further conceivable that these soap solutions can have a dispersing effect on solid debris, etc. In the first place, experiments were devoted to the dispersion of iron powder, representing the worn debris during lubrication; 0.5 wt% iron powder was used for the dispersion. The results are shown in Table V. The test solution used in the dispersing effect was a solution in which the iron powder had been brought in contact with the liquid paraffin solution of stearic acid at 100°C and then filtered. The second column of Table V shows the amount of iron contained in the solution before dispersion. The third column

shows the quantity of iron detected in the upper layer of solution after the iron powder had been dispersed at 50°C, and the solution then kept still at the same temperature for 7 h. The last column shows a difference between the two amounts of iron, *i.e.* the amount of dispersed iron powder. As it is possible that the soap is also formed when the dispersed iron powder reacts with the solution during this process, blank tests were made on the stearic acid solution of liquid paraffin. The results of these experiments are given in the last line of Table V.

No distinct relation is found between the concentration of iron soap and the amount of dispersion of iron powder. However, since the amount of dispersion is over ten times as much as that of $0.8 \cdot 10^{-6}$ g/g obtained when the iron powder is dispersed in the stearic acid solution alone, it is evident that these iron soap solutions have a dispersing action on the iron powder. Meanwhile, even in the stearic acid solution of liquid paraffin, a small quantity of iron soap may be formed by the slight oxidation effect of the hydrocarbon at 50°C. No dispersing effect was, however, observed in the iron powder.

TABLE V

DISPERSION OF IRON POWDER IN STEARIC ACID–LIQUID PARAFFIN SOLUTION CONTAINING IRON SOAP

Contact time(h)*	*Amount of iron, 10^{-6} g/g*		*Suspended iron power, (column 3) – (column 2), 10^{-6} g/g*
	Before the dispersion of iron powder	*After the dispersion of iron powder*	
2	3.8	14.3	8.5
3	5.7	14.5	8.6
5	7.8	20.6	12.8
7	8.9	18.1	9.2
10	10.1	21.9	11.8
Blank	—	0.8	0.8

* A $3.6 \cdot 10^{-3}$ *M* solution was heated with iron powder at 100°C and then filtered.

TABLE VI

DISPERSION OF CARBON IN STEARIC ACID–LIQUID PARAFFIN CONTAINING IRON SOAP

Contact time(h)*	*Light transmission in μA***		
	27 h	*75 h*	*100 h*
2	8.7	55.0	74.0
3	4.2	48.0	64.3
5	2.2	31.8	54.8
7	1.1	25.1	43.2
10	1.0	25.0	43.7
Blank	—	54.0	75.0

* The same solution as was used in Table V.
** The clean test solution having 100% light transmission.

Dispersion of carbon. In relation to the dispersion of carbon, the same experiments were carried out. In these experiments, the 0.5 wt % carbon was dispersed in the iron soap solution, which was kept still for 27, 75 and 100 h, respectively, after the dispersion. The experimental results are shown in Table VI.

The dispersing effect was expressed by the light transmission in microamperes, which was measured with the photoelectric photometer. The light transmission immediately after the dispersion of carbon was 0%, while that for the pure liquid paraffin was 100%. The dispersion of the carbon in the soap solution has been greatly improved with the increase in the soap concentration.

The results in Table V and VI have shown that the hydrocarbon solution forming the iron soap has a dispersing effect upon the iron powder and carbon. Such a dispersion mechanism seems to be attributable to the possibility that the fine solid particles are contained in the soap micelle.

The iron soap solution prepared by using a iron powder reached a concentration above the critical micelle concentration for iron soap after 3 h. The dispersion of iron powder shown in Table V has a dispersing effect even in the case of the solution left for only 2 h. Though the reason for it is not clear, this dispersion effect seems to be due to the co-existence of free fatty acid. This is also conceivable from the fact that in the dispersion experiments reported in Table VI, the solution after 2 h and the solution after 3 h differ greatly in their dispersing effect.

DISCUSSION

It is generally inevitable that worn debris is formed by the contact between metals during lubrication. TAMAI[6] has observed that worn oxide debris is formed on the friction surfaces. It is also possible that, as abrasive matter, worn oxide debris would adversely affect the lubrication effect. The dispersion of carbon sludge, etc., formed in engine lubrication is an important problem, since it influences the action of the engine oils. It has been observed that carboxylic acid formed by the oxidation of hydrocarbon oils and sulfonic acid or carboxylic acid initially contained in lubricating oils reacts with metal surfaces to form a soap, and that the soap solution disperses the iron powder, carbon, and other fine solids into the oils, and smoothes the lubrication. In this case, however, the oxidation of hydrocarbon caused by the formation of iron soap must be taken into consideration. Meanwhile, it has also been observed that the soap adsorbs on the metal surface even at a relatively high temperature, since its T_{max} is high, and that this adsorption effect checks the dissolution of metal into the solution and curbs the rapid oxidation.

Critical micelle concentration and thermal critical concentration

It has been generally observed that abrupt changes in the physical property–concentration curves take place over a narrow concentration interval when micelles are formed in solution. This critical concentration is called a critical micelle concentration in which the constitution of the polar solute in solution changes from the molecular of disperse state to an equilibrium between molecules and aggregates.

Thermal critical concentration was defined in the INTRODUCTION; we shall refer to it as T.C.C. Even if the concentration of the solute is increased to the above T.C.C., the critical temperature does not rise. In other words, the T.C.C. is the minimum

concentration at which the maximum critical temperature can be reached. The T.C.C. not only varies greatly with the solutes and metals concerned but also varies according to the combination of solute and solvent.

The T.C.C. for the refined Al stearate is $1.2 \cdot 10^{-4}$ M, while that for the refined Fe stearate is $3.6 \cdot 10^{-5}$ M[1]. Each T.C.C. is slightly lower than the critical micelle concentration.

It is quite conceivable that the critical micelle concentration of the surfactant, which can form the micelles in the solution, should generally be somewhat higher than the T.C.C.

It may also be necessary for the concentration of the surfactants in the lubrication to be more than the T.C.C., and for the dispersing effect at the high temperature to take place in a concentration more than sufficient to form the micelles at this temperature; in other words, at least in a concentration greater than the T.C.C. the concentration of the stearic acid in the cetane solution could be decreased to as little as $4.45 \cdot 10^{-4}$ M.

In connection with the liquid paraffin solution of refined Al and Fe stearate or the solution in which the iron powder was dissolved, the absorption and fluorescence spectra were measured, by adding the rhodamine B to the respective solution. It was then observed that the maximum of absorption spectrum was 546 mμ, while that of the fluorescence spectrum was 560 mμ, and further that the micelles were formed in these soap solutions.

The critical micelle concentration values for the liquid paraffin solutions of refined Al and Fe stearate measured by a fluorescence spectrum method were $1.05 \cdot 10^{-5}$ M and $4.0 \cdot 10^{-5}$ M, respectively. Meanwhile, it was observed that the iron soap concentration of the solution in contact with iron powder was more than the above concentration after 3 h. The solutions with the above soap concentration showed a dispersing effect upon iron powder and carbon.

From the above, it can be concluded that the metal soap formed in the lubricating oils will serve to disperse worn debris and other solid matter, and that an effective adsorption film can be formed by bringing about the formation of metal soap and so increasing the critical temperature.

REFERENCES

1 T. Sakurai and T. Baba, *J. Japan Petrol. Inst.*, *1* (1958) 33.
2 L. Arkin and C. R. Singleterry, *J. Am. Chem. Soc.*, *70* (1948) 3965.
3 W. A. Zisman, *Ind. Eng. Chem.*, *45* (1953) 1406.
4 J. B. Peri, *Symposium on Additives in Lubricants*, Am. Chem. Soc. Atlantic City Meeting, 1956.
5 G. H. Denison and F. W. Kavanagh, *4th World Petrol. Congr. 1955*, Sect. VI Preprint.
6 Y. Tamai, *Wear*, *1* (1957/58) 377.
7 J. H. Schulman, R. B. Waterhouse and J. A. Spink, *Kolloid Z.*, *146* (1956) 77.
8 E. B. Greenhill, *Trans. Faraday Soc.*, *45* (1949) 625.

Received for review June 20, 1959

Accepted November 15, 1959

A STUDY OF THE WEAR OF STEEL UNDER HEAVY LOADS WITH LUBRICANTS CONTAINING SULPHUR-BASED ADDITIVES*

G. V. VINOGRADOV AND O. E. MOROZOVA

Institute of Petrochemical Synthesis, Academy of Sciences of U.S.S.R., Moscow (U.S.S.R.)

SUMMARY

A four-ball friction machine is described. It was employed to study the wear of hardened steel at considerable contact stresses in highly purified dearomatized bright stock and solutions of sulphur and dibenzyldisulphide in the latter. Profilometric measurements were carried out, microhardnesses were determined and a metallographic study was made in the friction zone.

It is shown that estimation of the anti-wear properties of lubricants by scar diameters is only of qualitative value. The depth of the wear scars depends on the nature of the lubricant and on the sliding speed. It decreases under the action of anti-welding additives and when the sliding speed is lowered.

Under seizure conditions non-etching surface layers of great hardness up to 20 or 30 μ thick are formed. They probably arise in the process of rubbing as a result of diffusion to the surface of the alloy components and enrichment of the surface layers in carbon, because the hydrocarbon lubricant may act as a carburizer. The formation of very hard surface layers alleviates the heavy friction conditions at seizure.

Reaching down to a considerable depth below the nonetching layer is a layer of partially annealed steel, which forms under the action of the heat flow from the surface. The appearance of this layer facilitates plastic deformation of the steel in the friction zone and the development of adhesion between the rubbing surfaces, resulting in seizure.

The theory has been put forward that on seizure in the presence of sulphur-containing anti-welding additives submicroscopic relatively soft films of iron sulphides form first on the very hard surface layers.

The structural changes that occur in the surface layers of steel worked for a long time under heavy friction conditions in a hydrocarbon medium are different from those occurring when wear is produced in the same hydrocarbon medium in the presence of anti-welding additives.

The specific nature of heavy friction conditions is defined by the formation of a multi-layer structure in the friction zone of the steel.

In heavily loaded sliding processes, high temperatures and pressures occur which significantly alter the structure of the metal surfaces in the contact zone. The conditions of friction are alleviated by the presence between the rubbing surfaces of a lubricating material, especially if it contains substances that are chemically active towards metals. In the case of the lubrication of steel by oils, the active substances most frequently used are organic compounds of sulphur, chlorine, and phosphorus. In the frictional process these compounds react with the iron surface and form on it a layer of compounds of iron with sulphur, chlorine, and phosphorus[1-3]. The presence of this layer changes the nature of the friction and, what is very important, affects the origin and development of seizure. The result of modifying the rubbing surfaces

* Translation: Courtesy F. W. SMITH, Fuels and Lubricants Laboratory, National Research Council, Ottawa, Canada.

by substituting layers of other compounds of iron in place of the oxide layers can be estimated by studying the intensity of the wear and the qualitative difference in the structure of the surface layers, in friction with a pure oil and with an oil containing active additives.

The present work is concerned with studying the surface of the wear scar on steel balls of 12.7 mm diameter of hardened chrome ball bearing steel.

The experiments were carried out in a 4-ball friction machine, which is shown schematically in Fig. 1, and which consists of the friction assembly A, the loading arrangement B, the driving system C and the mechanical recorder D. The shaft carrying the rotating ball is driven by an asynchronous motor 1, and coupled through a hydraulic transmission consisting of a hydraulic pump 2 and a hydraulic motor 3. The speed of rotation of the shaft is controlled by varying the output of the pump and is measured with the aid of the stroboscopic disc 4. The load is applied with a hydraulic press 5, usually used for calibrating manometers, and is determined from the pressure of the hydraulic fluid as measured by the manometric panel 6.

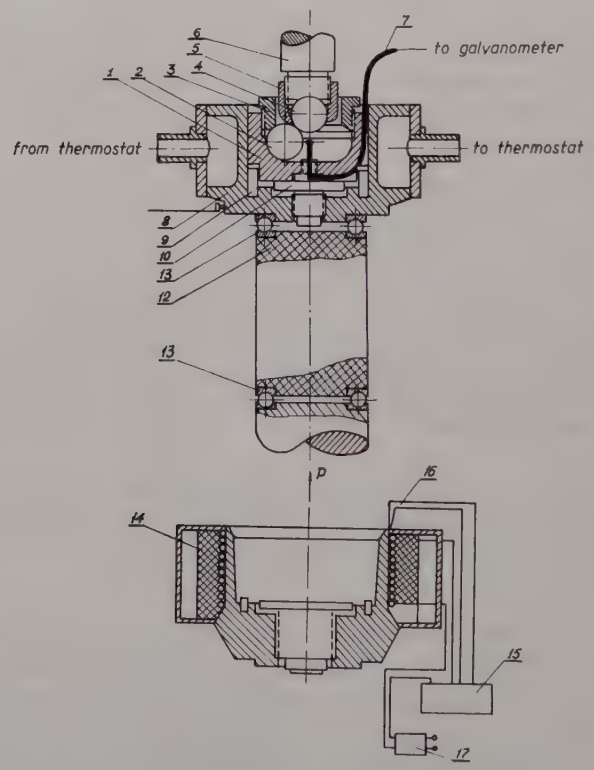

Fig. 1. Schematic diagram of 4-ball friction machine.

The hydraulic fluid acts on the piston 7 and the textolite spacer 8 to press the cup with its three balls against the ball fixed to the rotating shaft. The coefficient of friction is recorded with a mechanical recorder which consists basically of a spring 9 connected to a pointer, and a uniformly rotating paper-covered drum.

The friction assembly is shown in Fig. 2. The three lower balls 2 are placed in the cup 1 and clamped with the screw 3. The upper ball 4 is retained in the end of the shaft 6 by the nut 5. The cup is filled with 3.7 ml of the experimental oil. Its temperature is measured with the thermocouple 7. The cup is placed in the double-walled thermostat 8 and located by the pins 9. The exterior

surface of the cup and the interior surface of the thermostat have a taper of 1 : 50. The plate 10 mounted on a screw at the bottom of the thermostat ensures easy assembly of the cup and prevents its becoming jammed when heated. The frictional assembly slides under a force transmitted to the cup 1 by the textolite spacer 12. The thrust ball-bearings 13 permit easy assembly of the self-centering cup 1 containing the lower balls 2 relative to the upper ball 3.

The lower part of Fig. 2 shows an electric heater 14 used as an alternative to a circulating fluid for controlling the temperature. In this case the desired temperature is maintained automatically by a regulating pyrometric voltmeter 15 controlled by a thermocouple 16. The transformer 17 secures smooth control of the heating.

A more detailed description of the friction machine is given in ref. 4.

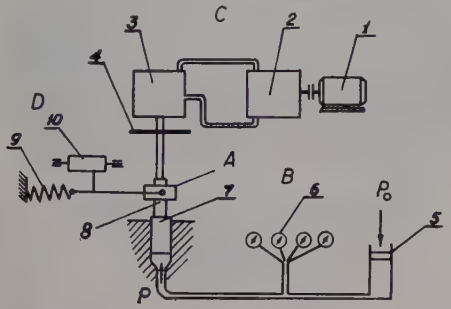

Fig. 2. Friction assembly, showing alternative heating arrangements.

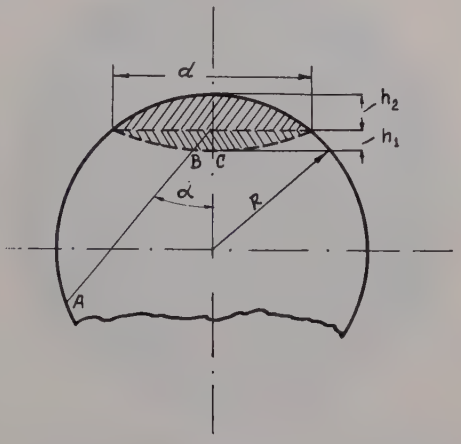

Fig. 3. Diagram of ball wear.

Some of the experiments described below are based on the oil which forms the bright stock napthenic–paraffinic fraction (NPF) of the oil MS-20. The NPF of a transformer oil was also used. Dibenzyldisulphide, and sulphur prepared from sodium thiosulphate, were used as active additives. They were dissolved in the NPFs to give a sulphur content of 1%. The NPFs were isolated from the original oils by a chromatographic method on pulverized aluminosilicate catalyst[5]. These fractions contained no trace of sulphur, gave a negative formalite reaction, and had the following characteristics:

NPF of MS-20: mean mol. wt. 540; $d_4^{20} = 0.8812$; $n_D^{20} = 1.4859$, $\nu_{20} = 780$ cS, $\nu_{50} = 105$ cS, $\nu_{100} = 14.5$ cS

NPF of transformer oil: mean mol. wt. 294; $d_4^{20} = 0.8617$; $n_D^{20} = 1.4730$; $\nu_{20} = 25$ cS; $\nu_{50} = 8.3$ cS

A study of the surfaces on which seizure had occurred was made on the lower balls. Following the method given in ref. 6, etched metallographic specimens of polished sections were prepared from the balls. Microhardness measurements were made with the MPT-3 instrument. The diameter d of the wear scar was measured with a binocular microscope as the mean of six measurements on the three lower balls. Fig. 3 shows a schematic diagram of the wear on the lower balls. Here and subsequently it will be assumed that the shape of the wear scar is approximately that of a spherical

depression. The maximum depth of this depression was measured profilometrically or with the Linnik two-beam interference microscope. The height h_2 of the spherical segment cut off by friction was calculated from the values of R and d. In this figure AB is the plane of the surface of the specimen, which intersects the ball and makes an angle α with the line perpendicular to the ball at the point C in the wear scar.

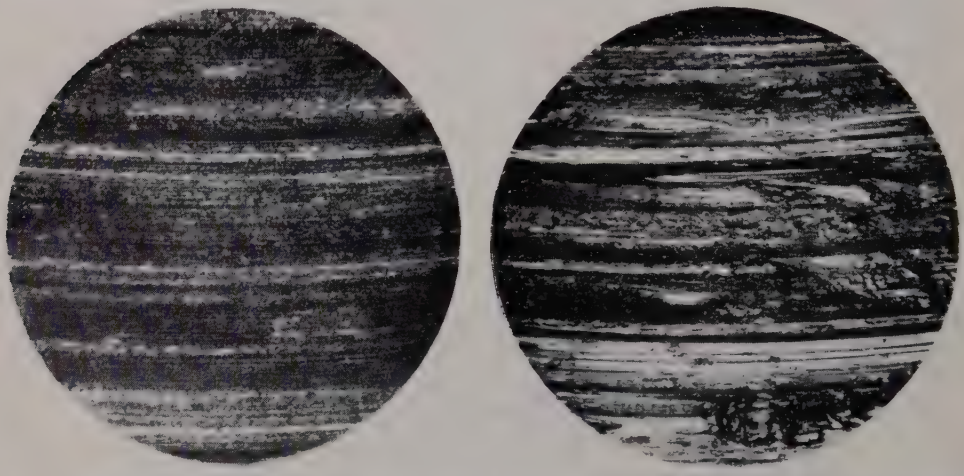

Fig. 4. Photomicrographs of wear scar surfaces. Left, with dibenzyldisulphide in bright stock NPF. Right, with pure bright stock NPF.

In Figs. 4 and 5 are shown the results obtained at very high specific loads for the bright stock NPF and for solutions in it of active additives. The experimental conditions are given in Table I.

The loads in the experiments on the NPF with and without the addition of sulphur were chosen so that the wear scar had approximately the same diameter in either case after one minute of running. This facilitated comparison of the shapes of the wear scars.

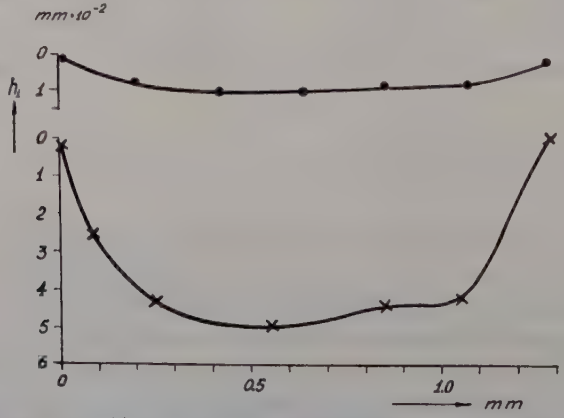

Fig. 5. Profiles of wear scars. Above, with dibenzyldisulphide in bright stock NPF. Below, with pure bright stock NPF.

TABLE I

EXPERIMENTAL CONDITIONS — 4-BALL MACHINE

Oil	Loading		Sliding speed (cm/sec)	t(°C) [b]	Duration of expt. (sec)	d(mm)
	Axial load (kg)	Initial contact stress [a] (kg/mm²)				
NPF + 1% S	300	460	23	50	60	1.3
NPF	120	340	23	20	60	1.3

[a] Calculated (mean) Hertz stress.
[b] Initial oil temperature.

In Fig. 4 the surface of the wear scar for the oil with added sulphur is shown on the left, and that for the pure NPF is shown on the right.

Fig. 5 shows the profile of the scars taken at their diameters and across the direction of sliding. There is naturally a difference in scale for the depth of the profile and for the diameter of the scar. The lines in Fig. 5 follow the peaks of the asperities of the scars. The upper part of the figure shows the profile for the NPF containing sulphur; the lower, that for the pure NPF.

Fig. 5 shows that the presence of sulphur in the oil sharply reduces the depth of the scar. In friction with the pure NPF an intense process of micro-welding is evident, and associated with it is the gouging-out of metal from the frictional surface. This gives considerable depth to the wear scar in the case of the NPF. It follows that when the diameters of two wear scars are identical, their volumes of wear may be different.

Consideration of Fig. 3 shows that the total volume of wear v may be given by the expression:

$$v = v_1(h_1) + v_2(h_2) = v_1(h_1) + v(d)$$

where the notation corresponds to Fig. 3. To disregard the value of h_1 in determining the volume of wear entails a percentage error equal approximately to $100\, h_1(h_1 + h_2)^{-1}$. Only when h_1 is sufficiently small can the determination of v be confined to the measurement of d.

In general, it is of only qualitative interest to determine the amount of wear and the wear-preventive characteristics of lubricating oils from the diameter of the wear scars alone. Particular care is required in approaching the problem of comparing the wear-preventing characteristics of oils with and without additives.

The results of measurements of d and h_1, and the calculated values of h_2, v_1, v_2 and v are shown in Table II for a series of experiments with NPFs and solutions of dibenzyl-disulphide in an NPF. The difficulties involved in making profilometric measurements and in preparing metallographic specimens did not permit the study of conditions milder than those shown in this table.

From Table II it can be seen that under heavily loaded conditions the volumetric wear depends to a significant extent upon the value of h_1.

Consideration of these data reveals two important peculiarities of the wear of balls in the presence of oil containing active additives. Firstly, as was already noted above, there is a smaller depth of wear scar (smaller h_1) at low sliding speeds. Secondly,

TABLE II

EXPERIMENTAL CONDITIONS — MEASURED VALUES OF h_1, CALCULATED VALUES OF h_2, v_1, v_2, v

Expt. No.	Exptl. conditions				d(mm)	h_1	h_2	Volume ($mm^3 \cdot 10^{-3}$) of wear		
	Axial load (kg)	Sliding speed (cm/sec)	t (°C)	Duration (sec)		($mm \cdot 10^{-3}$)		v_1	v_2	v
NPF of transformer oil										
1	120	23	25	60	1.15	4.3	2.7	22.5	14.5	37.0
NPF of bright stock										
2	117.5	23	25	60	1.3	3.2	3.4	21	23	44
3	120	23	120	300	1.75	4.3	6.0	52	72	124
NPF of bright stock + 0.15 mole/l $(C_7H_7S)_2$										
4	150	23	150	5	0.73	—	0.6	—	0.7	
5	150	23	150	20	0.84	1.0	1.3	2.8	3.5	6.3
6	150	23	150	40	0.91	1.1	1.7	3.3	5.4	8.7
7	150	23	150	60	0.99	1.1	1.9	4.2	7.2	11.4
8	150	23	150	140	1.05	1.2	2.2	5.1	9.6	14.7
9	150	23	150	300	1.34	1.1	3.6	7.6	25.7	33.3
10	300	23	20	600	1.7	1.1	5.8	12.4	66.9	79.3
11	150	23	20	1800	1.33	1.2	3.6	5.1	25.7	30.8
12	300	23	120	60	1.08	1.0	2.4	4.7	12.0	16.7
13	120	57	20	60	1.06	1.1	2.3	5.1	10.5	15.6
14	105	76	20	60	1.16	3.0	2.7	17.7	14.5	32.2
15	75	115	20	60	1.58	4.1	5.0	39.2	48.9	88.1

there is a very insignificant increase in the value of h_1 with increasing diameter of the wear scar. Higher sliding speeds greatly alter the frictional behaviour and adversely affect the ratio h_1/h_2, so that with increasing sliding speeds the value of h_1 increases commensurately with h_2. These results demonstrate well that the volume of worn metal can be found only by taking v_1 into account as well as v_2.

From the foregoing we conclude that the relative effectiveness of the wear-preventing properties of sulphur-containing compounds decrease with increasing sliding

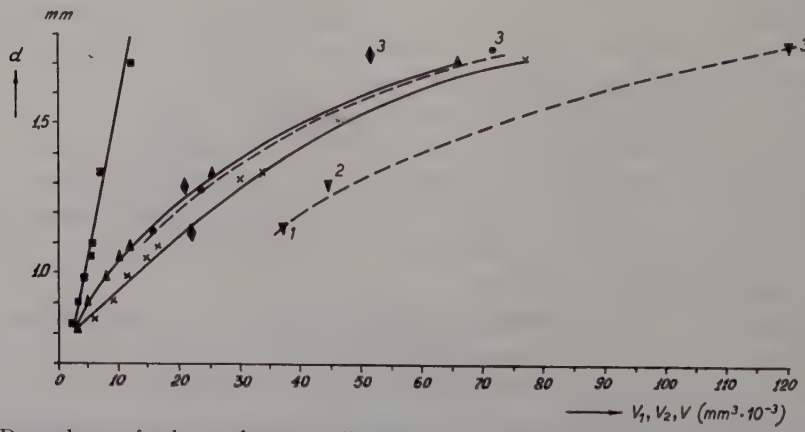

Fig. 6. Dependence of volume of wear on diameter of wear scar. ♦, ●, ▼; v_1, v_2, v, respectively, for experiments with NPFs. ■, △, ×; v_1, v_2, v for solutions of dibenzyldisulphide in bright stock NPF.

speed. In special experiments we showed that there is an optimum in the effectiveness of additives, depending on the speed of sliding.

In Fig. 6 the relation between the volume of wear and the diameter of the wear scar is shown graphically, for experiments 1–3 with NPFs and experiments 4–12 for solutions of dibenzyldisulphide in the NPF of oil MS-20 (see Table II).

Invariably, in the regime of seizure, there is a profound alteration in the structure of the metals, as is shown by the data of Table III. This table shows the experimental conditions and the value of cos α (see Fig. 3). In all experiments the sliding speed was 23 cm/sec. The mean value of the microhardness of the metal of the original balls was $8.62 \cdot 10^2$ kg/mm^2.

Figs. 7 and 8 show photomicrographs (magnification 400 ×) of certain specimens

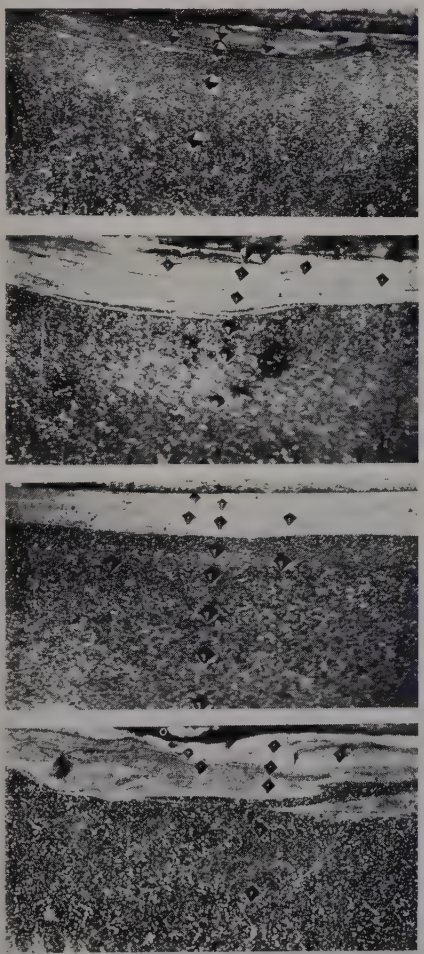

Fig. 7. Photomicrographs (400 ×) of specimens run in NPF bright stock fractions. A, expt. 1; B, expt. 2; C, expt. 3. (*cf.* Table III).

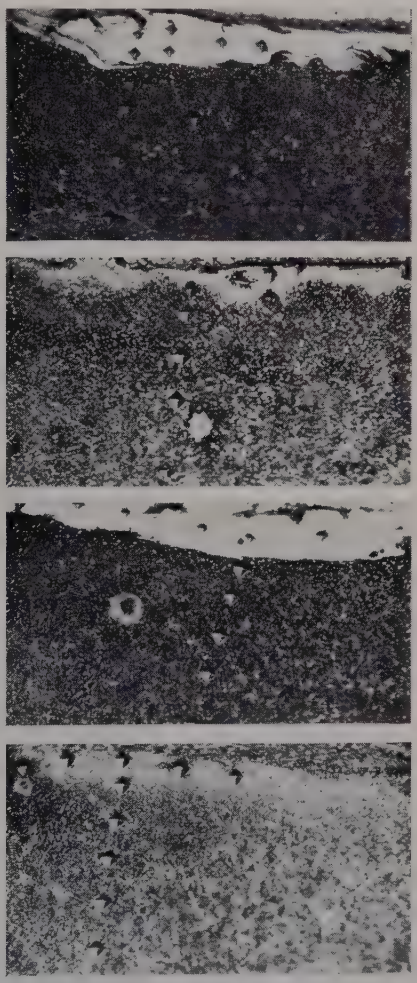

Fig. 8. Photomicrographs (400 ×) of specimens run in dibenzyldisulphide solutions. A, expt. 6; B, expt. 10; C, expt. 12; D, expt. 13. (*cf.* Table III).

after etching. These photographs show impressions made by a diamond pyramid, which demonstrate variations in microhardness at the frictional surface.

In the case of the NPF, a non-etching layer of high hardness and sometimes of considerable thickness is evident on the frictional surface at various bulk oil temperatures and various durations of the experiment. Increasing the temperature causes some increase in the thickness of the layer. An increase in the duration of the experiment increases the wear and hence decreases the specific pressure on the frictional surface. Nevertheless, the thickness of the non-etching layer increases as the duration of the experiment increases.

Beneath the layer of great hardness there occurs a partially annealed layer. Usually, if the experimental conditions are such that the layer of high hardness has relatively low thickness, then immediately beneath it occurs a layer of steel of hardness close to the hardness of the original hardened metal. When the layer of high hardness is of greater thickness, an annealed layer may appear immediately beneath it.

The thickness of the layer of lower hardness varies little with increasing duration of the experiment.

TABLE III

METALLOGRAPHIC DATA ON FRICTIONAL SURFACES

Expt. No.	Experimental conditions			d(mm)	Mean stress after expt.* (kg/mm²)	cos α	Non-etching layer		Softened layer	
	Axial load (kg)	t(°C)	Duration of expt. (sec)				Thickness (limits) (μ)	Micro-hardness (limits) (kg/mm² · 10²)	Thickness (mm)	Micro-hardness (kg/mm² · 10²)
NPF of bright stock										
1	120	20	20	1.1	52	0.39	1.7	8.5–7.6	0.1	4.5
2	120	20	300	1.75	22	0.55	28–16	10.8–7.1	0.1	4.5
3	120	120	60	1.68	28	0.51	30–23	11.2–8.4	0.2	3.9
4	120	120	300	2.1	14	0.47	25–22	9.9–7.2	0.2	4.4
NPF of bright stock + 0.15 mole/l $(C_7H_7S)_2$										
5	300	20	20	0.91	188	0.47	22–4	9.5–7.6	0.09	5.5
6	300	20	60	1.05	138	0.39	16–5	9.5–7.2	0.2	3.9
7	300	20	120	1.13	119	0.39	11–8	8.0–7.1	0.2	4.5
8	300	20	180	1.20	105	0.47	10–2	6.5	0.4	3.9
9	300	20	300	1.38	80	0.47	6–4	6.3	1.2	4.1
10	300	20	600	1.70	53	0.55	4–2	–	2.1	3.4
11	150	20	3600	2.08	18	0.58	Layer disappears	–	Layer disappears	—
12	300	120	60	1.08	134	0.47	24–4	7.1	0.3	3.9
13	300	120	300	1.70	53	0.55	Layer disappears	–	2.3	3.6
NPF of bright stock + 1% S										
14	300	20	60	1.50	68	0.39	17–15	8.4	0.09	3.9
15	300	20	300	2.10	34	0.55	Layer disappears	–	1.3	3.3
16	300	120	60	1.96	40	0.43	25	9.1–8.0	0.2	3.6
17	300	120	300	2.20	32	0.55	Layer disappears		1.9	3.3

* Calculated as relative normal stress over area of wear scar.

The processes of friction and wear develop in a completely different way with oils containing substances capable of producing compounds of sulphur with iron.

It can be seen from the data of Table III and Fig. 8 that in the presence of dibenzyl-sulphide a very hard, non-etching surface layer may be formed as in the case of the pure NPF. However, in contrast to the results with NPF, increasing the duration of the experiment diminishes the thickness of the layer, and eventually it disappears altogether. The disappearance or reduction in thickness of the very hard layer is accompanied by an increase in the underlying layer of partially annealed metal. In experiments of greater duration, both the non-etching layer and the annealed layer are absent. The surface layer of metal then has the hardness of the original hardened steel.

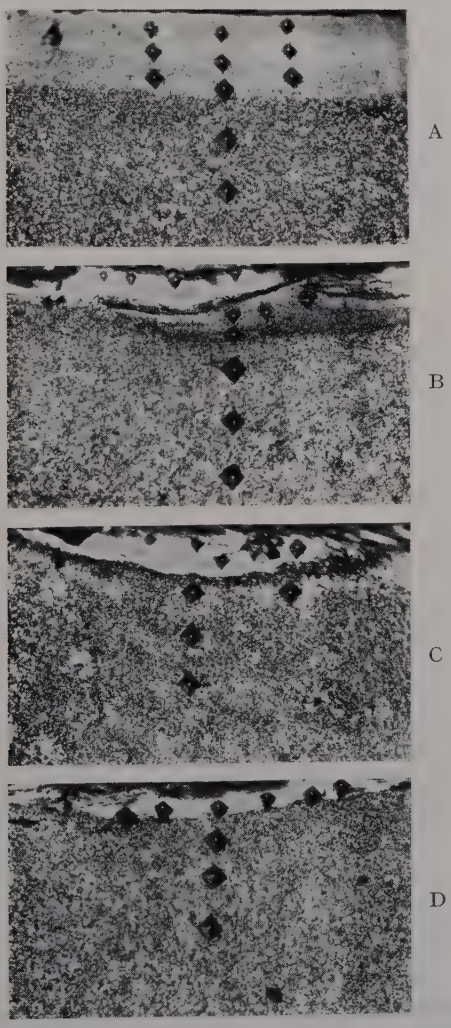

Fig. 9. Photomicrograph of partially annealed specimens (400 ×). A, expt. 2; B, expt. 4; C, expt. 6; D, expt. 12. (*cf.* Table IV).

The occurrence of the very hard, non-etching layer may be connected with quenching in the sudden cooling of the metal after stopping the experiment, or in the course of the same experiment while seizure of the frictional surfaces is occurring. The existence of a layer of lower hardness and of substantial thickness is conditional upon the partial annealing of hardened steel, and must occur during the experiment.

To solve the problem of the nature of the non-etching surface layer some specimens were partly annealed by prolonged heating in an electric furnace. In one series of experiments a temperature of 600°C was maintained for 2.5 h, and in another similar series the heating was continued for a further 2.5 h. The microhardness of the original metal of the balls after the annealing process was $2.7 \cdot 10^2$ kg/mm^2.

The results obtained are shown in Table IV and in the photomicrographs of Fig. 9. They show that partial annealing somewhat reduces the hardness of the non-etching surface layer. However, for friction in NPF medium this decrease is very insignificant. Furthermore, the fact is very noteworthy that this layer does not vanish even on prolonged annealing. It follows that in experiments with the NPF, the hard surface layer does not originate purely in a tempering process, but apparently is produced in the frictional process.

The hard non-etching layer on polished specimens prepared from frictional surfaces run in oils containing sulphur and dibenzyldisulphide gradually vanishes on partial

TABLE IV

METALLOGRAPHIC DATA ON ANNEALED SPECIMENS

Expt. No.*	*Thickness of non-etching layer (limits, in μ)*	*Microhardness (limits) (kg/mm² · 10²)*	*Comments*
Annealed 2.5 h			
2	23–14	10.0–8.9	Hard layer unevenly distributed on wear scar
3	27	8.5–7.1	Hard layer unevenly distributed on wear scar
4	27–15	8.6–6.6	Hard layer unevenly distributed on wear scar
6	10	9.5–8.0	Hard layer in form of small inclusions
12	3	6.2–4.0	Hard layer in form of small inclusions
14	Layer disappears	–	
16	Layer disappears	–	
Annealed 5 h			
2	10–7	13.0–4.3	Hard layer in form of separate inclusions
3	21	6.4–4.3	Hard layer unevenly distributed on wear scar
4	27–9	5.0–4.3	Hard layer unevenly distributed on wear scar
6	Layer disappears	–	
12	Layer disappears	–	

* No. of expt. corresponding to Table III.

annealing. In this case its production is very likely to be connected with the tempering process. By analogy with the experiments carried out with the NPF, one can assume that here also it is produced in the process of friction and not by the rapid cooling of metal after stopping the experiment.

At very high initial specific loads seizure of the frictional surfaces occurs even in the presence of substances having anti-seizure properties (sulphur and dibenzyldisulphide). It is accompanied firstly by production of the very hard surface layer, and secondly by chemical reactions and the appearance of a layer of sulphur compounds of iron of submicroscopic thickness.

The production of the very hard layer in experiments with sulphur, dibenzyldisulphide, and additives of similar general type, is connected first of all with the fact that the time required for conversion of sulphur and sulphur-containing compounds to a state of reactivity towards metals, and for the progress of reactions on the surface of the steel, is greater than the time in which the process of seizure may develop. The temperature flash at the surface during seizure results in the production of the very hard layer and in an extraordinarily fast reaction between iron and sulphur or sulphur-containing additives, with the result that a submicroscopic layer of iron sulphides appears on the surface of the steel. The formation of the very hard layer and of the plastic submicroscopic layer of reaction products of iron with sulphur and sulphur compounds substantially alleviates conditions at the frictional surface, especially if it decreases the specific load.

The present work shows that even in the presence of seizure-preventing additives, production of a hard surface layer alleviates the frictional conditions under heavy loads. In experiments of greater duration, the very hard layer occurs only at the beginning of the experiment; thereafter, it is gradually abraded away in the process of friction and is not renewed since the continuous production of sulphur compounds of iron alleviates the frictional conditions.

It is known[7–10] that the thickness of the layer of sulphur compounds of iron on the surface of the steel is of the order of 10^{-5} cm. It cannot therefore be detected on the specimens with the use of the metallurgical microscope. The thinness of the layer of sulphur compounds of iron is well illustrated by the following experiments.

The powdered iron used was from the thermal decomposition of iron pentacarbonyl. The mean diameter of the iron particles was about 3 μ. The powder was heated in cetane containing about 0.15 mole/l of dibenzyldisulphide for periods of from 3 to 20 h at temperatures from 80 to 160°C. The solution was then removed from the powder by filtration. It was found that the decrease in sulphur content of the solution, as determined by the method of double combustion[11], was within the limits of error of the method — of the order of 0.05%.

The direct investigation of the surface layers of sulphur compounds of iron formed in the friction of steel is possible only by using the electron microscope, or by methods based on radioactive indicators.

At the same time, the present work shows that profilometric measurements, determinations of microhardness, and metallographic analysis may be applied to

experiments in the widely used 4-ball machine, using oils with and without seizure-preventing additives; this gives a visual picture of the structural changes in steel during the frictional process, essential in understanding the nature of wear.

ACKNOWLEDGEMENTS

The authors are deeply grateful to N. T. PAVLOVSKAYA for advice and assistance in carrying out these experiments.

REFERENCES

1 C. F. PRUTTON, D. TURNBULL AND G. DLOUHY, *J. Inst. Petroleum, 32* (1946) 90.
2 W. DAVEY, *Petroleum (London), 13* (1950) 279.
3 G. SPENGLER *et al., Schmiertechnik, 2* (1955) 5.
4 M. D. BEZBOROD'KO *et al., Zavodskaya Lab.*, (No. 10) (1958) 1267.
5 O. A. ARTEM'EVA *et al., Composition and Properties of the High Molecular Weight Petroleum Fraction*, (collection), Academy of Sciences, U.S.S.R., p. 90.
6 N. T. PAVLOVSKAYA *et al., Zavodskaya Lab.* (No. 7) (1957) 840.
7 V. N. BORSOFF *et al., Lubrication Eng., 13* (1957) 91.
8 G. V. VINOGRADOV *et al., Khim. i. Tekhnol. Topliva*, (No. 6) (1956) 87.
9 G. V. VINOGRADOV *et al., Zhur. Priklad. Khim., 32* (No. 5) (1959) 1136.
10 C. G. WILLIAMS, *Proc. Roy. Soc. (London), A, 212* (1952) 512.
11 N. P. VOLYNSKII, I. K. CHUDAKOVA, *Zavodskaya Lab.*, (No. 12) (1955) 1435.

Received (Russian version) October 14, 1959

Wear, 3 (1960) 297–308

Brief Note

PYROLYSIS OF ZINC DIALKYL PHOSPHORODITHIOATE AND BOUNDARY LUBRICATION

I-MING FENG

Detroit Research Laboratories of the Ethyl Corporation, Detroit, Mich. (U.S.A.)

The pyrolysis of zinc dialkyl phosphorodithioate is under study. This note reports some interesting results and discusses their significance in relation to boundary lubrication.

250 g of zinc dialkyl (mixture of C_3, C_4 and C_6) phosphorodithioate (containing approximately 20% mineral oil) was heated in a three-neck flask. The flask was flushed with prepurified nitrogen prior to heating and was kept under a nitrogen atmosphere. When the temperature reached 168–169°C, a few gas bubbles appeared in the liquid. The amount of gas evolved increased with time and temperature. At 176–177°C, the rate of evolution of gas became so large that the liquid appeared to boil. As heating was continued, the temperature of the liquid remained at 176–177 °C, and the material in the flask changed from a dark liquid into a light-colored, viscous mass. The thickened material foamed and soon became a waxy solid of golden-yellow color. At the end of ten minutes heating at 176–177°C, the waxy solid could no longer be heated evenly, evolution of volatile material appeared to have stopped, and the heating was discontinued. A total of 28.9 g of volatile materials was evolved. The volatile material was collected in a dry ice trap and analyzed by mass spectrometry. Various components which have been identified include H_2S, propene, butene, hexene, and a very small amount of mercaptans (C_3 and C_6). The volatile materials collected at different stages of the experiment had the same composition. No precise quantitative analysis was made with mass spectrometry; however, the two major components, H_2S and olefins, were estimated to have a molar ratio of 1:2. Chemical analysis showed that the material collected in the trap contained 0.44 wt.% phosphorus. However, no phosphorus compound was detected by mass spectrometry. This small amount of phosphorus could have come from entrainment of the original material by the nitrogen flowing through the flask.

The solid material left in the flask weighed 221.1 g. Chemical analysis yielded 10.5 wt.% Zn, 10.4 wt.% P and 17.2 wt.% S. This gave a 1:2.08:3.35 atomic ratio for Zn:P:S, indicating that no significant change occurred in the atomic ratio of Zn

to P. These results seem to indicate that the P–S–Zn–S–P linkage was probably undisturbed. From the nature of the volatile material evolved on heating, and the weight balance, it would appear that each molecule of zinc dialkyl phosphorodithioate has lost one alkyl group and one-half sulfur atom. The estimated molar ratio of H_2S and olefins (1:2) is in good agreement with this conclusion.

From the results obtained so far, the following chemical changes of zinc dialkyl phosphorothioate during heating seem to be reasonable:

The first step involves the loss of olefin to give a product which may be present in either the thiono or thiolo form:

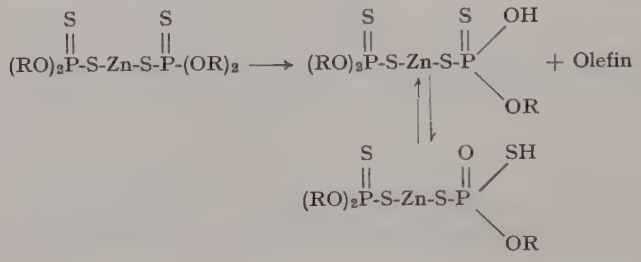

In the second step, the thiolo product forms a thioanhydride and liberates H_2S.

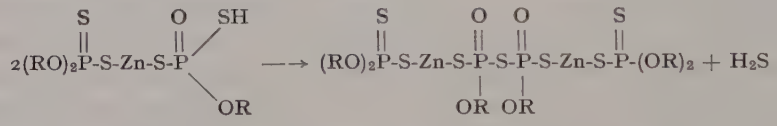

The end product has a Zn:P:S ratio of 1:2:3.5, which is very close to that which was found by chemical analysis as mentioned above. The molecular weight of the end product could be determined only roughly for the following reasons: (1) The end product contained mineral oil which was originally present in the material; although it had no effect on the Zn:P:S ratio in the analysis, the mineral oil lowered the molecular weight of the mixture. (2) H_2S and other volatile materials entrapped in the solid interfered with the molecluar weight determination. From the data available, the molecular weight of the end product was estimated to be greater than 600. The work of positive identification of the end product is in progress.

In another experiment, zinc dialkyl phosphorodithioate was heated quickly to 195°C in a prepurified nitrogen atmosphere. At that temperature, there was a sudden rapid evolution of a large amount of volatile material, the mass became viscous, and then changed to a golden-yellow waxy solid. The entire change occurred within thirty seconds.

The significance of these observations in their relation to boundary lubrication is obvious. The release of active sulfur in the form of free sulfur or H_2S starts at about 169°C. The rate of release of active sulfur increases with temperature. The formation of solids starts at about 176°C and becomes increasingly rapid as temperature increases. These temperatures are above the maximum normally found in the crankcase of an

internal combustion engine. The localized temperature rise caused by sliding at the areas of actual contact of wear surfaces raises the temperature above the ambient temperature. Thus the liberation of H_2S to provide the commonly called chemical "E.P." action takes place under moderately severe conditions. When higher localized temperatures are caused by very severe rubbing, the more effective mechanism of polymerization *in situ* sets in. This correlates very well with the observed light-colored thin surface layer on the areas of very severe rubbing in gasoline engines tested with crank-case oil containg zinc dialkyl phosphorodithioate.

The polymerization *in situ* may also explain the effectiveness of zinc dialkyl phosphorodithioate in reducing corrosion, and may partly explain its effectiveness as an oxidation inhibitor. A thin surface layer covers the metal surfaces and minimizes catalytic action.

Received January 25, 1960

Wear, 3 (1960) 309–311

Letter to the Editor

Sir,

The results of a recent research programme on concentrated tool wear in the finish turning of steel[1] suggest a general assumption in regard to the existence of "critical points" in cutting tools. Observations based on a comparative study of the working characteristics of drills of various chemical composition carried out at the Faculty of Mechanical Engineering of the University of Belgrade lend support to the above assumption.

0.35% Carbon steel has been machined with 8 mm diam. drills made of W–Mo high-speed steel (grade DMo 5) under severe cutting conditions, namely, cutting speed 37.7 m/min, drill feed s = 0.1 mm/rev, and without cutting fluid. The wear magnitudes on the clearance face and margin after a total length of cutting L = 1.120 mm can be seen in Figs. 1 and 2 and the development of wear with cutting length is shown in Fig. 3 (B = the medium value of the wear land on the clearance

Fig. 1. Clearance face of an 8 mm drill after a wear experiment in drilling grade St 50.11 steel, v = 37.7 m/min, s = 0.1 mm/rev, without cutting fluid. Photographed on a microscope, magnification 16.5×.

Fig. 2. Margin of the drill shown in Fig. 1 after the same experiment.

face, B_{max} = the wear value at the outer corner adjacent to the margin and B_f = the marginal wear). Chisel edge wear is not shown in Fig. 3 because its order of magnitude was only 0.1 mm. Fig. 3 shows that, as is usual, the outer corner of the drill carries the greatest load, and also that the curve of B_{max} differs in character from other curves.

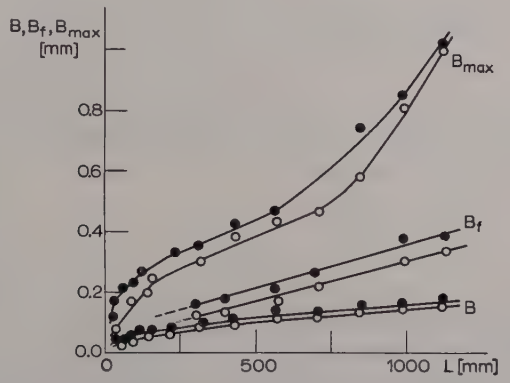

Fig. 3. The dependence of wear magnitudes B_{max}, B and B_f on the length of cutting L for the drill shown in Figs. 1 and 2. Circles and full circles correspond to the two edges, *viz.* margins.

It is now a well established fact that there are generally three periods of adhesive wear: (i) high initial wear rate, (ii) normal wear rate and (iii) increased wear rate before the final breakdown of the sliding surfaces, and some authors applied this finding to an analysis of turning tool wear[2].

Contrary to what might have been expected from the results with turning tools, not only is the gradient of the second period of the wear curve steeper at the outer corner, but the third period is reached usually long before any serious second-period wear develops at the rest of the surfaces that are subjected to friction. Thus, both the phenomena superimposed in their effect make the outer corner of a drill a critical point.

The author would like to thank the management of the tool factory "Industrija Alata", Trebinje, Yugoslavia, for providing experimental drills and workpieces, and Mr. H. L. HUGHES of the Wolverhampton and Staffs. College of Technology, Wolverhampton, England, for help with the English version.

V. ŠOLAJA

Faculty of Mechanical Engineering
University of Belgrade
Belgrade (Yugoslavia)

[1] V. ŠOLAJA, *Wear*, 2 (1958/59) 40.
[2] M. C. SHAW AND S. O. DIRKE, *Microtecnic*, 10 (1956) 187.

Received May 3, 1960

Authors' Abstracts

Einige Grundlagenversuche zur Oberflächenverformung und Pittingbildung*

A. Bartel und E. Kuss (Institut für Erdölforschung, Hannover) – *Freiberger Forschungsh.* B 35, August (1959), Akademie-Verlag, Berlin, 17 Seiten, 13 Abbildungen, 37 Lit. Zitate.

Die Verfasser geben einen Beitrag zu dem akuten Thema „Metallverformung und Pittingbildung". Sie stellen das Öl in den Mittelpunkt ihrer Versuche und Betrachtungen und heben besonders die Bedeutung des Öls im Gebiet des Zahnrad-Getriebebaus und im Gebiet der Grenzreibung hervor.

1. *Zahnradgetriebebau*

Die Untersuchung von Schäden an hochbeanspruchten Zahnrädern (aber auch an Ventilstösseln, Wälzlagerlaufringen und dergl.) hat ergeben, dass man zwischen Mikropittings und Makropittings unterscheiden muss. Mikropittings entstehen beim Einlaufen eines Zahnrades, wenn die Zähne noch nicht ausreichend grosse Tragflächen bekommen haben. Am Ende des Einlaufvorgangs ist ein relativ grosser Teil der Zahnflanke mit Mikropittings bedeckt. Da diese Pittingbildung nicht weiter fortschreitet, ist sie relativ ungefährlich.

Gefürchtet sind dagegen die Makropittings. Sie entstehen meist in der Nähe des Teilkreises in Form von scharf geränderten, zackigen Grübchen. Die begonnene Zerstörung schreitet rasch weiter fort und zwar bei Pfeilverzahnung (grossgetrieberäder für Schiffe!!) vom Rand des Zahnrades zur Mitte hin. Das Schnittbild eines Zahnradpittings zeigt, dass zunächst ein trichterförmig erweiterter Aufbruch mit Anrissen im Grund entsteht. Wird beim nächsten Zahneingriff erneut Öl in den Spalt gepresst und beim Weiterlauf des Zahnrades schnell entlastet, so werden diese Risse verlängert und erweitert, bis schliesslich die gefürchteten Ausbrüche entstehen. Besonders bemerkenswert ist hier die Feststellung, dass Pittings nur bei Anwesenheit von Schmiermitteln auftreten.

2. *Grenzreibung*

Versuche auf dem IfE-Ölprüfgerät nach A. Bartel zeigten, dass die bei hohen Flächenpressungen auftretenden Verschleisserscheinungen bei verschiedenen Ölen recht unterschiedlich sein können. Das Gerät arbeitet so, dass ein feinpolierter Prüfzapfen bei gleichmässiger Anpressung gegen zwei feststehende Rollen gedreht wird. Dabei wird während eines Dreistundenversuchs das Aussehen der Laufspur, der Verschleiss, der Reibungskoeffizient und die Temperatur beobachtet.
Berichtet wird über Versuche, die mit Prüfzapfen unter gleichen mechanischen Bedingungen (anfängliche Flächenpressung 4,500 kg/cm², Gleitgeschwindigkeit 0.2 m/sec)

* Verfasser des Auszugs: Dr. Ing. E. F. Göbel, Frankfurt a/M.

mit dem gleichen Grundöl, aber mit verschiedenen Ölzusätzen durchgeführt wurden. Mit Bezug auf die Verschleissmenge ergaben sich die nachstehenden Werte, wobei der Verschleiss im Trockenlauf $V = 1{,}200$ gesetzt wurde.

	V
(a) Trockenlauf	1,200
(b) Grundöl	14
(c) Grundöl mit schichtaufbauendem Zusatz (P, S, MoS_2)	0.1
(d) Versuche c, jedoch anschliessend noch 3 Stunden ohne Ölzufuhr (Notlauf)	0.2
(e) Grundöl mit ölsäurehaltigem Zusatz	4
(f) Grundöl mit einer ungeeigneten Additivkombination oder Verschleiss-schmierung	30

Auch das Aussehen der Laufflächen brachte wertvolle Hinweise für die Praxis. Bei ungeeignetem Öl entstehen Fressstellen und tiefe Rillen. Ölzusätze führen zur Bildung von charakteristischen Schichten, die zuweilen laufend abgetragen und neu gebildet werden (Verschleisschmierung). Dabei entstehen spiegelblanke Oberflächen mit einer sehr viel geringeren Rauhigkeit als zu Beginn der Versuche. Hierdurch kann unter anderem herausgefunden werden, welche Zusätze z.B. speziell zum Einfahren hochbelasteter Maschinen verwendet werden können usw.

3. *Versuche in einer geschlossenen Hochdruckapparatur*

Die Verfasser stellten sich die Frage, inwieweit das Öl für das Auftreten von Metallverformungen und für die Bildung von Pittings verantwortlich gemacht werden kann. Zur Beantwortung dieser Frage baute E. Kuss eine physikalisch und regeltechnisch sehr einfache Hochdruckapparatur, die es ermöglichte, oberflächenpolierte Metallproben einem allseitigen, konstanten Druck von 12,000 bezw. 16,000 atü auszusetzen. Die Metallprobe kam dabei mit keiner anderen Metallfläche in Berührung. Der Öldruck konnte beliebig lange aufgebracht werden. Schliesslich wurde plötzlich entspannt. Untersucht wurden Proben aus Stahl, Feinsilber, Feinzink und Gusseisen.

Die Arbeit bringt eine Reihe von ausgezeichneten metallmikroskopischen und elektronenmikroskopischen Aufnahmen der Oberfläche der Metallproben vor und nach dem Versuch bei 100-, 6,000- und 20,000-facher Vergrösserung. Sie zeigen deutlich die eingetretenen Oberflächenveränderungen. Die Resultate von Rauhigkeitsmessungen mit dem Forster – Leitz-Gerät und mit einem Talysurfgerät zeigen, dass nach der Druckentlastung bis zu 12 μ tiefe Grübchen entstanden waren. Schliesslich wird emissionsspektroskopisch mit dem Fuess-Quarzspektrographen M 110 nachgewiesen, dass tatsächlich Metall aus der Oberfläche in das Öl übergegangen war.

Unter Einbeziehung der einschlägigen Literatur kommen die Verfasser zu der Erkenntnis, dass bei der Pittingbildung die *Anisotropie des Elastizitätsmoduls* eine entscheidende Rolle spielt. Man versteht darunter die Erscheinung, dass sich die einzelnen Metallkristallite unter allseitigem Druck in verschiedenen Richtungen verschieden stark zusammendrücken lassen wodurch Spannungen auftreten, die zur Ausbildung feiner Risse führen. Bei hohen Drücken, die auch praktisch lokal in der Grössenord-

nung von mehreren tausend Atmosphären auftreten können, wird das Öl in die Risse hineingedrückt*. Bei schnellen Druckentlastungen, wie sie beim Lauf eines Zahnrades an den Zahnflanken auftreten, kann das Öl jedoch nicht so schnell aus den Rissen heraustreten. Es entsteht eine Druckdifferenz zwischen dem inneren ölgefüllten Hohlraum und der äusseren Umgebung, die zum Aufreissen der Oberfläche von innen heraus führt. Die Oberflächenverformungen werden daraus erklärt, dass die Metalloberfläche bei den angegebenen hohen Drücken über die Fliessgrenze hinaus beansprucht wird. Bei solchen Kaltverformungen entsteht dann auch eine grössere Oberflächenhärte.

* Siehe auch: Referat H. Scharnhorst-VDI über Vortrag A. BARTEL: Zahnradschäden im Betrieb, *VDI-Nachrichten*, 13 (Nr. 4) (1959).

A Theory of the Abrasion of Solids such as Metals

J. GODDARD, H. J. HARKER AND H. WILMAN, *Nature*, *184* (1959) 333–335.

The friction coefficient μ, and wear M g/cm, are measured for Al, Ag, Cu, Pt, Fe, Mo and W blocks 1–2.5 cm in diam. (initially surfaced by sliding on the abrasive to be tested, wet with propyl alcohol) sliding under $\sim$ 1 kg load at a few cm/sec on emery papers (either dry or wet with propyl alcohol) of particle diam. D = 5–150 microns (grades 0000 to 3).

It is shown that μ does not increase linearly with D as suggested by previous authors (using much smaller specimens and smaller range of D), but that for each metal μ is practically constant ($\mu_{max.}$) at $D >$ about 70 microns, being then smaller the harder the metal. At $D <$ 70 microns μ decreases (less the shorter the specimen) because part of the load is borne on metal (+ oxide)/metal (+ oxide) contacts between the specimen and the metal worn off by the abrasive and partly clogging it. The high and constant $\mu_{max.}$ on the coarser emery and on glass papers is due to the angular shape of the abrasive particles, since μ is only 0.15 for Ag and Cu on an array of glass spheres of $D \sim$ 125 microns, which cause ploughing but virtually no wear.

At the final equilibrium state of pick-up of emery by the metal, M also increases with D to become practically constant at $D >$ 70 microns, and M then varies practically linearly with μ, *i.e.* $M = kW(\mu - \mu_0)$, where W = load, and μ_0 is a constant in general $> \mu_{mm}$ of metal (+ oxide?) on metal (+ oxide?) in air, because of pick-up of abrasive particles by the metal surface. Most of the abrading particles cause wear in the form of long strips of metal analogous to those caused by machine tools, but there is also much plastic flow (and lateral pile-up by the grooves), as electron diffraction also indicates.

Theoretical expressions are developed for μ of spheres and for triangular or square pyramids and cones, and the $\mu_{max.}$ found corresponds well to the observed angularity of the abrasive particles (semi-apical angle $\sim$ 60–70°). The wear (g/cm) if pick-up is absent is concluded to be: $M = (fW\varrho/p'_m) \cdot \alpha \{1 - (A_0/A_1)\} \cdot \mu_p = (W\varrho/p'_m) \alpha$

$\{1 - A_0/A_1)\} \cdot \{1 + (\mu_a - \mu_0)/\mu_p\}^{-1} (\mu - \mu_0), = kW(\mu - \mu_0)$, as observed, where ϱ and p'_m = density and operative flow pressure of the metal, f = proportion of load carried on emery/metal ploughing contacts, μ_a and μ_p = adhesion and ploughing components of total μ, α = fraction of the contacting emery particles producing wear, A_1 = mean abrasion-groove cross-section area of which A_0 represents metal displaced by plastic flow but not removed as wear. Comparison with the experimental data shows that only $\sim$ 10% of the total abrasion groove volume is removed as wear.

It is also shown that when $f = 1$ (at $D > 70$ microns), $(M/\varrho) \cdot H_D$ = constant, where H_D = Vickers diamond-indentation hardness of the metal; and this, together with Khruschov's (1957) results indicates that for all pure metals H_D at the state of maximum work hardening (*e.g.* the abraded surface) is practically the same factor times the minimum hardness, *i.e.* for the annealed metal.

Wear, 3 (1960) 316–317

Studies on Surface Layer of Polished Metals by Means of Electron Diffraction and by Electrical Contact Resistance Measurements

M. MATSUNAGA (Institute of Industrial Science, University of Tokyo, Chiba, Japan) –
Rept. Inst. Ind. Sci. Univ. Tokyo, 7 (1958) 225–252; (50 fig., 41 ref.).

In metallic contact relatively low values of the electrical contact resistance have been obtained by many workers, for instance, 10 Ω at a load of 100 g. The resistance is unstable and is not always reproducible. It has been found, however, that stable and reproducible electrical contact resistance is measured using a graphite slider as a contact member because its softness and lubricating nature avoid breakdown of the surface oxide layer on the metals. The resistance is connected with surface roughness, preparing methods and the electron diffraction pattern of the surface with some metals and alloys. The low resistance values (about 2 or 3 Ω) are obtained with roughly polished surfaces, whereas high resistance values (over 100,000 Ω) are obtained with finely polished surfaces whose diffraction pattern has diffuse rings.

Thus, taking the electron diffraction pattern and contact resistance values of the surface of various metals into account it is concluded that the diffuse electron diffraction pattern is probably due to amorphous oxide.

Wear, 3 (1960) 317

Einfluss der Schweissbedingungen auf das Verschleissverhalten von Auftragsschweissungen
(Influence of Welding Conditions upon the Wearing Properties of Hard-faced Surfaces)

K. WELLINGER UND H. UETZ, (Stuttgart) –
Schweissen und Schneiden, 11, no. 12 (1959) 458–474; 41 fig.

Welding alloys for hard facing and their application — Filler metals under investigation — Resistance to wear under the action of grinding media of different hardness — Influences of the type

of alloy used — Welding processes — Number of layers — Diameter of filler wire — Flame setting — Welding current — Parent material — Micro-structure and hardness — Unintentional faults due to lack of skill on the part of the welder.

Verschleißfeste Auftragsschweißungen mit niedriglegiertem (2% Mn; 1% Cr + Ti) und hochlegiertem (3.5/3.8% C; 33% Cr) Schweißzusatzwerkstoff, mit Sinter-Hartmetall sowie mit Hartlegierungen, ferner zwei eisenfreie Legierungen, wurden unter verschiedenen Bedingungen hergestellt und ihr Gleitverschleißverhalten geprüft.

Die Auftragsschweißungen standen hierbei unter der Einwirkung verschieden harten Schleifkornes (Glas, Flint, Korund, Siliziumkarbid) und wurden, abhängig vom Schweißverfahren und Grundwerkstoff, der Lagenzahl, Durchmesser des Schweißdrahtes, Flammeneinstellung, Stromstärke, Dicke des Grundwerkstoffes, Gefügeausbildung und Härte und auch vom Einfluß der menschlichen Unzulänglichkeit des Schweißers, untersucht.

Die Zusammensetzung der Zusatzwerkstoffe bleibt in der Schweiße nicht erhalten. Der Gehalt an Kohlenstoff und Legierungselementen wird je nach den Schweißbedingungen infolge Abbrand und Vermischung mit dem Grundwerkstoff niedriger. Die hierdurch entstehenden Verluste sucht man insbesondere beim Lichtbogenschweißen durch Verwendung von Stäben mit Kohlenstoff und Legierungselemente enthaltenden Umhüllungen auszugleichen.

Die Mangan-Chrom-Titan-legierte Gasschweißung mit mittlerem oder großem Azetylenüberschuß verhält sich auf Grund der hartgußähnlichen Gefügeausbildung bedeutend günstiger als die Gasschweißung ohne Azetylenüberschuß und die Lichtbogen- sowie Schutzgasschweißung, die sorbitisches und perlitisches Gefüge haben.

Bei der chromlegierten Auftragsschweißung hängt das Verschleißverhalten in hohem Maße von der Gefügeausbildung ab, nur bei übereutektischem Gefüge mit genügend großem Anteil von Primärchromkarbiden wird die erwünschte Verschleißfestigkeit erzielt. Ein solches Gefüge wird bei der Gasschweißung bereits in der ersten Lage, bei der Lichtbogenschweißung mit umhüllten Elektroden in der ersten oder zweiten Lage erreicht, dagegen bei der Schutzgasschweißung selbst in der zweiten Lage trotz verhältnismäßig hoher Härte nicht oder nicht sicher erreicht. Das Verscheißverhalten der Auftragsschweißung unter Schutzgas ist deshalb gegenüber den beiden anderen Verfahren ungünstiger.

Die Anzahl der Lagen hat bei der Gasschweißung keinen Einfluß, bei der Lichtbogen- und Schutzgasschweißung mit der Mangan-Chrom-Titan-Legierung einen nur geringfügigen, mit der Chromlegierung und insbesondere mit der Sinterhartmetallschweißung sowie der Schweißung mit Hartlegierungen einen bedeutenden Einfluß. Der Einfluß macht sich um so mehr bemerkbar, je größer legierungsmäßig der Unterschied zwischen Grundwerkstoff und Auftragsschweißung ist.

Bei der Mangan-Chrom-Titan-legierten Auftragsschweißung wurde kein Einfluß des Drahtdurchmessers, dagegen bei der chromlegierten Auftragsschweißung ein geringfügiger Einfluß festgestellt. Eine hohe Stromstärke wirkt sich auf das Verschleißverhalten bei der chromlegierten Auftragsschweißung, insbesondere bei der

Schutzgasschweißung nachteilig, bei der Mangan-Chrom-Titan-legierten Auftragsschweißung nicht aus.

Bei der Mangan-Chrom-Titan-legierten Auftragsschweißung auf 37 MnSi 5 als Grundwerkstoff ergaben sich günstigere Verschleißwerte als auf St 37. Bei den chromlegierten und den Hartaufschweißungen wurde kein Einfluß des Grundwerkstoffes festgestellt. Ein Einfluß der Dicke des Grundwerkstoffes auf das Verschleißverhalten ergab sich unter den angewandten Verhältnissen nicht. Zweckmäßig wäre, Schweißungen auf größeren Grundwerkstoffdicken nachzuprüfen.

An Gasschweißungen mit Mangan-Chrom-Titan-Legierungen, die von verschiedenen Schweißern und zu verschiedenen Zeiten hergestellt wurden, ergab die Prüfung, daß die Flammeneinstellung nicht richtig eingehalten worden war. Durch solche menschlichen Unzulänglichkeiten des Schweißers kann das Verschleißverhalten einer Auftragsschweißung beeinträchtigt werden.

[1] K. Wellinger und P. Gimmel, Auftragsschweißung, *Das Industrieblatt*, *52* (1952) 2.
[2] O. Müller, Verschleißprüfungen an verschieden hoch und lang geglühten Auftragsschweißen, *Dissertation*, TH Danzig, 1935.
[3] R. D. Haworth, Einfluß des Schweißverfahrens auf den Verschleißwiderstand von Hartaufschweißungen, *Iron Age*, *162* (15) (1948) 82.
[4] H. Wahl, Verschleißfestigkeit und Wirtschaftlichkeit von Auftragsschweißungen, *Metalloberfläche*, *2* (1948) 169.
[5] F. Rapatz und A. Schmidt, Auftragsschweißung als Instandsetzungs- und Fertigungsverfahren, *Schw. Schn.*, *2* (1950) 320.
[6] I. Kunz und H. Jansen, Herstellen und Instandsetzen von Werkzeugen durch autogene Auftragsschweißung mit verschleißfesten Werkstoffen, *Schw. Schn.*, *2* (1950) 137.
[7] K. Wellinger und H. Gaisser, Untersuchungen von Auftragsschweißungen an Schienen, *Schw. Schn.*, *3* (6) (1951) 173.
[8] W. Hummitzsch und A. Schmidt, Verschleißfeste Auftragsschweißungen auf Werkzeugen aus Manganhartstahl, *Schw. Schn.*, *3* (1951) 147.
[9] W. Hummitsch, Leistungssteigerung durch Auftragsschweißen, *Fachbuchreihe Schweißtechnik*, Bd. 3, Düsseldorf, 1955, S. 31.
[10] H. S. Avery, Hardfacing alloys for steel mill use, *Iron and Steel, Engineer Year Book 1951*, S. 601.
[11] H. S. Avery und H. I. Chapin, Hardfacing alloys of the chromium carbid type, *Welding J.*, *31* (1952) 917.
[12] H. Benfeld, Auftragsschweißung an verschlissenen Roststäben, *Brennstoff-Wärme-Kraft*, *4* (1952) 119.
[13] K. Krüger, Über Auftragsschweißungen an Straßenbahnschienen, *Schw. Schn.*, *4* (1952) 50.
[14] E. Kauhausen, Auftragsschweißung im Berg- und Hüttenwesen, *Schw. Schn. 4* (1952) 26 (S).
[15] K. Wellinger und H. Uetz, Gleit-, Spül- und Strahlverschleiß unter Wirkung von körnigen Stoffen, *VDI-Forschungsheft 449*, B 21 (1955).
[16] O. Knotek und I. Birk, Hochverschleißfeste Auftragsschweißung, *Fachbuchreihe Schweißtechnik*, Bd. 7, Düsseldorf, 1956.
[17] S. Lundin, Richtiges Hartschweißen, *Kjellberg-Esab-Schriften*, IV (1956) 8.
[18] M. Puschner, Der Verschleißwiderstand von Auftragsschweißungen und seinen Beziehungen zu anderen Werkstoff-Kennwerten, *Kjellberg-Esab-Schriften*, III (1957) 1.
[19] H. Grix, H. Siebel und R. Fleck, Autogenes Panzern von Verschleißteilen unter besonderer Berücksichtigung von Drehwerkzeugen, *Schw. Schn.*, *9* (1957) 437.
[20] H. Koch und E. Bernholz, Der Einfluß der Schweißbedingungen auf die Zusammensetzung und Gefügebildung aufgeschweißter Chrom - Hartlegierungen, *Schw. Schn.*, *10* (1958) 71.
[21] A. E. Chevalley, Einführung in die Frage des Schutzgasschweißens von Stahl, *Schweißtechnik*, (1958) H. 4 bis H. 6.
[22] R. Schulze, Belastungsabhängigkeit der Vickers-Mikrohärte, *Feinwerktechnik*, *55* (1951) 190.
[23] W. Tofaute, C. Kuttner und A. Buttinghaus, Das System Eisen-Chrom-Chromkarbid Cr_7Cr_3-Zementit, *Arch. Eisenhüttenwesen*, *9* (1936) 607.
[24] A. L. Schaeffler, Selection of Austenitic Electrodes for the Welding of Dissimilar Steels, *Welding J.*, *26* (1947) 601.
[25] K. Wellinger und H. Uetz, Strahlverschleißuntersuchungen an Hartmetallen, erscheint demnächst.

Systematic Abstracts of Current Literature

Selected from Battelle Technical Review 1960
and from other sources

1. Deformation and Fracture

Practical Solution of Plastic Deformation Problems in Elastic-Plastic Range.
A. Mendelson and S. S. Manson. *NASA Technical Report R-28.* (Supersedes *NACA TN 4088*) 1959. i, 24 pp., diagrs., tab. GPO price, $0.40
A practical method for solving plastic deformation problems in the elastic-plastic range is presented. The method is one of successive approximations and is illustrated by four examples, which include a flat plate with temperature distribution across the width, a thin shell with axial temperature distribution, a solid cylinder with radial temperature distribution, and a rotating disk with radial temperature distribution.

Fracture Appearance of Impact Specimens Taken From Fractured Ship Plates.
John A. Bennett. *U. S. Ship Structure Committee, SSC-113,* June 29, 9 pp.
Several thousand broken V-notch Charpy specimens from service failures were studied to determine the relation between fracture appearance and impact energy of steel from fractured ships.

Micromechamism of Brittle Fracture in a Low-Carbon Steel.
G. T. Hahn, W. S. Owen, B. L. Averbach and M. Cohen. *Welding Journal,* v. 38, Sept. 1959, p. 367s-376s.
Tensile data, elastic-limit measurements, and metallographic observations of slip, twinning and microcracks, as well as standard Charpy data, for a low-carbon steel in a coarse- and a fine-grained condition.

Effect of Hardness and other Mechanical Properties on Rolling-Contact Fatigue Life of Four High-Temperature Bearing Steels.
Thomas L. Carter, Erwin V. Zaretsky and William J. Anderson. *NASA Technical Note D-270,* March 1960. 51 pp., diagrs., photos., tabs. OTS price, $ 1.50.
The rolling-contact fatigue life of groups of AISI M-1, AISI M-50, Halmo, and WB-49 alloy steel balls tempered to various hardness levels was determined at room temperature in the fatigue spin rig and the five-ball fatigue tester. A continuous increase in fatigue life and load capacity of each steel was observed with increased ball hardness. These results did not correlate with elastic-limit and yield-strength measurements for bar specimens, which showed optimum values at an intermediate hardness; the results, however, did correlate with resistance to plastic deformation as measured with spherical specimens in rolling contact.

Drop Formation from Rapidly Moving Liquid Sheets.
P. Eisenklam, N. Drombrowski and D. Hasson. Directorate of Guided Weapons Research and Development (Gt. Brit.) *DGWRD DGGW Report/EMR/59/3.* May 1959. 23 pp., illus. (Ask for N-81306)
The three types of instability manifested in flat sheets produced by fan spray nozzles and their effects on drop size are discussed. Recent analyses of aerodynamic instability are reviewed, experimentally tested, and extended to provide a drop size expression which is compared with that for the aerodynamically stable sheet under the action of surface tension forces. The conditions for and the properties of instability as a result of turbulence are discussed.

2. Adhesion and Friction

2.1. *Adhesion*

The Adhesion Capacity of Powders.
P. Patat and W. Schmid. *Chemie-Ingenieur-Technik,* v. 32, no. 1 (1960) p. 8; 2 fig., 7 tables, 31 ref.
The adhesion capacity of powders impairs many technical processes. An apparatus has been developed for measurement of this capacity and permits experiments to be carried out *in vacuo* and in various gas atmospheres; the slide surface plate and powder can be heated separately for the removal of adsorbed layers, and the slide plate can also be electrically charged. With this apparatus it has been possible to explain the essential factors influencing the adhesion behaviour, which is characterized by the two indices: adhesion force and friction. These factors are: the particle size and the composition of the powder; the material (glass, metal, plastics), the nature (oxidized, wetted with liquid) and the electrical charge of the plate. Frequently, exchange reactions exist between these influencing indices. A general, empirical re-

lationship has been found for the relationship between the particle size and the adhesion force. The influencing indices are discussed with respect to their physical content.

Experiments on Peeling.
J. J. Bikerman. *Journal of Applied Polymer Science*, v. 2, no. 5 (1959) pp. 216–224; 9 fig., 4 tables, 10 ref.
The force required to peel an aluminium (or nickel) ribbon glued to a rigid glass plate with a polyethylene or polyvinyl acetate was determined. It proved to be smaller than expected (from a theory partly new) both for adhesives which were almost Hookean solids and for those whose stress–strain curve could approximately be represented as stress = const. $(\text{strain})^{0.5}$. In the latter group, the difference between the theory and the experiment was due to stress concentrations at the right-hand and the left-hand edges of the adhesive layer; these stress concentrations formed because, when a pull was applied, the adhesive contracted in the directions perpendicular to that of pull. As a consequence of this effect, the peeling force W_0 was not proportional to the width w of the ribbon; sometimes, a linear relation $W_0 = aw + b$ seemed to be valid. On the other hand, near-Hookean adhesives of a low total elongation required a peeling force proportional to w; the stress concentration dangerous for these materials occurred at the boundary between the adhesive and the bent ribbon at the sharp bend. The damage to the brittle adhesive caused by the ribbon deformation could be reproduced without bending, namely by extension of the ribbon beyond its yield strength.

2.2. *Friction Processes*

Skin-Friction Measurements in Incompressible Flow.
Donald W. Smith and John H. Walker. (*NASA Technical Report R-26*. Supersedes *NACA TN 4231*) 1959. i, 35 pp., diagrs., photo., tabs. GPO price, $ 0.45.
Experiments have been conducted to measure the local surface-shear stress and the average skin-friction coefficient in incompressible flow for a turbulent boundary layer on a smooth flat plate having zero pressure gradient. Data were obtained for a range of Reynolds numbers from 1 million to 45 million. The local surface-shear stress was measured by a floating-element skin-friction balance and also by a calibrated total head tube located on the surface of the test wall. The average skin-friction coefficient was obtained from boundary-layer velocity profiles.

Experimental Investigation of Spin-up Friction Coefficients on Concrete and Nonskid Carrier-Deck Surfaces.
Walter B. Horne. *(NASA Technical Note D-214)*. April 1960. 50 pp., diagrs., photos., tabs. OTS price, $ 1.25.
A series of landing-impact tests was conducted with a carrier-type jet airplane main landing gear to obtain data on spin-up friction coefficients for both concrete and nonskid deck surfaces for tire-inflation pressures of 260, 320, and 400 p.s.i. The sinking speeds investigated ranged between 12 and 19 ft/sec over a forward speed range between 54 and 104 knots. Several impact and taxiing tests over a 1-3/8 in.-diameter arresting cable were also conducted. Results indicated somewhat lower spin-up friction coefficients for the non-skid deck than for the concrete surface.

Flight Tests to Determine the Coefficients of Friction Between an Aircraft Tyre and Various Wet Runway Surfaces. Part I.
Ministry of Aviation (Gt. Brit.) *MOA S & T Memo. 15/59*. September 1959. 16 pp., diagrs., photos. (Ask for N-79925)
Covers the initial instrumentation-proving trials carried out at Wisley Airfield prior to comprehensive tests on selected runway surfaces to determine the variation of coefficient of friction between an aircraft tire and wet runway. Instrumentation is described and a brief history of the initial proving tests is given. Results are presented showing the variation of friction coefficient with aircraft speed for the 100-percent slip (wheel locked) case at constant aircraft weights and tire pressure. A curve is included showing variation of friction coefficient with slip at a speed of 75 knots.

Kinematics of a Rolling Tire and Its Application to Tire Performance.
M. Berger. *Journal of Applied Polymer Science*, v. 2, no. 5 (1959) 174–180; 11 fig., 1 ref.
A geometrical analysis is given of the tread motions occurring in the contact length of a rolling tire. Both the case of a free rolling wheel and that of a wheel under torque are discussed. Expressions and curves are derived for the relative slip and compressions which occur at the contact length for the two conditions. It is found that two important structural features control the nature of tread motions. These are the torsional rigidity of the sidewall and the compressibility of the tread. In addition, the implication of the analysis in tire design and performance are discussed.

2.3. *Friction Materials*

Les alliages antifriction à base d'aluminium et d'étain.
Aluminum- and Tin-based Antifrictional Alloys.
Ch. Guinard. *Métaux Corrosion-Industries*, v. 34, Sept. 1959, p. 317–323.

A study of the qualities of antifrictional Al-Sn alloys in relation to the Sn content, Sn distribution, properties of the Al-based substratum, and methods used in modifying these properties by means of additions, thermal treatment, welding or plating.

Effect of Alloy Content on Frictional Properties of Titanium.
I. S. Kaptyug and V. I. Syshchikov. *Metal Science and Heat Treatment of Metals* (Cover-to-cover translation of *Metallovedenie i Termicheskaya Obrabotka Metallov*), 1959, no. 4, Apr., p. 27–32.
Alloying of Ti only slightly decreases the static coefficient of friction — from 0.55 to 0.45 against unalloyed Ti, and from 0.20 to 0.15 against brass — and the depth of damage done by dry sliding friction. Titanium metal and the Ti alloys investigated show a very low resistance to wear in sliding friction, the wear being 15 to 30 times that of brass, bronze, and stainless steel. The Ti alloys and the Ti metal investigated cannot be used in components subjected to friction at high specific pressures. They can be run against brass or bronze only under relatively small loads.

Les plastiques comme matériaux de frottement.
G. Fabre. *Industrie des plastiques modernes*, v. 11, no. 8 (1959), 40–44, 47, 48; 5 tables, 22 ref.
A review with numerous data selected from current literature.

3. Lubrication and Lubricants

3.1. *Lubrication*

Lubrication of Bearings.
E. I. Radzimovsky. 338 pp. 1959. Ronald Press Co., New York.
Theoretical principles; design factors.

Gas Lubrication.
J. A. Cole. *Research*, v. 12, Aug.-Sept. 1959, p. 348–355.
Most machine bearings are lubricated with petroleum lubricants, but in some applications there are advantages to be gained from the use of gaseous lubricants, usually air. This article describes the principles and development of gas lubrication, and surveys some current applications.

The Lubrication of Radiused-Pad Thrust Bearings. (in Italian)
S. I. El-Sisi. *Tecnica Italiana*, v. 24, no. 5, Aug. 1959, p. 349–364.
An experimental investigation of the operating conditions of this type of bearing where a full convergent-divergent lubricating film exists. Load per unit width, absolute viscosity of the lubricant and surface speed were accounted for in the curves representing the experimental results. A more precise study of the local oil pressures at the "on" and "off" boundaries of the lubricant film is also included.

3.2. *Lubricants*

Fuels and Lubricants.
M. Popovich and Carl Hering. 312 pp. 1959. John Wiley & Sons, New York.
Discusses the important fuels, including boiler, internal combustion engine, and jet fuels, as well as rocket propellents and nuclear fuels. Examines the desirable properties of fuels and lubricants, the ASTM tests which are used to measure properties, and the interpretation, limitation and significance of these tests.

The Performance of Lubricating Oils.
H. H. Zuidema. 2nd ed. 205 pp. 1959. Reinhold Publishing Corp., New York.
Evaluates data on the performance characteristics of lubricating oils under various conditions; data to facilitate the conversion of various viscosity units; lubrication processes; rheology; oxidation; bearing corrosion; sludge and lacquer deposition; emulsification and foaming; manufacturing methods.

The Development, Testing, and Application of Petroleum Based Launching Lubricants.
G. H. Clark and D. A. Davidson. *Institute of Petroleum, Journal*, v. 45, July 1959, p. 175–196.
Use of lubricants specially developed for launching ships.

Hypoid Gear Lubricants and Additives.
J. S. Elliott, N. E. F. Hitchcock and E. D. Edwards. *Institute of Petroleum, Journal*, v. 45, Aug. 1959, p. 219–235.
A brief history is given of the development of hypoid gear oils and the methods used for their evaluation.

The Effects of Surface-Active Lubricants on Resistance to Shear in Friction.
I. S. Avetisian and G. I. Epifanov. *Akademiia Nauk SSSR, Doklady*, v. 128, no. 5, Oct. 1959, p. 973–976.
Effects of the boundary layers of hard lubricants on the coefficient of friction, the shearing strength, and the degree of surface friction in the case of Fe, Cu, Zn, Sn, Al, and Pb. Effects of liquid hydrocarbons and their derivatives on the coefficient of friction and the shear strength in the case of Cu, Al, Fe, and the alloy EI-437.

Über die Schmierfähigkeit organischer Molybdänverbindungen.
Lubricating Power of Organic Molybdenum Compounds.
Günter Spengler and Adalbert Weber. *Chemische Berichte*, v. 92, no. 9, 1959, p. 2163–2171.
An attempt was made to explain the improvement of the lubricating effect of mineral oils by addition of organic Mo compounds in the presence of S. Molybdenum-oxy-sulfide has good lubricating properties; during the thermal decomposition of organic Mo compounds, it is probable that molybdenum-oxy-sulfide is formed.

4. Bearings

A Study of the Metallurgical Properties That Are Necessary for Satisfactory Bearing Performance and the Development of Improved Bearing Alloys for Service up to 1000°F.
T. V. Philip, A. E. Nehrenberg and G. Steven. *U. S. Air Force, Wright Air Development Center, WADC Technical Report 57–343*, (pt. 2), Oct. 1958, 56 pp.
Fifty-one experimental compositions were studied. Describes the theoretical considerations which formed the basis of the formulation of these steels as well as the annealing cycle, austenitzing temperature survey, and the tempering survey. The results of the tempering studies are plotted as "master tempering curves".

Roller Bearings for Use to 600°F.
Notes from Battelle, *Battelle Rev.*, v. 9, April 1960, p. 15.
Battelle established load-life characteristics for oscillating, self-aligning roller bearings of materials suitable for the 300–600°F temperature range. A total of 1,080 bearings was evaluated to establish load-life charts.
William A. Glaeser reports that, as expected, bearing life drops off as temperatures increase. The gradual drop-off in strength appears to be related to plastic deformation and oxidation and wear. It is assumed that plastic deformation predominates at heavier loads, wear and oxidation at lighter ones.
Among materials considered for the 450–600°F range, M-2 tool steel and 440-C stainless steel seem most satisfactory. The latter showed better resistance to oxidation, but a greater tendency for segregation of carbides in "bands", which surface cracks tend to follow inward. Of materials for temperatures up to 450°F, the technologists found SAE 52100 satisfactory, though its life in bearings should be expected to be shorter than 440-C or M-2 tool steel.
Sample size of about 15 bearings is sufficient to establish a point in load-life determinations of high-temperature grease-lubricated oscillating roller bearings.

Cast Bronze Sleeve Bearings.
Harry C. Rippel. *Machine Design*, v. 31, Sept. 17, 1959, p. 174–206.
Comprehensive manual of principles and practices for simplified design and application of 360-degree cast-bronze bearings. Sleeve-bearing fundamentals; full-film lubrication; complete boundary lubrication; mixed-film lubrication.

Grooving for Sleeve Bearings.
Harry C. Rippel. Machine Design, v. 31, Nov. 12, 1959, p. 170–177.
Selection of type, width, depth, and configuration of groove for effective lubrication.

Position of the Shaft and Friction in a Triple-Wedge Bearing.
H. H. Ott. *Brown Boveri Review*, v. 46, no. 7, July 1959, p. 395–406.
By using an approximation method, the position of the shaft and friction are calculated for the standard Brown Boveri triple-wedge bearing considering the steady state. The forces in the three segments and the maximum pressures produced in the oil film are also calculated. Flow in the oil film is assumed to be two-dimensional, and the viscosity of the oil to be constant. For the calculation, the wedge-shaped segments are replaced by equivalent circular segments. The results are depicted in the form of curves. From these it is an easy matter to determine the quantities which are important for the employment of triple-wedge bearings.

On the Behaviour of Rollers in a Cylindrical Roller Bearing.
Kōsaku Iida and Akio Igarashi. *Bulletin of JSME*, v. 2, no. 8, Nov. 1959, p. 538–545.
Each roller in a cylindrical roller bearing performs both two-dimensional planetary motion (*i.e.*, rotation and revolution), and three-dimensional skewing action. This behaviour, along with many other factors, affects the bearing characteristics such as running noise, friction, etc. To study the relations between roller motion and such characteristics, rotation and revolution of rollers were observed and photographed by stroboscope.

Tapered Roller Bearings in Kiln Car Design.
R. E. Martinsen. *American Ceramic Society Bulletin*, v. 39, Jan. 1960, p. 7–9.
Dead axle design utilizing high quality anti-friction tapered roller bearings provides the best service and is, over the years, the most economical. Advantages of this type design are discussed as well as the limitations it places on the design of the kiln itself and on the lubricants used.

A Special Analytical Study of Air-Lubricated Bearings for Jet Aircraft Engines.
George M. Robinson. Final Technical Report. Prepared on NACA Contract NAw-6473.

Laboratories for Research and Development, Franklin Inst. Report F-A1914. (Ask for N-79697) March 7, 1956 to February 15, 1957. 75. pp., diagrs.
The analytical study of air-lubricated bearings, which is covered in this report, had as its major objective the feasibility of adaptation of this type bearing to aircraft turbojet engine applications. Design formulas and methods for a simple step bearing were derived. Bearing loads encountered in maneuvers listed in MIL-E-5007A were analyzed. These analyses and formulas indicate that air-lubricated bearings may be adaptable to aircraft turbojet engines. However, large bearings, small clearances, and large volumes of air will be involved.

Dynamic Stability of Gas-Lubricated Bearings. (in English)
V. N. Constantinescu. *Rev. Mécanique Appliquée (Bucarest)*, v. 4, no. 4, (1959) 627–642; 10 fig., 6 ref.
Calculations on the influence of dynamic operation conditions on the bearing characteristics. Application of small perturbation method to cases of constant load and centrifugal load.

Investigations on the Operating Conditions of Journal Bearings.
I. Influence of Viscosity Variation (in English).
V. Tipei and Al. Nica. *Rev. Mécanique Appliquée (Bucarest)*, v. 4, no. 4 (1959) 609–625; 29 fig., 9 ref.
Theory of pressure distribution. Experiments on lubricant film viscosity as a function of loading and temperature.

5. Wear and Wear Resistance

Preliminary Investigation of Graphite, Silicon Carbide, and Several Polymer-Glass-Cloth Laminates in a Mach Number 2 Air Jet at Stagnation Temperatures of 3,000°F and 4,000°F.
Francis W. Casey, Jr., and Russell N. Hopko. *NACA RM L57K15.* January 1958. 18 pp., diagrs., photos.
An investigation of the possibility of utilizing the mechanisms of radiation, latent heat of fusion, pyrolysis, and ablation as methods of alleviating aerodynamic heating was conducted. Tests on graphite, silicon carbide, and several polymer laminates were conducted.

The Effect of the Duration of a Pulse on the Electric Erosion of Metals.
B. N. Zolotykh. Ministry of Aviation (Gt. Brit.) translation from *Elektrichestvo*, v. 8, 1956, p. 55-57. January 1960. 5 pp. MOA TIL/T.5088. (Ask for CN-80724)
The electric spark method of treating metals shows that the physical basis of the electric erosion of metals is the electrothermal process. The rate of heat distribution in a metallic electrode has almost no effect on the duration of the pulse and cannot be greater than the value determined for the given material. The erosion value is determined by the volume of of the metal melted during the pulse.

Increase of Resistance to Wear of Rolls for Continuous Strip Mills. (in Russian)
A. E. Krivosheev, L. S. Rudnitskiĭ, Iu. N. Taran, and I. E. Lev. *Stal'*, v. 19, no. 7, July 1959, p. 629–636.
Determination of the optimum chemical composition and structure of high-alloy rolls for finishing and intermediate stands has led to considerable increase of their resistance to wear.

Performance Study of a Piston-Type Pump for Liquid Hydrogen.
Arnold E. Biermann and William G. Shinko. *NASA Technical Note D-276.* March 1960. 26 pp. diagrs., photos. OTS price, $ 0.75.
Data covering the performance of a low-speed, submerged, piston-type pump for handling boiling hydrogen are presented. Tests were made with JP-5 fuel, liquid nitrogen, and liquid hydrogen at flows up to 78 gal./min, speeds to 360 r.p.m., and with pressures to 130 lb./in.^{2} gage. The overall performance of the pump was satisfactory with all fluids pumped. The effect on pump delivery of subcooling or of liquid level above the pump was slight. Internal leakage (slip) was greatest with hydrogen and least with JP-5 fuel. The cavitation losses were slightly greater with nitrogen than with hydrogen. The mechanical endurance of the pump in its final configuration was satisfactory for the intended application.

6. Analysis and Testing

Use of Radioactive Isotopes for Measurement of Cutting Tool Wear.
Georg Engstrand. *Kungliga Tekniska Högskolans Handlingar*, no. 143, 1959, 17 pp.
Deals with methods and applications of the isotope technics in determination of wear resistance of cutting tools. Relative measurements were performed by means of a scintillation detector.

Bearing Dynamometer.
R. V. Klint and R. S. Owens. *Review of Scientific Instruments*, v. 30, Sept. 1959, p. 775–777.
A bearing dynamometer was devised and built which enables ready evaluation of bearing materials. Coefficient of friction and shaft speed are presented on an X-Y recorder. At present, bearings of $\frac{1}{2}$-in. diameter are being studied to speeds of 2000 r.p.m. and coefficients of friction to 0.7.

7. Surface Treatment and Finishing

Protective Coating Systems for Molybdenum.
R. I. Jaffee. Paper from *Fabrication of Molybdenum*, p. 119–133. 1959, American Society for Metals, Cleveland.
The problem of application of coated Mo at elevated temperatures is extremely complex. There are a large number of potentially useful coatings but no one coating is without fault. Laboratory evaluation of silicide, Al-Si-Cr, Ni, Cr, Ni-Cr, Al coatings, and frit-type coatings is reported.

Coatings on Molybdenum for High Temperature Sliding.
G. W. Rowe. *Scientific Lubrication*, v. 11, Oct. 1959, p. 12–15.
The lowest friction is obtained with MoS_2 and provided that oxidation is prevented, for example by sliding *in vacuo*, lubrication is maintained up to 800°C (1,500°F). If the sliders are to operate in air it is possible to provide a protective coating of $MoSi_2$.

Limited Tests of Molybdenum Coated with Molybdenum Disilicide in a Supersonic Heated-Air Jet and Brief Description of the Coating Facility.
E. M. Fields and N. T. Wakelyn. *NACA RM L57112*, January 1958. 21 pp., diagrs., photos., tabs.
A laboratory-scale vapor-deposition coating facility (hydrogen reduction process) has been constructed and used in basic research in the field of high-temperature coatings. A molybdenum disilicide coating applied to molybdenum in this facility has been tested in a supersonic hot-air jet at jet stagnation temperatures of about 3,500° to 4,000°F. A coated model reached an equilibrium temperature of about 3,100°F and was undamaged after 470 sec at this equilibrium temperature in the jet, while an uncoated model was virtually destroyed in less than 6 sec.

The Vacuum Brazing of Nimonic 80A and Nimonic 90.
J. M. Shaw. Ministry of Supply (Gt. Brit.) *MOA S & T Memo 14/59*, August 1959. 14 pp., illus. (Ask for N-80730)
Describes the investigation which has been carried out to establish the necessary conditions for vacuum brazing the Nimonic alloys 80A and 90. The use of three typical brazing alloys — copper, coast metal 52, and N.M.P. 1. — has been examined. The limiting vacuums, optimum joint clearances, and brazing temperatures have been determined and the effect of prolonged heating and superheating has been observed. A limited number of tests have indicated the shear strength of brazed joints, at room temperature and at 800°C.

A Method of Depositing Metallic Films on Non-metallic Surfaces. Part 2. Electrical Resistance and Fine Structure of Copper Deposits and Polyester-Iron Substrates.
N. C. W. Judd. Royal Aircraft Establishment (Gt. Brit.) *RAE Tech. Note Chem. 1357*, November 1959. 15 pp., diagr., photos., tabs. (Ask for N-80725)
A method of depositing copper films on non-metallic materials by the replacement of iron present in a surface coating thereon has been considered for certain electrical applications. This note records some experiments to determine the resistance of the deposited copper films, and the surface resistivity of the substrates. Photomicrographs of the substrates and of the deposited copper films are presented.

8. Machining and Tool Wear

Does Compensation of Thermoelectric Currents Influence Cutting Tool Wear?
George Engstrand. *Kungliga Tekniska Högskolans Handlingar*, no. 144, 1959, 11 pp.
In machining with cemented-carbide tools the oxidation phenomenon is a contributive cause to the wear of the cutting edge. An account is given of the influence of compensating thermocurrents on the wear process.

Study of Machinability of Metals.
H. Takeyama and E. Usui. *ASME, Transactions, Series B, Journal of Engineering for Industry*, v. 81, no. 4, Nov. 1959, p. 289–292.
If the definition of the so-called machinability is simplified, a rather scientific treatment of machinability is possible. Reveals that machinability of a metal in terms of chip formation, which is one of the most important aspects, is closely related to the ratio of the shearing strain to the shearing stress near the fracture point of the shearing-test curve of the metal. The larger the ratio, the poorer the machinability from the viewpoint of chip formation.

The High Speed Routing of Stainless and High Tensile Steels.
Ministry of Aviation (Gt. Brit.) *MOA S & T Memo. 10/59*, June 1959. 10 pp., illus. (Ask for N-80732)
Determines the cutting speeds, feeds, cutter geometry, cutter life, surface finish on workpiece and limits using the Ferrand Luttmer Limited process, cutters, and injector head incorporating CO_2 cooling on nine aircraft and other steels including stainless steel.

The Broaching Characteristics of Titanium R. C. 130 A.M.
J. Purcell and J. A. Leitch. Ministry of Aviation (Gt. Brit.) *MOA S & T Memo. 6/59*, June 1959. 20 pp. illus. (Ask for N-80731*)
An investigation to find the optimum tool angles, and to determine the effects of cutting speed, tooth-to-tooth increment of cut, and other variations of conditions on the tool life when broaching the high strength titanium alloy R. C. 130.

Grading of Abrasive Grain on Coated Abrasive Products.
U. S. Department of Commerce OTS; Commercial Standard CS217–59; 39 pp., 10 tabs.
Determination of the grading or grain size of the abrasive grain on the coated product.

Coated Abrasives—Modern Tool of Industry.
Harold B. Maynard, editor. 426 pp. 1958. McGraw-Hill, New York.
Describes how abrasives are manufactured, and their use in the metalworking (ferrous and nonferrous), woodworking, glass, and plastics industries, in applications ranging from heavy material removal to fine polishing. Also describes recent advances, including new automatic machinery, applications such as strip scouring, preplate finishing, contour finishing, and discusses such special topics as cutting oils, coolants, and lubricants specifically for use with coated abrasives.

Bibliographies

Rubber Technology

Proc. Intern. Rubber Conference, Washington, D.C., 1959
Sponsored jointly by:

Division of Rubber Chemistry,
American Chemical Society

Committee D-11 on Rubber and Rubber-like Materials,
American Society for Testing Materials

Rubber and Plastics Division,
American Society of Mechanical Engineers

Preprints of the papers presented at the International Rubber Conference, Washington, D.C., November 8–13, 1959. Edited and produced for the Conference by the staff of the Applied Publications of the American Chemical Society; 613 pp., numerous fig. and ref. (no discussion remarks are included).

There were 12 Sessions on the various aspects of rubber technology. No attempt is made here to abstract those papers of particular importance to readers of this Journal since most of the results have been or will be reported elsewhere in technical rubber literature.

Three Sessions dealing with the technology of tyres give a comprehensive survey on problems of friction and wear as related to tyre structure, choice of materials and service conditions.

A concise analysis of the contents of this volume has been published by a group of specialists in: *Rubber and Plastic Age, 41* (1960) 37–51.

Testing of Materials

Proc. Second Japan. Congr. on Testing Materials, 1958

Compiled by The Editorial Committee of the Japanese Congress on Testing Materials, with the cooperation of The Science Council of Japan.

Published by the Japanese Society for Testing Materials, Kyoto, Japan 1959. 246 pp., numerous fig. and ref.

67 papers on metallic and non-metallic materials, testing methods and apparatus. An appendix deals with the present industrial situation in Japan (Equipments and Techniques).

KUMAKURA reports on a metal compression test, using Teflon films and MoS_2 as a lubricant. Large deformations with little bulging of the specimen and conditions of constant low friction are observed. (4 pp., 4 fig., 5 ref.)

IMAIZUMI reports on a new machine for testing the wear resistance of timber. A combination of rubbing, sand erosion and impact action is used. The importance of wear due to impact on flooring surfaces is emphasized. (4 pp., 11 fig., 4 ref.)

Wear, 3 (1960) 327

Tyre and Road Problems

Rev. gén. caoutchouc, 36 (10) (1959), Numéro Spécial, about 300 pages. 23 papers (and discussion remarks) read by experts from nine countries at a Symposium held in the Institut Français du Caoutchouc, Paris, May 20–22, 1959.

The topics of discussion are subdivided under the following headings:
- Tyre Dynamics (6 papers)
- Sliding (9 papers)
- Wear (see also the contribution by SCHALLAMACH in this Journal)
- Rolling Resistance (3 papers)
- Special Tyres (2 papers)
- Tests (2 papers)

All contributions are published in English and French.

Wear, 3 (1960) 327

Forthcoming Event

1960 INTERNATIONAL CONFERENCE ON THE NATURE OF SOLID FRICTION

Midwest Research Institute, Kansas City 10, Missouri

September 26, 27, 28, 1960

Nine invited papers will be discussed. The speakers are: Dr. J. F. ARCHARD; Dr. A. I. BAILEY; Dr. D. G. FLOM; Dr. E. RABINOWICZ; Mr. C. RUBENSTEIN; Dr. R. H. SAVAGE; Dr. S. SKINNER; Dr. R. T. SPURR; Dr. Y. TAMAI.

Wear, 3 (1960) 327

Book Reviews

TEXTILE TECHNOLOGY

Textile Engineering Processes, edited by A. H. NISSAN, Butterworths Scientific Publications, London, 1959, 14 × 22 cm, ix + 366 pp., £3.0.0 (American edition: Academic Press Inc., New York, $ 9.25).

Moisture in Textiles, edited by J. W. S. HEARLE AND R. H. PETERS, The Textile Institute and

Butterworths Scientific Publications, Manchester and London, 1960. 14 × 22 cm; ix + 203 pp., £ 2.0.0 (American edition: Textile Book Publishers Inc., $ 6.50).

The first volume, a text for students, should also be useful for mechanical and chemical engineers who wish to explore the mysteries of textile technology. Properties of textile fibres, basic principles spinning, yarn production, weaving, knitting, finishing and drying are considered in eleven chapters by almost as many contributors.

Two chapters on humidity control and automatic control, respectively, should be of interest to the general reader.

There are several references to friction, abrasion and wear but, considering the scope of this monograph, they cannot be exhaustive. The well-balanced and concise text, however, should be of particular value to lubrication engineers who intend to preach the gospel of modern lubrication techniques to the textile industry.

The contents of the second monograph are of more limited scope. The 13 chapters contributed by 7 well-known British specialists, are the outcome of a refresher course held at the Manchester College of Science and Technology. An exposition of the classical physical chemistry of moisture sorption by fibres and its effect on some physical and mechanical properties is given. The literature quoted refers mostly to the period 1930–1954. Some fibre materials such as polyvinylalcohol are not mentioned at all. No reference is made to the friction properties of fibres as related to moisture content, and the treatment of frictional electricity is rather superficial. One might also have expected that the editors would explain the subtle differences in the usage of the terms, sorption, *ad*sorption and *ab*sorption. Apart from these minor points of criticism the book can be recommended as a convenient introduction.

It is difficult in books of this type to avoid the use of British measures, at least in some places. Addition of conversion tables seems therefore recommendable for future volumes of this Series.

The moderate prices of these effectively illustrated monographs make them eligible for addition to the private libraries of students and technologists. G.Sa.

Wear, 3 (1960) 327–328

Notes on Contributors

ORSON L. ANDERSON, Ph.D., M.S., B.S.; a native of Price, Utah; studied at the University of Utah, where he obtained his B.S. in mechanical engineering and his Ph.D. in physics for a thesis on plasticity in 1951. After a short term as assistant professor of physics at the University of Utah, joined the research department of Bell Telephone Laboratories, where he is still employed; his field is the mechanical properties of solids. He has written papers on fracture and flow of glass, as well as on adhesion. [See p. 253]

I-MING FENG, Ph.D., M.S., B.Sc.: born in Shanghai; educated at Chiao-Tung University and did his graduate work at the University of Michigan; from 1950 to 1955 was at Mass. Inst. of Technology where, as an assistant professor, he taught and supervised research on applied mechanics, modern research techniques, and fundamentals of wear and lubrication. Since joining Ethyl Corporation in 1956, has continued basic and applied research in lubrication and wear mechanisms; is the author of some twenty papers in these fields. [See p. 309]

G. W. ROWE: (for biographical note see *Wear*, 1 (1957/58) 530). [See p. 274]

TOSHIO SATA: born in Tokyo, Japan; obtained B.Sc. in mechanical engineering and D.Sc. at Tokyo University; in 1948 joined the research staff of the Institute of Physical and Chemical Research, Tokyo, where he has been engaged in studies on wear, metal cutting and plastic-working. [See p. 104]

G. V. VINOGRADOV: born in Moscow; graduated from the Higher Technical School of Moscow; in 1941 received degree of Candidate of Chemical Sciences at Karpov Institute of Physical Chemistry; in 1951, after taking a post-graduate course, was awarded a D.Sc. degree; specializes in lubrication and lubricants and is at present at the Institute of Petrochemical Synthesis of the U.S.S.R. Academy of Sciences. [See p. 297]

VOL. 3 NO. 4 JULY/AUGUST 1960

CONTENTS

The role of surface shear strains in the adhesion of metals. Part I
by O. L. ANDERSON (Murray Hill, N.J.) 253

Some observations on the frictional behaviour of boron nitride and of graphite
by G. W. ROWE (Cambridge) 274

Surface chemical behavior of polar compounds in nonaqueous liquids. Dispersing effect of the soap solution
by T. SAKURAI AND T. BABA (Tokyo) 286

A study of the wear of steel under heavy loads with lubricants containing sulphur-based additives
by G. V. VINOGRADOV AND O. E. MOROZOVA (Moscow) 297

Brief note: Pyrolysis of zinc dialkyl phosphorodithioate and boundary lubrication
by I-MING FENG (Detroit) 309

Letter to the editor 312

Literature and current events 314

Authors' abstracts 314

Systematic abstracts 320

Bibliographies 326

Forthcoming event 327

Book reviews 327

Notes on contributors 328

SOME PAPERS ACCEPTED FOR PUBLICATION

Solution for a high speed bearing problem
by G. R. NORTHRUP (Wayne, Penna.)

Directional effects in friction
by M. HALAUNBRENNER (Cracow)

Ein Beitrag zum Zylinder- und Kolbenring-Verschleiss bei Dieselmotoren für Traktoren
by A. SEIFERT (Braunschweig)

A technique for investigating reactions between e.p. additives and metal surfaces at high temperatures
by F. T. BARCROFT (Chester)

The phenomenon of seizure and its investigation
by A. P. Semenov

The friction and strength of clean graphite at high temperatures
by G. W. Rowe

Some measurements of rail-tyre adhesion
by R. T. Spurr

CONTRIBUTIONS

Types of Contributions:

(a) Original research work not previously published in other periodicals.
(b) Surveys of work that has already been published either in languages other than those of this Journal or in reports on laboratory activities that are not generally accessible.
(c) Reviews on recent developments in specialized fields.
(d) Case histories or analyses of service problems, if they are of a more general interest.
(e) Short notes or letters to the editors.
(f) Authors' abstracts, Bibliographies and Systematic abstracts.

Language

Papers will be published in English, French or German.

Notes for Authors

'Notes for Authors' for the guidance of contributors can be obtained from all Members of the Editorial Board and the Advisory Board and from the Editor's Office.

Submission and Acceptance of Papers

Original contributions, surveys or case histories can be submitted to Members of the Editorial Board or the Advisory Board in the Author's geographic region, or to the Editor.

Office of the Editor: P.O.Box 71, Delft, The Netherlands.

Review Articles are scheduled well in advance. Authors wishing to contribute a review article should communicate first with a Member of the Editorial Board or with the Editor for detailed arrangements.

Short Notes, Letters, and Abstracts of papers published in other languages should, however, be sent directly to the Editor.

Competent referees will assist the Editorial Board in deciding whether a paper is to be accepted. Papers which, in the opinion of the Editorial Board, can be shortened will be referred back to the author for modification.

Reprints

Twenty-five reprints will be supplied free of charge. Additional reprints can be ordered at quoted prices. They must be ordered on order forms which are sent together with the proofs.

PUBLICATION

WEAR will have six issues to the volume, approx. 500 pages per volume.
Subscription price: £ 5.7.6 or $ 15.00 or Dfl. 57.— per volume.

Subscriptions should be sent to:

ELSEVIER PUBLISHING CO., Spuistraat 110–112, Amsterdam-C, The Netherlands.

For advertising rates apply to the publishers.

All rights reserved

ELSEVIER PUBLISHING CO., AMSTERDAM
Printed in The Netherlands by
NEDERLANDSE BOEKDRUK INRICHTING N.V., 'S-HERTOGENBOSCH